Dottorato di Ricerca in Neuroscienze

Curriculum: Neuroscienze e Neurotecnologie

Coordinatore: Prof. Angelo Schenone

Ciclo XXXIII

Coordination in space and time of excitatory and inhibitory synaptic plasticity at dendritic synapses

Author: Massimo Ruben

Supervisor: Andrea Barberis

UNIVERSITÀ DEGLI STUDI DI GENOVA

ISTITUTO ITALIANO DI TECNOLOGIA

Contents

List of Figures

ABSTRACT

For years, GABAergic synapses were considered poorly plastic. However, an increasing body of evidence demonstrated that, similarly to excitatory synapses, inhibitory synapses formed by interneurons onto pyramidal cells can be modulated in response to neuronal activity. The spiking output of a neuron is determined by the opposite but concomitant action of excitation and inhibition. In this view, it is crucial to understand how plasticity at excitatory and inhibitory synapses is coordinated. In this thesis, I will describe two different types of plasticity interplay between excitation and inhibition, in space and time domains. In our previous work (Petrini et al., 2014) we characterized the induction and the expression of postsynaptic inhibitory long term potentiation (iLTP) following the administration of NMDA and CNQX (chemical protocol of induction of iLTP). Here we induced postsynaptic iLTP by administering electrophysiological stimulations intended to better mimic physiological neuronal activity. We observed that the delivery to the postsynaptic neuron of a train of action potentials at frequency of 2Hz, (that we define here low frequency stimulation, LFS) potentiated the amplitude of the inhibitory postsynaptic currents (iPSCs) up to 30 minutes. This particular form of iLTP depended on moderate calcium increase in the postsynaptic neuron and the activation of the Calcium calmodulin kinase II (CaMKII). The concomitant investigation of excitatory transmission revealed the depression of excitatory postsynaptic currents (ePSCs) amplitude thus indicating that LFS induced excitatory (LTD). In order to further study the interaction between excitatory and inhibitory synaptic plasticity, we paired the protocol of iLTP together with simultaneous photorelease of glutamate on a single spine. This particular type of Hebbian stimulation induced LTP at the photostimulated spine (Lee et al., 2009; Matsuzaki et al., 2001, 2004) and LTD on the other spines. In contrast, we observed that the GABAergic synapses located distant from the potentiated spine showed an iLTP while the ones located in a range of 3 micron from the potentiated spine were depressed. Such “inversion of plasticity” was promoted by a massive influx of calcium and the activation of calpain, a protease involved in the cleavage of the gephyrin.

In the second part of this thesis, I will show a new type of structural inhibitory short term depression plasticity (siSTD) that occurs during the induction of the plasticity protocol, before the expression of iLTP. In particular, the depolarization of the postsynaptic neuron induced a transient depression of inhibitory synapses that was dependent on the fast activation of the protease calpain. We propose

that such “early” calpain activation pathway competes with that of the CaMKII thus defining the extent of long-term inhibitory plasticity.

INTRODUCTION

In the central nervous system, higher brain functions are determined by the interplay between excitatory neurons (principal cells) and inhibitory cells (interneurons). While principal cells are rather homogeneous and are the largest neuronal population, interneurons represent the 15-20% of the total neuronal number and show substantial diversity (Somogyi et al., 1998). For instance in the region of hippocampus more than 20 types of interneurons have been described (Freund and Buzsáki, 1998; Klausberger and Somogyi, 2008). Interneurons play a crucial role in the modulation and the control of the neuronal network (Bartos et al., 2007; Bragin et al., 1995; Klausberger and Somogyi, 2008; Sohal et al., 2009). Interneurons subclasses have been created based on different criteria including i) electrophysiological activity, ii) morphology, iii) biochemical properties and iv) localization of their afferences in pyramidal neurons (Bacci et al., 2003; Bartos et al., 2007, 2011; Kullmann and Lamsa, 2007; Pelkey et al., 2017). Their diversity allows an accurate tuning of the activity of the principal cells and the emergence of the higher brain function. Specific interneuronal subclasses have been described to play distinct roles in shaping specific aspects of neuronal activity, such as generation of rhythmic activity, signal integration and dendritic filtering of excitatory inputs and generation of cell assemblies. For instance, the intrinsic electrophysiological characteristic of two interneurons targeting the soma of pyramidal neurons expressing either parvalbumin (PV+) (Bartos et al., 2007; Gabernet et al., 2005; Geiger et al., 1997) e or cholecystokinin peptide (CCK+) (Daw et al., 2009; Hefft and Jonas, 2005) define their role in shaping neuronal circuit. Both interneurons are present in the region of the hippocampus. Indeed PV+ interneurons are fast spiking, the CCK+ are regular spiking and show accommodation interneurons: this indicates that while PV interneurons control the network with high temporal precision (clock interneurons), the CKK interneurons have been shown to determine the slow and fine modulation of the network (mood interneurons), being involved in motivation and emotions (Freund and Katona, 2007) and also in pathologies as schizophrenia and anxiety (Benes, 2001; Croarkin et al., 2011; Levitt et al., 2004; Orekhova et al., 2007; Sanacora et al., 1999). Besides their role in shaping the network properties, interneurons have been shown to be substantially diverse also in terms of location of their synapses on the excitatory neurons. In particular, in the hippocampus, bi and tri-stratified cells (Klausberger and Somogyi, 2008; McBain and Fisahn, 2001), ivy cells (Fuentealba et al., 2008) and neuroglialform cells (Capogna, 2011; Karayannis et al., 2010; Kawaguchi and Kubota, 1997; Szabadics et al., 2007) show synapses in the more apical part of the dendritic tree of the excitatory

neurons. Viceversa, basket cells as PV+, CK+ interneurons (Freund and Katona, 2007) and chandelier cells (Freund and Buzsáki, 1998; Kawaguchi and Kubota, 1997; Markram et al., 1997) contact the excitatory neuron on the perisomatic portion of the dendrites or on the axon.

Synaptic transmission:

From aplysia, to mammalians, it is clear that the communication among neurons is crucial for the brain functioning, thus allowing the individual's survival and reproduction. Neurons can communicate through specialized structures called synapses that can be both electrical and chemical. While electrical synapses are faster, chemical synapses are slower and energy consuming but better suited for signal processing and integration. We will focus our attention on the chemical synapses and how they can be modulated during neuronal activity. Synaptic transmission is a dynamic process where an electrical signal from the presynaptic neuron is converted into a chemical signal to be delivered to the postsynaptic neurons, where it can be re-converted in an electrical postsynaptic signal. The release of the neurotransmitter vesicles after the electrical signal invades the presynaptic terminal, occurs through the calcium influx mediated by the voltage gated calcium channels (VGCC). The vesicles release their content in the synaptic cleft, where the neurotransmitter diffuses to bind its receptor located on the postsynaptic membrane. Next, the postsynaptic receptor activation allows a flow of ions between the extracellular and intracellular compartments, generating an electrical signal in the postsynaptic membrane. Chemical synapses can be excitatory or inhibitory, depending on different factors including distribution of ions across the membrane, and the membrane potential. A hyperpolarizing current is typically observed following the activation of GABA or Glycine receptors at inhibitory synapses, and is generated by chloride and HCO_3^- ions. Viceversa, a depolarizing current is observed during the action of an excitatory synapse, due to the permeation of sodium, calcium and potassium ions. Postsynaptic receptors can be divided in ionotropic and metabotropic. Ionotropic receptors mediate fast postsynaptic currents elicited by the conformational change induced by the binding neurotransmitter that directly open the channel pore, thus allowing the ions flow. Metabotropic receptors are usually slower and their activation determines a signalling cascade that ultimately activates ion conductances able to tune and fine regulate postsynaptic signals. Among ionotropic receptors, the most abundant in the CNS are the AMPA, NMDA and Kainate receptors at excitatory synapses, while inhibitory synapses express GABAA and Glycine receptors.

Excitatory synapses:

Most of the excitatory neurons are defined as spiny cells, meaning that they present on their surface small protrusions, called spines. Spines typically harbor excitatory synapses that, in pyramidal cells are distributed along the dendritic arborisation (McKinney, 2010; Nimchinsky et al., 2002). The physiological role of the spine is not completely defined, although the most common hypotheses point at the spines as strategy to increase neuronal surface and to compartmentalize proteins and factors important for synaptic transmission and plasticity (Tønnesen and Nägerl, 2016). In addition, spines could favour non-linearity, prevent the excito-toxicity (Korkotian and Segal, 1999; Segal, 1995; Segal et al., 2000), and modulate synaptic efficacy. The morphology of a spine shows a head, where the receptors are located, and a neck, that link the head with the parent dendrite. Spines can be divided in different classes, as "mushroom" spines, "thin" spines or "stubby" spines, based on the shape of both head and neck (Harris et al., 1992; Peters and Kaiserman-Abramof, 1970). It is thought that the morphology of the spine is crucial for its synaptic function as mushrooms spines with big head are more stable respect to "thin" spines that are more susceptible to removal. It is also demonstrated that morphology of spines on the same dendrite can significantly differ. For instance, afferences from the cortex contact "thin" spines on neuron located in the later nucleus of the amygdala, while afferents from the thalamus contact "mushroom" spines located on the same dendrite (Humeau et al., 2005). Spines are strongly compartmentalized: the neck width is crucial for the control of the signal's transmission from the spine head to the dendrite (Tønnesen et al., 2014). It is known that during plasticity the width of the spine neck can be modulated, facilitating or limiting the passage of molecules and regulating the neck electrical resistance (Araya et al., 2014; Bloodgood and Sabatini, 2005; Fifková and Anderson, 1981; Tanaka et al., 2008). The head of the spines is filled with receptors, scaffold proteins, organelles and other proteins necessary for the transmission of the signal. Glutamatergic spines are enriched in AMPA, NMDA and kainite receptors that are anchored to scaffold proteins such as stargazing, PSD95 and Homer1 (Chidambaram et al., 2019). Calcium influx through NMDA, Kainate receptors and specific subclasses of AMPA receptors is fundamental for the transmission of the signal and the induction of plasticity (Hill and Zito, 2013; Yang et al., 2014). The amplitude of calcium transient generated by the activation of a spine is proportional with the size of the spine (Arellano, 2007; Harris and Stevens, 1989; Koch and Zador, 1993; Majewska et al., 2000; Matsuzaki et al., 2001; Noguchi et al., 2011). Wider spines present more NMDA receptors on their surface, allowing a higher influx of calcium (Bloodgood and Sabatini,

2007; Bywalez et al., 2015; Noguchi et al., 2005). After influx, calcium is buffered by several proteins such as for instance the calcium calmodulin binding protein (CaM) (Chang et al., 2019). Several works show that CaM is activated by different concentration of intraspine calcium, activating different synaptic pathways leading to different types of plasticity (Higley and Sabatini, 2008; Sabatini et al., 2001; Sanhueza et al., 2011; Soderling, 2000). Calcium and CaM lead to the activation of the CaMKII, a kinase known to be involved in several type of excitatory synaptic plasticities (Sanz-Clemente et al., 2013; Xia and Storm, 2005). In particular, one of the principal role of the CaMKII is to phosphorylate AMPA receptor, an event that triggers their recruiting at synapses thus promoting LTP. Another important protein involved in plasticity is calcineurin, a phosphatase mostly implicated in the depression of excitatory transmission (LTD) (Mulkey et al., 1994a; Yasuda et al., 2003; Zeng et al., 2001) by removing the phosphorylation of AMPA receptors (Weitlauf and Winder, 2001). Calciuneurin shows higher affinity for calcium with respect to CaMKII, allowing preferential activation of this protein in presence of low concentration of calcium. Hence, different calcium influx can induce the activation of different pathways promoting opposite plasticity. In this concern, it is believed that massive influx of calcium leads to LTP while mild calcium entry induces LTD. A third important protein involved in spine plasticity is the calcium-dependent protease calpain. So far, several families of calpain proteins have been described, but calpain type 1 and 2, have been shown to play a major role in synaptic plasticity. While the capain type 1 is mostly required in the LTP induction, cleaving rapidly regulatory and cytoskeleton proteins, calpain 2 is involved in the block of the plasticity (Briz and Baudry, 2017). The cytoplasm of the spines is rich of filamentous actin, which allows the rapid shaping of the spine morphology during plasticity (Capani et al., 2001; Fifková and Delay, 1982; Hlushchenko et al., 2016; Lei et al., 2016). Several works have demonstrated that spines can be continuously formed and destroyed, being this plasticity occurring with kinetics raging from minutes to days (De Roo et al., 2008; Wosiski-Kuhn and Stranahan, 2012). In particular, it has been demonstrated that spine heads showing the scaffold protein PSD95 are bigger and more stable with respect to others (Cane et al., 2014).

Inhibitory synapses:

While excitatory synapses are typically formed on spines, the majority of inhibitory synapses are located on the dendritic shaft. The reason of this difference is still debated and might suggest major functional differences between excitatory and inhibitory synapses. The role of inhibitory synapses is to shape excitation by both generating hyperpolarizing currents and by shunting excitatory currents. It has been shown that the activation of individual inhibitory synapses located in the right position on the dendritic shaft can strongly impact on the modulation of synaptic signals (Chklovskii et al., 2004; Poirazi and Mel, 2001). While the significant depolarization of the neuron requires the concomitant actions of several excitatory synapses, inhibitory synapses can effectively silence excitatory signals with a relatively "weaker" activation. The most important neurotransmitter mediating inhibition in the brain is GABA. GABA is synthesized from the glutamate by glutamic acid decarboxylase (GAD). After being synthesized, GABA is accumulated inside inhibitory synaptic vesicles by vGAT, a co-transporter of GABA and hydrogen ions. The action of the enzyme is facilitated by the different electrochemical gradient of the vesicle respect to the cytosolic compartment, which in turn is maintained by the V-ATPase. After the fusion of the vesicle with the presynaptic membrane, GABA is released in the synaptic cleft and binds postsynaptic receptor located on the postsynaptic neuron, allowing an influx of chloride that leads to a hyperpolarization or shunting of the postsynaptic membrane thus decreasing the probability of generating an action potential. Receptors for GABA are divided in 2 classes: i) GABAA receptors (ionotropic) (Barnard et al., 1998; Sieghart, 2006), including the ex-GABAC receptors that are present only at the level of the retina and ii) GABAB receptors (metabotropic) (Bowery et al., 1983; Isaacson et al., 1993). At inhibitory synapses, GABAA receptors are stabilized by scaffold proteins, among which the most important is gephyrin. The chloride entry mediated by the opening of GABAA receptors is ensured by the presence of a chloride electrochemical gradient across the membrane which, in turn, is maintained by the action of KCC2 cotransporters that extrude chloride exploiting the K^+ gradient actively generated by the K-Na ATPase pump (Rivera et al., 1999, 2005). It is interesting to note that the process of chloride extrusion by the KCC2 enzyme is rather slow (seconds to tens of seconds) (Payne et al., 2003; Rivera et al., 1999, 2005). Since GABAergic synaptic transmission occurs in millisecond this means that, under specific conditions of sustained activation of GABAergic transmission, the Cl gradient can be dissipated and in some cases even inverted, leading to depolarization instead of hyperpolarization with important consequences at network level (Doyon

et al., 2011; Rinke et al., 2010). Interestingly, in the developmental period, GABA is mostly depolarizing, since KCC2 is poorly expressed, and the high presence of the cotransporter of sodium, potassium and chloride NKCC1 leads to the accumulation of intracellular chloride and to a more negative value of the reversal potential of the ion respect to the resting membrane potential, with the consequent depolarizing action of GABA (Ben-Ari, 2001, 2002; Ben-Ari and Spitzer, 2004).

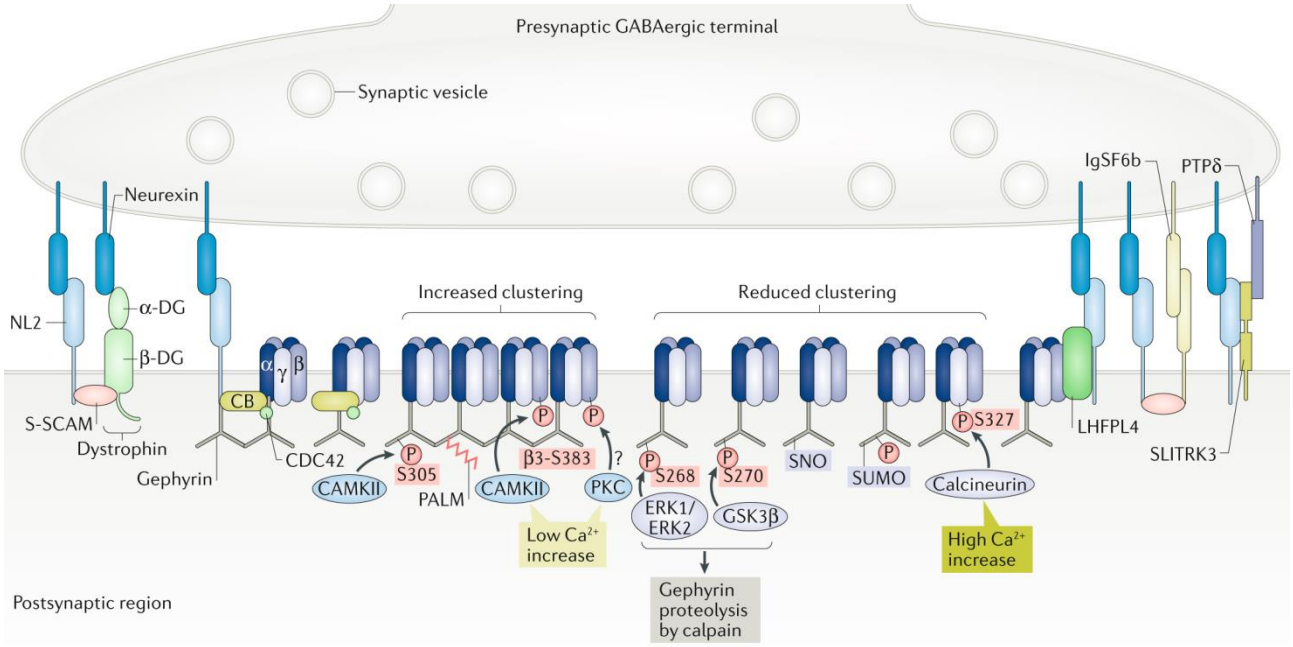

Figure: Schematic representation of the molecular components involved in the structure and regulation of ionotropic GABAergic synapses.

(Chiu et al., 2019)

Dually innervated spines:

The classical view of a clear separation in the space domain between synaptic excitation (on the spines) and inhibition (on the dendritic shaft) synapses has been recently questioned. The ability to simultaneously visualize excitatory and inhibitory synapses in vivo and ex vivo allowed to reveal that a considerable percentage of spine (about 30% in visual cortex) also harbour an inhibitory synapse (Chen et al., 2012). These spines that are defined as dually innervated spines (DiS) are bigger and more stable respect to the single innervated spines (SiP). In addition, inhibitory synapses on spines have been shown to finely modulate the excitatory transmission (Chiu et al., 2013). In particular, while inhibitory synapses on the dendritic shaft are uniformly distributed along all the dendrites, the GABAergic synapses on spines are twice distributed in the distal dendritic portion. The reason of such distribution could represent a "division of labor" between synapses on dendritic shaft and spines. GABAergic synapses on the dendritic shaft might regulate the activity from multiple spines and the depolarization brought by back-propagating action potentials (bAPs). Since bAP are heavily filtered in distal dendrites, the only excitatory driven in these dendritic regions are represented by spines: in this scenario inhibitory synapses on spine could represent an efficient and energy-saving strategy to control and modulate distal dendritic excitation (Chen et al., 2012). As mentioned above, dually innervated spines are more stable with respect to singly innervated ones thus highlighting their important role in shaping dendritic synaptic signals (Villa et al., 2016). In addition gephyrin clusters on spines are extremely dynamic with respect to those ones located on the dendritic shaft, continuously appearing and disappearing in the same position (Villa et al., 2016). Thus while dually innervated spines are very stable, inhibition on spines can be "tuned on demand" thus ultimately regulating the output of the neurons and contributing to circuit remodeling.

Dendritic synaptic integration:

The integration of synaptic inputs on dendrites involves the summation in space and time of several excitatory and inhibitory inputs and is crucial for ultimately shaping neuronal output. The original hypothesis was that synaptic inputs are linearly summated in the soma and thresholded in the axon hillock. This theory also defined "point neuron" would offer the same chance to be integrated to every synapse in the neurons. However by analysing the cable theory it became soon clear that such integration strategy dramatically favours synapses close to the soma at the expenses of synapses in small dendrites or in the distal apical region that, due to the heavy cable filtering negligibly contribute to changing the somatic potential (Berger et al., 2001; Harnett et al., 2013, 2015; Larkum et al., 2009; Magee, 1998; Nevian et al., 2007; Stuart and Spruston, 1998; Williams and Stuart, 2002). To compensate this biophysical limit, it has been proposed that more distal synapses are bigger, thus mediating larger potentials that may have the chance to reach the soma, a phenomenon defined "synaptic scaling". In addition, since the dendritic impedance (Z) depends on dendrite diameter (Katz et al., 2009; Losonczy and Magee, 2006), postsynaptic potential elicited in smaller dendrites will be larger than that evoked in large dendrites: this dendritic feature known as "passive normalization" would also contribute to increase the weight of electrotonically distant synapses. Although these strategies partially mitigate dendritic cable filtering, the weight of synapses distant from the soma remains very low and the main contributors to "linear integration" are synapses very close to soma or in the apical trunk dendrite that show large diameter.

Even if most of dendritic synapses are not strong enough to be linearly integrated at the level of the soma, it has been shown that their activation can contribute to the induction of local regenerative potentials defined as "dendritic spikes" (Llinas et al., 1968; Rall and Shepherd, 1968; Spencer and Kandel, 1961). Such dendritic activity is sustained by active conductances that include voltage dependent sodium channels, voltage dependent calcium channels and NMDA receptors: the interplay between these conductances can lead to sustained dendritic depolarization (or plateau potentials) (Hoffman et al., 1997; Magee and Johnston, 1995; Magee et al., 1998; Migliore and Shepherd, 2002; Stuart and Sakmann, 1994). An important requisite for the generation of such active dendritic potential is that synaptic inputs are sufficiently clustered within a dendritic branch in order to reach the threshold for triggering the aforementioned regenerative processes (Stuart and Spruston, 2015). The amplitude and duration of dendritic spikes is not fixed, suggesting that the more colocalized synapses are activated simultaneously, the stronger will be dendritic potential

(Losonczy and Magee, 2006; Polsky et al., 2004; Williams and Stuart, 2002), a phenomenon that may regulate the time window for the synaptic integration. The occurrence of dendritic spikes has inspired a more updated model for dendritic integration, in which each dendritic branch showing dendritic spikes acts as a “unit” that can be integrated in the soma. Interestingly these dendritic branches are integrated linearly in the soma, thus leading to the “two layer” integration model. It is worth to note that the linear summation and the two layer model may coexist and the relative weight of these two “integration modes” can vary according to dendritic region and the neuronal activation state. Although less studied, inhibitory synapses play a crucial role in dendritic integration, acting as a “shutter” allowing or blocking depolarization from excitatory synapses and, ultimately, dendritic spikes (Larkum et al., 1999), thus highlighting that dendritic branches are functional domains where excitatory and inhibitory synapses that act together in modulating the output of neurons.

Synaptic plasticity:

Synaptic plasticity is maybe one of the most distinctive ability of the central nervous system (CNS) that refers to the ability that to functionally and physically change the neuronal network in response to specific conditions or external stimuli. Since the majority of neurons of the central nervous system do not replicate, plasticity represent an essential feature to "renovate the network" in order to adapt to novel scenarios presented during an individual's life. Given the aforementioned importance of plasticity in phenomena like learning and memory, during the last 50 years an extraordinary effort has been made to investigate this phenomenon at several levels, from the molecular to the circuit and behaviour ones. Several types of synaptic plasticity were extensively identified and described involving functional but also structural synaptic changes in response to specific stimuli or activity patterns. Different forms of learning and memory (Bailey et al., 2000; Huang and Kandel, 2005; Ito, 2001), as well as of neuronal circuit development (Chen and Olsen, 2007), have been associated to synaptic plasticity. Modifications can differ in their time of action, usually defined as short-term plasticity (when it occurs in tens of milliseconds) or long-term plasticity (when it lasts for more than 30 minutes). In the present thesis I will focus on long term plasticity analysed either at early stage (1 minute after induction) or in the long term (30 min).

Excitatory and inhibitory plasticity:

As mentioned above plasticity at excitatory synapses has been extensively studied for almost 5 decades and several types of glutamatergic plasticity have been characterized. Surprisingly, plasticity of inhibition has received much less attention. An increasing body of evidence is showing that inhibitory synapses are extremely susceptible to be modulated by neuronal activity and similarly to excitatory synapses they show both short and long term plasticity expressed at pre and postsynaptic levels (Lamsa et al., 2005; Maffei and Turrigiano, 2008; Maffei et al., 2006).

Presynaptic plasticity:

Presynaptic form of excitatory plasticity:

A well characterized form of plasticity expressed at presynaptic level was identified in the hippocampus, at synapses formed by dentate gyrus (DG) granule cells and CA3 neurons (mossy fibers). Indeed it has been shown that high frequency stimulations trigger an increase in the probability of glutamate release (Mellor and Nicoll, 2001; Zalutsky and Nicoll, 1990). In particular, the increase of calcium concentration in the presynaptic terminal mediated by R-type voltage gated calcium channels (VGCC) leads to the activation of an intracellular cascade that ultimately activates PKA. In turn, PKA phosphorylates presynaptic substrates, as VGCC, causing a long-lasting increase in their activity and leading to a persisting enhance of the glutamate release probability from granule cells ending with LTP (Breustedt et al., 2003; Villacres et al., 1998; Wang et al., 2003; Weisskopf et al., 1994). Interestingly these synapses, under specific conditions, could also show presynaptic LTD (Kobayashi et al., 1996) mediated by the metabotropic glutamate receptors mGluR2 located on the presynaptic neuron (Kobayashi et al., 1999; Tzounopoulos et al., 1998). From a molecular point of view, the stimulation of the G protein coupled with the mGlur2 decrease the activity of the PKA, leading to an inverse phenomenon respect to the LTP, triggering a reduction in vesicles release (Castillo, 2012).

Presynaptic form of inhibitory plasticity:

At presynaptic level, inhibitory GABAergic synapses have been shown to be modulated by the activation of NMDA receptors inducing two different processes that can lead to either potentiation (iLTP) or a depression (iLTD) of inhibitory transmission. For instance, in the cerebellum, the stimulation of the parallel fibers and the consequent release of glutamate, activates the NMDA receptors on the stellate interneurons, resulting in increase of GABA release through a pathway involving calcium influx and PKA activation (Lachamp et al., 2009; Liu and Lachamp, 2006). The enhancement of the inhibitory transmission mediated by the stellate cells enables Purkinje cells to integrate excitatory inputs with a high temporal fidelity (Scelfo et al., 2008). Moreover, stellate cells show reciprocal connectivity, thus suggesting that the increase in GABA release is likely to modulate the network activity also by regulating neuronal disinhibition. On the contrary, in the xenopus retinotectal system, the activation of interneurons NMDA receptors following repetitive seems to be required but not sufficient for the induction of iLTD, since it is necessary also the coincident

GABAergic interneuron activity that promotes a boosting of calcium influx in the presynaptic terminal (Lien et al., 2006; Liu et al., 2007).

Retrograde messengers on excitation and inhibition:

A different form of presynaptically induced plasticity involves the release of retrograde messengers from the postsynaptic element. Importantly this form of plasticity has been found at both excitatory and inhibitory synapses. The retrograde messenger diffuses to the presynaptic terminal where it binds to specific presynaptic receptors. There are several types of retrograde messengers, some of which are inducing plasticity both at excitatory or inhibitory synapses. The best characterized retrograde messengers are: i) endocannabinoids (eCBs), ii) nitric oxide (NO), iii) peptides as the neurotrophic factors, among which one of the most important is the BDNF.

Endogenous Cannabinoids:

Endocannabinoids (eCBs) are lipid derived retrograde messengers synthesized and released from the postsynaptic neuron and are able to affect both excitatory and inhibitory transmission. The first demonstration of retrograde eCBs signalling in synaptic plasticity was characterized in the depolarization-induced suppression (DIS) of inhibition (Ohno-Shosaku et al., 2001; Wilson and Nicoll, 2001) and of excitation (Kreitzer and Regehr, 2001). In the hippocampus, the depolarization of pyramidal neurons leads to the release and diffusion of eCBs that activate the G-protein coupled with CB1 receptor located presynaptically. CB1 activation reduces the calcium influx in the presynaptic terminal through the inhibition of VGCC, thus affecting the release of GABA from interneurons and promoting inhibitory depression. eCBs are also involved in depression of excitatory synaptic transmission on cerebellar purkinje cells. In particular, the depolarization of these neurons induces the release of eCBs that reduces the release of glutamate from the climbing and parallel fibers, promoting short term depression (STD). Concerning long term plasticity, in the hippocampus (but also in other brain regions) the binding of eCBs to CB1 receptors activates the alpha subunit of G protein triggering a signalling cascade, which finally results in the downregulation of the cAMP/PKA system and the persistent depression of synaptic transmission (Castillo et al., 2011; Chevaleyre et al., 2006; Heifets and Castillo, 2009). In conclusion, endocannabinoids are able to modify the signal transmission of excitation and inhibition both in short or long manner. Interestingly, in all the aforementioned plasticity forms the final action of eCBs is to reduce presynaptic release, without affecting the postsynaptic element.

Nitric oxide:

Nitric oxide (NO) is an ubiquitous signalling molecule involved in several aspects of brain function, including synaptic plasticity (Hölscher, 1997), development (Contestabile, 2000), cellular functions (Garthwaite, 2008) and blood flow (Gordon et al., 2007). In particular, in synaptic plasticity, NO is usually synthesized in the postsynaptic neurons and influence the release of neurotransmitter at presynaptic side. In the CNS the most common isoform of NO synthase is NOS1 that usually is located in spines head and is a part of the post synaptic density (PSD) by interacting with the PDZ domain of the PSD95 (Brenman et al., 1996; Eliasson et al., 1997). Several works show that NO is implicated in the modulation of release of neurotransmitter at excitatory and inhibitory synapses by modulating the fusion of synaptic vesicles with the presynaptic membrane. In particular, NO is able to increase the influx of calcium in the presynaptic terminal by enhancing the N-type calcium channel conductance via PKG and also induces the binding of synataxin1 with the VAMP on the vesicles and SNAP 25 on the release site, thus promoting the vesicle fusion. The role of NO has been observed in several brain regions including the hippocampus (Phillips et al., 2008), amygdala (Lange et al., 2012) and neocortex (Hardingham and Fox, 2006). In the hippocampus, NO modulates excitatory and inhibitory synaptic plasticity. For example, the activation of NMDA receptors in pyramidal cells induces the release of NO from the postsynaptic neuron, stimulating the release of GABA from the presynaptic terminal and potentiating the spontaneous IPSCs mediated by GABAA receptors (Xue et al., 2011). In the layer 5 of the neocortex, somatic depolarization or short bursts of action potentials of pyramidal neurons induce an iLTP of GABAergic synapses increasing the release of nitric oxide (Lourenço et al., 2014, 2020a). Moreover it has been shown that exogenous NO application in hippocampal slices increases spontaneous EPSCs (O'Dell et al., 1991).

Neurotrophins:

Another important family of molecules involved in the retrograde signalling are the neurotrophins. Similar to NO and eCBs, they are secreted from the postsynaptic neurons following neuronal activity and express plasticity at presynaptic side. Neurotrophins are involved in the regulation of excitatory and inhibitory transmission. Among all the neurotrophins, the most important in the modulation of Glutamate and GABA plasticity is the brain derived neurotrophic factor (BDNF). BDNF, after being released, binds and activates TRKb receptor, located on nerve terminals, spines and axons (Drake et al., 1999) triggering three main pathways of signalling cascade that are crucial for the plasticity expression: i) Ras–mitogen-activated protein kinase (MAPK) pathway, ii) the phosphatidylinositol 3-

kinase (PI3K)–Akt pathway, and iii) the PLCγ–Ca2+ pathway (Atwal et al., 2000). In the hippocampus, bath application of BDNF induces an LTP of the synapses formed between CA3 and CA1 (Kang and Schuman, 1996, 1995; Korte et al., 1998). Moreover, dendritic BDNF application facilitates LTP induced by weak burst synaptic stimulation in dentate granule cells through a postsynaptic mechanism (Kovalchuk et al., 2002). During the development, BDNF is crucial for the strengthening of GABA currents. The calcium influx mediated by NMDA receptors in the postsynaptic neuron induces the release of BDNF that modulates the presynaptic activity (Inagaki et al., 2008; Kuczewski et al., 2008; Sivakumaran et al., 2009). In adulthood BDNF can modulate the postsynaptic plasticity acting on GABA receptors (Abidin et al., 2008; Brünig et al., 2001; Jovanovic et al., 2004; Mizoguchi et al., 2003; Tanaka et al., 1997). Interestingly BDNF is also involved in the regulation of the density of GABA terminals (Kohara et al., 2007; Marty et al., 2000) and the control of chloride homeostasis tuning the expression of KCC2 (Aguado, 2003; Wardle and Poo, 2003).

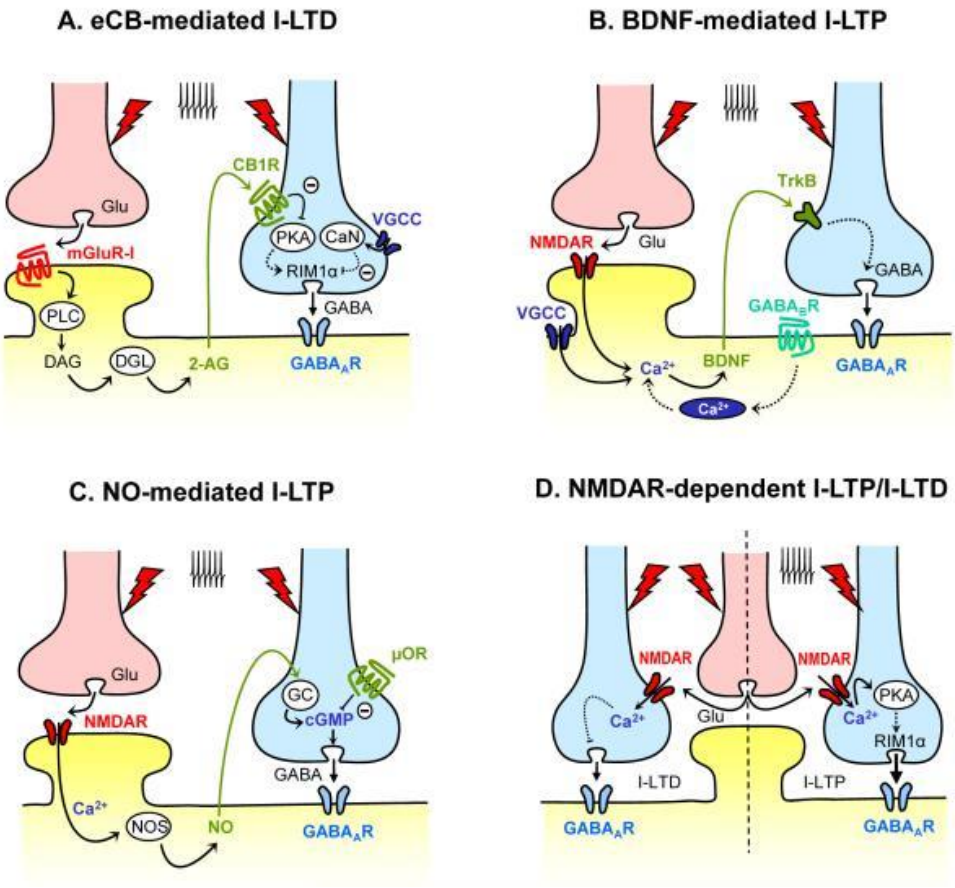

Figure: inhibitory presynaptic plasticity

(A) i-LTD mediated by eCBs. (B) iLTP mediated by BDNF. (C) iLTP mediated by NO. (D) NMDAR-dependent plasticity.

(Castillo et al., 2011)

Postsynaptic plasticity:

Excitatory postsynaptic plasticity:

Synaptic plasticity has been intensely investigated in Schaffer collaterals, e.g. at synapses formed by CA3 pyramidal neurons onto CA1 pyramidal neurons of the hippocampus. These synapses that are believed to play a fundamental role in the mnemonic process were found to be extremely plastic. In particular, depending on the stimulation delivered, Schaffer collateral synapses can be either potentiated or depressed. In particular, theta burst stimulations (short bursts at high-frequency, 100Hz delivered at the theta rhythm (5 to 7 HZ)) are able to induce long term potentiation (LTP). On the contrary, the induction of long term depression (LTD) is observed after low frequency stimulations (LFS) at 1Hz. This archetypal form of LTP involves the activation of NMDA receptor and, the coincident activation of the pre and post synaptic neuron (Hebbian plasticity) to remove the NMDA receptors from magnesium block thus leading to an influx of calcium in the postsynaptic membrane. Calcium entry triggers the activation of the CaMKII, leading to an increase AMPA receptors number induced by the modulation of the AMPA receptors binding with scaffold proteins at excitatory synapses. Indeed, following high frequency stimulations, new AMPA receptors are inserted in the synaptic area promoting an increase in the postsynaptic signals and the LTP. In contrast, following the low frequency stimulation, the activation of the calcineurin induces a dephosphorylation of the AMPA receptors at the synapse, promoting an endocytosis and leading to an LTD (Lee and Kirkwood, 2011).

Inhibitory postsynaptic plasticity:

As mentioned above several studies have demonstrated that inhibitory synapses express postsynaptic plasticity. As for its excitatory counterpart, the most consistent forms of inhibitory postsynaptic plasticity rely on the modulation of GABAA receptors number expressed at postsynaptic side. It has been shown that, the phosphorylation of GABA receptors is modulated by the action of CamKII and calcineurin, activated by defined intracellular calcium concentration. In the 5 layer of the cortex, the induction of a high frequency stimulation on the pyramidal neuron is able to potentiate the perisomatic inhibition through the calcium influx mediated by the activation of R-type VGCC. Interestingly, the induction of the same protocol on a hyperpolarized membrane (anti-

hebbian plasticity) triggers the activation of the L-type VGCC with a weakening of the synaptic strength, showing an opposite result. Both the effects can be easily prevented by adding botulinum toxin that interferes with the constitutive GABAA receptor recycling and trafficking (Chiu et al., 2019; Kurotani et al., 2008). In another region of the brain, the cerebellum, one of the first discovered form of postsynaptic iLTP, referred to as rebound potentiation, involves the depolarization of the Purkinje cells mediated by excitatory inputs coming from climbing fibers (Kano et al., 1992). The depolarization of the postsynaptic neuron leads to the activation of the CaMKII that phosphorylate the β2 subunit of the GABA receptors, favouring its binding with the scaffold protein GABARAP (Kawaguchi and Hirano, 2007). This protein plays a crucial role in the trafficking of GABAA receptors thus favouring receptor exocytosis and expression in the postsynaptic membrane. Moreover GABARAP seems to be involved in the modulation of the activity of the receptors, changing its kinetics (Chen and Olsen, 2007; Chen et al., 2000; Kittler and Moss, 2001; Kneussel, 2002; Kneussel et al., 2000; Leil et al., 2004; Lüscher and Keller, 2004; Moss and Smart, 2001; Nymann-Andersen et al., 2002). Another type of postsynaptic iLTP was found and described in hippocampus circuitry and involved the increasing expression of the main inhibitory scaffold protein gephyrin. In particular, in the CA1 pyramidal neuron the application of a chemical protocol (consist in NMDA and CNQX) is able to induce an increase in GABAaR and gephyrin at the level of the synapse, through the action of the CamKII (Marsden et al., 2007). Interestingly the induction of the same protocol promotes also the endocytosis of the AMPA receptor mediated by the calcineurin, and the depression of excitatory transmission (Mulkey et al., 1994a).

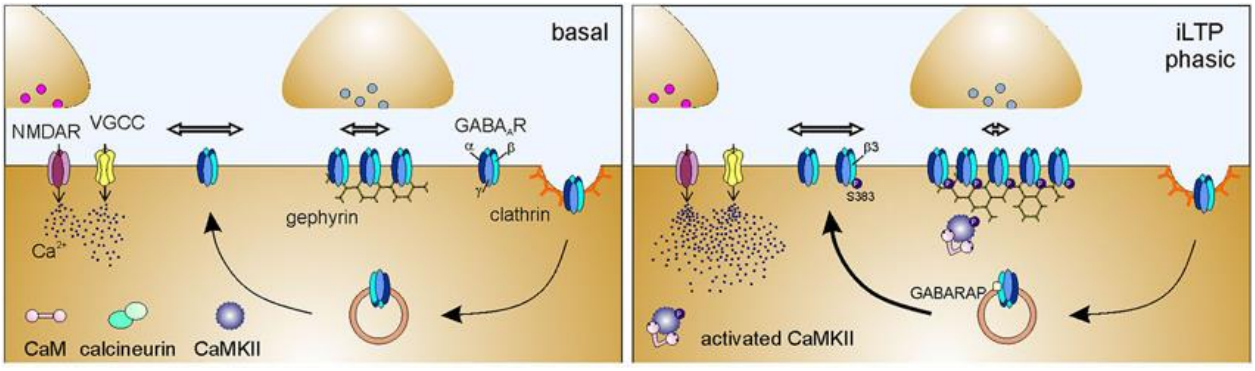

Figure: inhibitory postsynaptic plasticity

(Petrini et al., 2014)

Variation in ionic concentration:

Variations in inhibitory synaptic strength can also occur through the modulation of ionic concentration across the membrane (ionic plasticity). This form of plasticity is important at inhibitory synapses because the equilibrium potential of the chloride can be very close to the resting membrane potential so that small variations in the chloride concentration can strongly impact on the amplitude of the inhibitory synaptic signals. Several studies show that chloride concentration can be modulated by the neuronal activity through the expression of specific chloride transporters, (Fiumelli and Woodin, 2007; Payne et al., 2003). In particular, in mature hippocampal neurons, coincident pre and post synaptic activity can reduce GABAergic currents due to the reduced chloride gradient caused by the reduced activity of the KCC2 cotransporter (Woodin et al., 2003). Interestingly, since in early developmental stages the Nernst potential for chloride is depolarizing with respect to the resting membrane potential , coincident pre and post synaptic activity produced an opposite effect in immature neurons (Balena and Woodin, 2008). This was due to the reduced activity of NKCC1 that determined the hyperpolarization of the chloride equilibrium potential with consequent increase of GABAergic inhibition.

Spike timing dependent plasticity (STDP):

Spike timing dependent plasticity (STDP) is a type of postsynaptic plasticity that can be observed both at excitatory and inhibitory synapses. In STDP, the delay between the firing of the presynaptic and postsynaptic neuron can lead to either synaptic potentiation or the depression (Dan and Poo, 2006; Magee and Johnston, 1997; Markram et al., 1997). STDP can be considered an “extension” of the Hebbian coincidence and has been described in several region of the brain. For example, in pyramidal neurons of the neocortex (layer 5), a repetitive stimulation pre and post with a delay of 13 ms was able to induce a potentiation of excitatory currents. Such LTP required the activation of NMDA receptors with the consequent accumulation of calcium in the spine that triggered an actin-polymeralization dependent shrinkage of the neck and the diffusion of GluR1 receptors from the neck to the spine head, increasing the number of synaptic receptors. In contrast, if the post synaptic neuron is activated before the presynaptic one, the excitatory transmission was depressed, showing an LTD, not accompanied with changes in the morphology of the spine (Tazerart et al., 2020). When the presynaptic neuron is activated before the post, a higher influx of calcium is observed respect

to the opposite condition, in line with the model by which the preferential rise of the LTP respect to the LTD is dependent by the amount of calcium inflow. The first demonstration of GABAergic plasticity relies on the precise timing of pre and postsynaptic neuron activity was described in Woodin et al., (2003) where, in the hippocampus, the coincident activation within 20 ms led to the iLTD. As described above in the ionic plasticity paragraph, they showed that the calcium influx in the postsynaptic neuron through the L-type VGCC promoted modification in the KCC2 cotransporter resulting in the KCC2 loss of activity, reduced chloride driving force and depression of inhibitory transmission (iLTD). Three years after Haas and his colleagues found in the entorhinal cortex in the synapses made by the interneuron on the principal stellate cells that the rise of the iLTP or iLTD followed similar rules already described for excitation, by which the expression of potentiation or of the depression is dependent by the timing of activation of the presynaptic neuron respect to the postsynaptic. This form of STDP requires calcium influx mediated by the activation of L-type VGCC (Haas et al., 2006).

Plasticity mediated by astrocytes:

Astrocytes are “third rulers” that play an important role in both excitatory and inhibitory synaptic plasticity. Several studies, indeed, show that astrocytes actively modulate the induction of both LTP and LTD. In the hippocampus, the activation of a pyramidal cell in CA1 followed by the stimulation of the Shaffer collaterals was able to induce LTD in slices obtained from mice between P13 and P21. The generation of the LTD depends on the activation of the pathway that induces the synthesis of NO in the postsynaptic neuron and the decrease in the release of neurotransmitter from the presynaptic one. Interestingly, the application of the same protocol in the slices obtained from mice P22-30 did not induce any effect while in slices P30-45 was able to revert the plasticity, inducing LTP. Such inversion of plasticity is promoted by the action of the astrocytes. In fact, the production of NO triggers the release of adenosine and glutamate from the astrocytes that activate respectively the A1R and mGluR receptors on the presynaptic neuron, increasing the release of glutamate (Falcón-Moya et al., 2020). Moreover, astrocytes are also able to modulate inhibitory plasticity. For instance, the release of GABA and the following GABA binding to GABA receptors on the astrocytes, activates a signalling cascade that induce the release of glutamate in the intersynaptic space. The glutamate, acting on the presynaptic neuron, can modulate the strength of the transmission of the excitatory or inhibitory signal (Kang et al., 1998). Astrocytes are demonstrated being involve in excitatory and inhibitory synaptic plasticity and further studies could highlight an active role also in the interplay between the two plasticities, coordinating them in a precise manner.

Extracellular matrix role in synaptic plasticity:

Several studies have pointed at the extracellular matrix (ECM) as an important player in synaptic plasticity. ECM is a network of molecules secreted from neurons and glial cells. This component has several functions including support to neurons, separation between and inside different brain areas and facilitation of the existing communications between cells. For example in the CA1 region of the hippocampus the ECM molecule reelin contributes to the induction of excitatory synaptic plasticity. In particular, activation of Reelin's receptors, the very low density lipoprotein receptors (VLDLR) and the apolipoprotein E receptors type 2 (APOER2) trigger a signalling cascade leading to the phosphorylation of GluN1 subunits of NMDA receptors promote insertion of AMPA receptors at synapses the consequent potentiation of excitatory transmission (Beffert et al., 2005; Qiu et al., 2006; Weeber et al., 2002). Another important family of ECM molecules, the metalloprotease (MMP), are heavily involved in synaptic plasticity. In the hippocampus, the presynaptic activation of MMP9 is sufficient for the induction of spine enlargement and of synaptic potentiation (Wang et al., 2008). Moreover, MMP9 is involved in the maintenance of the NMDA-dependent LTP and in the NMDA lateral diffusion (Gorkiewicz et al., 2010). MMP have been also recently demonstrated to modulate crucial inhibitory plasticity: MMP 3 is fundamental for the induction of postsynaptic iLTP with the increase of IPSCs amplitude, the enlargement of gephyrin clusters and the decrease of the lateral diffusion of GABA receptors (Wiera et al., 2020). Synaptic plasticity is also modulated by the action of a third group of component of the ECM, the chondroitin sulphate proteoglycans (CSPGs), responsible of the inhibition of the axon's sprouting. The degradation of the CSPGs causes a restore in the ocular dominance plasticity, suggesting their involvement in the stabilization of the synapses and the "freezing" of the network (Pizzorusso et al., 2002). Hence, molecules of the ECM play an important role in the induction and maintenance of synaptic plasticity and, since they are required in both excitatory and inhibitory plasticity, they may represent as a possible player in the coordination of activity-dependent changes at glutamatergic and GABAergic synapses.

Interplay between excitatory and inhibitory synaptic plasticity:

So far, I have analysed different aspects of both excitatory and inhibitory synaptic plasticity assuming that they are two independent phenomena. With the exception of homeostatic plasticity in which excitation and inhibition are coordinated to maintain the level of neuronal excitability, the interplay between glutamatergic and GABAergic synaptic plasticity has been poorly studied. However since the neuronal spiking output depends on the integration of glutamatergic and GABAergic synapses it is vital to understand which are the mechanisms involved in reciprocal modulation of excitatory and inhibitory synaptic plasticity. In this concern, it has to be stressed that several molecular players involved in the excitatory plasticity are also acting at inhibitory synapses, and, often glutamatergic and GABAergic synapses are in close spatial proximity in proximal dendrites, thus creating the opportunity for efficient postsynaptic heterosynaptic interaction. It has been clearly shown that CaMKII is involved in the induction of postsynaptic excitatory LTP (Nicoll, 2017): nevertheless CaMKII is also necessary for some forms of postsynaptic inhibitory iLTP (Chiu et al., 2018; Flores et al., 2015; He et al., 2015a; Kano et al., 1996; Marsden et al., 2007; Petrini et al., 2014). Moreover, inhibitory depression requires the activity of calcineurin (Bannai et al., 2009, 2015; Muir et al., 2010), a phosphatase that was observed involved also in LTD (Mulkey et al., 1994b; Zeng et al., 2001). During inhibitory (Bannai et al., 2009; Chiu et al., 2018; He et al., 2015a; Kurotani et al., 2008; Muir et al., 2010; Nusser et al., 1998; Petrini et al., 2014) and excitatory plasticity (Diering and Huganir, 2018), receptors are continuously translocated from synaptic and extrasynaptic compartments, quickly modulating the postsynaptic response. For instance, in CA1 pyramidal neurons, the relocation of extrasynaptic α5-GABAa receptors towards inhibitory synapses after the induction of excitatory LTP is crucial to sustain learned associations. The authors demonstrated that the higher expression of α5-GABAa receptors at the inhibitory synapses prevents excitatory LTD and the induction of further LTP, preventing behavioural flexibility (Davenport et al., 2021).

The preservation of the correct E/I balance is crucial to maintain the functional stability of the network (Higley and Contreras, 2006; Isaacson and Scanziani, 2011). The issue of the interplay between glutamatergic and GABAergic synapses could also be important for pathology, since the alteration of the correct balance between excitation and inhibition has been shown to be involved in the physiopathology of neurological disorders such as autism (Hussman, 2001; Lee et al., 2017; Rubenstein and Merzenich, 2003a; Zorrilla de San Martin et al., 2018), epilepsy (Bernard, 2012; Bozzi

et al., 2018; Treiman, 2001) and schizophrenia (Benes, 2001, 1991; Marín, 2012). However a transient loss of the E/I balance can be important for the sensory processing (Froemke et al., 2007), since a restricted period of disinhibition may act as a synaptic correlate of heightened attentiveness for novel or meaningful stimuli and a synaptic trace for sensory information of increased significance (Hromádka and Zador, 2007; Thompson, 2005; Weinberger, 2004). On the other hand, a transient potentiation of the inhibitory transmission is crucial to control the temporal precision of spike generation at the level of the dendrites, by modulating the time window of synaptic integration of the excitatory inputs (Lourenço et al., 2014, 2020b). For example, postsynaptic activity of pyramidal neurons in layer 5 is able to alter the E/I balance by potentiating the feedforward inhibition mediated by parvalbumin interneurons recruited by pyramidal neurons of layer 2/3 (Lourenço et al., 2020a).

Distinct interneurons are modulated in different manners:

We described various stimulations or physiological activities able to induce different type of plasticity at excitation and inhibition. The same protocol can affect inhibition or excitation or both, inducing potentiation or depression. But, is it possible that a stimulation induces opposite or different plasticity at different inhibitory synapses? How a particular physiological activity can influence in a different manner two different inhibitory synapses on the same neuron? In the human brain there are different classes of interneurons that differ for many features as morphology, activity, synapses composition and location, but also in the induction of plasticity. In the cerebellum was discovered that a depolarization of a Purkinje cell potentiated the strength of somato-dendritic basket cell synapses without affecting distal dendritic stellate cell synapses (He et al., 2015). The β2-subunit-containing GABAA receptors are predominantly express in basket cells and are crucial to allow this form of plasticity, favouring the expression of potentiation. Moreover, in the neocortex the stimulation of NMDA receptors with a chemical protocol was able to potentiate the distal inhibitory synapses formed by somatostatin interneurons without affecting the transmission of perisomatic synapses of parvalbumin interneurons (Chiu et al., 2018). In this example, the potentiation occurs in distal synapses while in the previous one only somato-dendritic synapses were affected. This phenomenon of specific plasticity was described also in the hippocampus. In particular, during a physiological activity pattern, the currents mediated by the activation of somatostatin interneuron were potentiated while transmission mediated by PV interneurons was depressed (Udakis et al., 2020). With these works we show that, under specific condition, the synapses located in different part of the neurons can be differently influenced, highlighting how is crucial the exact localization on the dendritic tree. In particular, when an important signal is delivered to the apical part of the neuron, the inhibitory counterparts is depressed in the region, while is potentiated in the other areas of the neuron to silence other excitatory signals that can compete.

METHODS

Animals:

All the experiments were carried out in accordance with the laws of Italian Ministry of Health and the guidelines established by the European Communities Council (Directive 2010/63/EU, 2010). Parvalbumin-tdTomato (PV-tdTomato) mice were obtained at the IIT animal facility by breeding Ai9 mice with PVCRE mice. Ai9 (B6.Cg-*Gt(ROSA)26Sortm9(CAGtdTomato) Hze*/J - Jackson Laboratory, USA) mice carrying a *loxP*-flanked STOP cassette, that prevents the transcription of a CAG promoter-driven red fluorescent protein variant (tdTomato) were used as a Cre reporter strain. PVCRE (B6;129P2-Pvalbtm1(cre)Arbr/J - Jackson Laboratory, USA) mice express the Cre recombinase in Parvalbumin-expressing interneurons without disrupting the endogenous Parvalbumin locus (Pvalb) expression. The resulting offspring PV-td tomato has the STOP cassette removed in Parvalbumin-potitive interneurons and the consequent expression of tdTomato.

Primary neuronal cultures:

Cultures of hippocampal neurons were prepared from P1-P3 Parvalbumin-tdTomato mice of either sex using a previously published protocol (de Luca et al., 2017) modified from (Baudouin et al., 2012). Briefly, hippocampi were dissected, quickly sliced and digested with trypsin in the presence of DNAase, mechanically triturated, centrifuged at 80g and re-suspended. Neurons were plated at a density of 90 x 10^3 cells/ml on poly-D-lysine (0.1 µg/ml) pre-coated coverslips. Cultures were kept in serum-free Neurobasal-A medium (Invitrogen, Italy) supplemented with Glutamax (Invitrogen, Italy) 1%, B-27 (Invitrogen, Italy) 2% and Gentamycin 5 µg/ml at 37°C in 5% CO2 up to 30 days in vitro (DIV). During this period, half of the medium was changed weekly. Experiments were conducted at DIV 15-27.

Plasmid constructs:

Enhanced GFP (eGFP) was expressed from the pEGFP-N1 (Clontech). Homer1c-DsRed and Homer1c-GFP plasmids encoding for Homer1c fused with DsRed and GFP at the N terminus, respectively were kindly provided by Dr. D. Choquet (Petrini et al., 2009). EGFP-gephyrin was a gift from Prof. E. Cherubini. FingR-gephyrin-GFP (received from Dr C. Duarte) was expressed from

pCAG_GPHN.FingR-eGFP-CCR5TC, a plasmid encoding for FingRs (Fibronectin intrabodies generated with mRNA display), that bind endogenous gephyrin with high affinity and allow the visualization of gephyrin clusters using GFP as a reporter (Gross et al., 2013). Gephyrin-D269-GFP was kindly donated by Dott. G. Schwarz. GABAA receptor α1 subunit carrying the Hemagglutinin (HA) tag between the IV and V amino acid of the mature protein has been described previously (de Luca et al., 2017).

Transfection and synapse visualization:

Neurons were transfected with either using Effectene (*Qiagen*, Germany) at 6-7 days in vitro (DIV) or Lipofectamine 2000 (Thermofisher) 24/72 hours before the experiments, following the companies' protocols. All experiments were performed from 14 DIV to 21 DIV. In most experiments, excitatory and inhibitory synapses were visualized by transfecting Homer1c-DsRed and gephyrin-EGFP, respectively. GABAergic synapses were also identified by live immunolabelling of the presynaptic marker vGAT using the anti-vGAT-Oyster550 antibody (Synaptic Systems, Germany) which is directed against the luminal part of the protein, diluted in culture medium and incubated for 30 min at 37°C.

Antibodies and drugs:

Anti-vGAT-Oyster 550 antibody was purchased from Synaptic System (Goettingen, Germany). Anti-HA antibody was from Roche (Milan, Italy). BAPTA (1,2-bis(o-aminophenoxy)ethane-N,N,N',N'-tetraacetic acid), L-NAME (L-NG-Nitroarginine methyl ester), Nifedipine (1,4-Dihydro-2,6-dimethyl-4-(2-nitrophenyl)-3,5-pyridinedicarboxylic acid dimethylester),Bicuculline and Cyclosporin A were purchased from Sigma (Milan, Italy). KN-93 and KN-92 were acquired from Millipore Merck (Darmstadt, Germany). APV (D-(-)-2-Amino-5-phosphonopentanoic acid), CNQX (6-Cyano-7-nitroquinoxaline-2,3-dione), ω-conotoxin MVIIC, ω-conotoxin GVIA, DPNI-caged-GABA (1-(4-Aminobutanoyl)-4-[1,3-bis(dihydroxyphosphoryloxy)propan-2-yloxy]-7-nitroindoline) and MNI-caged-L-glutamate ((S)-α-amino-2,3-dihydro-4-methoxy-7-nitro-δ-oxo-1H-indole-1-pentanoic acid) were purchased from Tocris (Bristol, UK). Rhod-2 tripotassium salt was purchased from AAT Bioquest (Sunnyvale, CA, USA).

Electrophysiological recordings:

Inhibitory and excitatory postsynaptic currents (IPSCs and EPSCs, respectively) were recorded at room temperature in the whole-cell configuration of the patch-clamp technique. External recording solution contained (in mM): 145 NaCl, 2 KCl, 2 $CaCl_2$, 2 $MgCl_2$, 10 glucose, and 10 HEPES, pH 7.4. Patch pipettes, pulled from borosilicate glass capillaries (Warner Instruments, LLC, Hamden, USA) had a 4 to 5 MΩ resistance when filled with intracellular solution. In all experiments with the exception of paired-patch electrophysiological recordings, the intracellular solution contained (in mM): 10 KGluconate, 125 KCl, 1 EGTA, 10 HEPES, 5 Sucrose, 4 MgATP (300mOsm and pH 7.2 with KOH). Paired-patch recordings were performed with an intracellular solution containing (in mM): 130 KGluconate, 20 KCl, 1 EGTA, 10 HEPES, 5 Sucrose, 4 MgATP (300mOsm and pH 7.2 with KOH). In a subset of paired-patch recordings 20 KCl was replaced with 5 KCl. Since the use of these two intracellular solutions gave comparable results, data were merged. In the paired-patch experiments using BAPTA, 1mM EGTA was replaced with 11mM BAPTA in the presence of 120 mM KGluconate. Currents were recorded using Clampex 10.0 software (Molecular Devices, Sunnyvale, CA). The stability of the patch was checked by monitoring the input resistance during the experiments to exclude cells exhibiting more than 15% changes from the analysis. Currents were sampled at 20 KHz and digitally filtered at 3 KHz using the 700B Axopatch amplifier (Molecular Devices, Sunnyvale, CA). IPSCs and EPSCs were analyzed with Clampfit 10.0 (Molecular Devices, Sunnyvale, CA).

In paired-patch experiments, a small current was injected into presynaptic neurons in the current clamp mode to keep their membrane potential close to -65 mV. Action potentials, evoked in the presynaptic neuron by injecting depolarizing current pulses (0.8-1 nA for 5-7 ms) at a frequency of 0.1 Hz, elicited IPSCs or EPSCs that were recorded from the postsynaptic neuron voltage-clamped at -65 mV. When the paired-patch involved a presynaptic PV+ interneuron and a putative pyramidal neuron, GABAergic IPSCs were pharmacologically isolated by the continuous perfusion of CNQX (10 µM) to prevent glutamatergic synaptic transmission. When the presynaptic and postsynaptic neurons were two putative pyramidal neurons, EPSCs were isolated by the continuous perfusion of Bicuculline (10 µM) to prevent GABAergic transmission. IPSCs or EPSCs were continuously acquired from 5 min before to 30 min after the delivery of the electrical

plasticity-inducing protocol (see below). IPSCs and EPSCs data were binned in 1 min intervals and normalized to the mean of the baseline amplitude. Data are expressed as normalized values after/before. In the text, we report stimulation-induced average changes in current amplitude between 25 and 30 min after the protocol and expressed as fold-change of the baseline.

Neurotransmitter Uncaging:

GABA and Glutamate were photoreleased from DPNI-GABA and MNI-glutamate after illumination by a 378 nm diode laser (Cube 378, 16 mW, Coherent Italia, Italy). MNI-glutamate (5 mM) or DPNI-GABA (1 mM) were dissolved in extracellular solution and locally applied near the synapses through a pulled glass capillary (2-4 µm tip diameter) placed at 10-30 µm in the x-axis and at 5-10 µm in the z-axis from the region of interest (ROI), using a pressure-based perfusion system (5/10 psi) (Picospritzer, Parker, USA). The laser beam was focused on the sample by means of an Olympus Apo-plan 100X oil-immersion objective (1.4 NA). A beam expander was placed in the optical path between the laser source and the objective in order to achieve a complete filling of the objective pupil, a conditions that maximizes the focusing capability of the objective, thus minimizing the spot size on the sample. The measured point spread function (PSF) had a lateral dimension of 487±55 nm (FWHM, n = 6). The laser beam was steered in the field of view by using a galvanometric mirrors-based pointing system able to illuminate specific regions of interest outlined around glutamatergic and GABAergic synapses defined by Homer1c-DsRed and gephyrin-GFP (UGA32, Rapp OptoElectronics, Hamburg, Germany). Synchronization of optical uncaging and electrophysiological recordings was controlled with the UGA32 software interfaced with the Clampex 10.0 software (Molecular Devices, Sunnyvale, CA, USA). Both MNI-glutamate and DPNI-GABA uncaging currents (uEPSCs and uIPSCs, respectively) were elicited by 500-1000 µs laser pulses with a power intensity of 80-100 µW at the exit of the objective. In double-uncaging experiments, the same uncaging settings were applied, with MNI-glutamate and DPNI-GABA loaded in two glass capillaries independently positioned in the ROIs and independently controlled by the aforementioned pressure-based perfusion system. The time course of uncaging current amplitude changes upon plasticity induction was quantified by binning data in 10 min intervals and by normalizing them to the mean of the amplitude at baseline time points. In the text, we report

the values of stimulation-induced average changes in current amplitude at 27 min after the protocol expressed as fold-change of the baseline.

Plasticity induction:

The non-Hebbian plasticity-inducing protocol consisted of action potential (AP) trains elicited in the postsynaptic neuron at 2 Hz for 40 seconds (low frequency stimulation, LFS) in the current clamp configuration. AP was elicited by the injection of depolarizing current pulses (0.8-1 nA for 5-7 ms) (0.8-1 nA for 5-7 ms). Single spine LTP (for a Hebbian stimulation) was induced by pairing the aforementioned LFS with repetitive MNI- glutamate uncaging at 4 Hz at individual spines for 40 seconds (see Neurotransmitter Uncaging). In the text, this protocol has been referred to also as "LFS + MNI-glutamate uncaging". Experiments aimed at identifying the contribution of i) different calcium sources ii) CaMKII role, iii) nitric oxide (NO) role or calcineurin role in inhibitory plasticity were performed in the same conditions described above during the bath application of APV (50 µM), L-NAME (50 µM), KN-93 (5 µM), KN-92 (5 µM), ω-conotoxin MVIIC (2 µM), ω-conotoxin GVIA (3 µM) or Nifedipine (10 µM) as described in the text. In the experiments performed to study the involvement of the calpain or calcineurin, neurons were preincubated with the calpain inhibitor III MDL28170 (50 µM) or Cyclosporin A (20 µM) for 30 minutes before the delivery of the single spine LTP protocol, respectively.

Live-Cell Imaging:

Hippocampal primary cultures from PV-tdTomato mice were transfected with FingR-gephyrin-GFP or gephyrin-GFP. Samples were illuminated with a LED light source (Spectra X, Lumencor) through 475/34 nm and 543/22 filters (Semrock, Italy). GFP and tdTomato fluorescence was detected using a 520/35 nm and 593/40 nm filters respectively (Semrock, Italy). Neurons positive for GFP were identified, patched and stimulated with the both the non-Hebbian and Hebbian electrophysiological plasticity-inducing protocol. Neurons positive for both GFP and PV-tdTomato were excluded. Images were acquired with the digital camera Hamamatsu, EM-CCD C9100 mounted on a wide field inverted fluorescence microscope (Nikon Eclipse Ti) equipped with an oil-immersion 60X (1.4 NA) or with the digital camera EM-CCD Photometric QuantEM:512SC mounted

on a wide field inverted fluorescence microscope (Olympus IX 70) equipped with an oil immersion 100X objective (1.4 NA), for the imaging of gephyrin-GFP or FingR-gephyrin-GFP clusters, respectively. Acquisition and quantification of gephyrin clusters fluorescence were performed by using the MetaMorph 7.8 software (Molecular Devices).

Images of FingR-gephyrin-GFP or gephyrin-GFP clusters fluorescence was acquired before and after (up to 30 minutes) the application of the LFS protocol (non-Hebbian stimulation) or the LFS+MNI-glutamate uncaging protocol at individual spines (Hebbian stimulation). Focal plane was set by the operator and maintained fixed for the duration of the experiment. Gephyrin clusters that changed their focal plane after the delivery of the stimulation, were discarded from the analysis. The same light exposure time was used for the acquisition of all images and was set to avoid signal saturation. After background correction, a user-defined intensity threshold was applied to the maximal projection of each image-stack to create a binary mask for the identification of gephyrin clusters. For the analysis of gephyrin clusters, regions were created around each cluster in the binary mask after 2 pixel enlargement. As such, we aimed at avoiding the possibility of underestimating gephyrin fluorescence over time due to the changes in the cluster size/position after the delivery of the protocol. Average fluorescence intensity of each cluster was measured and normalized to control experiments in which the stimulation was omitted.

Calcium imaging:

Calcium imaging experiments were performed by using Rhod-2 (Minta et al., 1989). The rationale for the choice of this red shifted rhodamine-based calcium indicator with respect to the more commonly used green-emitting indicators was to maximize the separation between the wavelength of the laser used for neurotransmitter uncaging (378 nm) and the indicator absorption spectrum, thus minimizing the possible photobleach of the indicator. Previous studies have shown that the positive net charge of the Rhod-2 molecule favors intracellular Rhod-2 accumulation in mitochondria (Collins et al., 2001). However, this particular Rhod-2 partitioning between cytosol and mitochondria has been mainly observed with the cell permeant form of Rhod-2 (Rhod-2 AM). In contrast, the cell-impermeant form has been used to record bona fide cytosolic calcium in electrophysiological studies (Kaiser et al., 2004; Yasuda et al., 1998). In our calcium experiments

with Rhod-2, we observed that, while it efficiently dialyzed in dendrites, it showed limited diffusion into spines. However, since our goal was to study calcium dynamics in the dendritic shaft, we reasoned that such Rhod-2 feature could contribute to maintain unperturbed the spine calcium dynamics, while recording the dendritic one.

Neurons were loaded with Rhod-2 (80 µM) through the patch pipette for at least 5 minutes after reaching the whole-cell configuration to allow the diffusion of Rhod-2 in proximal dendrites. Rhod-2 fluorescence was acquired with the digital EM-CCD QuantEM:512SC camera (Photometrics) mounted on a wide field inverted fluorescence microscope (Olympus IX 70) equipped with an oil-immersion 100X objective (1.4 NA) and the MetaMorph 7.8 software (Molecular Devices). The LFS paired with MNI-glutamate uncaging was delivered at individual spines (Hebbian stimulation). During this protocol, we recorded calcium dynamics in a dendritic region centered below the photostimulated spine. Concomitantly, calcium dynamics was also recorded in another region on a different dendritic branch of the same neuron (at a similar distance from the soma) centered below a reference, non-photostimulated spine. Since the latter region was distant from the potentiated spine, it was receiving only the LFS, so hereafter it will be referred to as "LFS" conditions. The onset of calcium responses recorded in the two regions reached plateau in a few seconds after stimulation. Thus, the stimulation protocol duration was reduced to 10 seconds (instead of the full-length stimulation of 40 seconds) in order to minimize fluorescence photobleaching. Therefore, the total duration of the recording was 16 seconds (i.e., 160 frames acquired at 10 Hz) including 3 seconds before (baseline), 10 seconds during and 3 seconds after (recovery) the stimulation protocol.

For the data analysis, we considered dendritic portions of 14 µm centered below the stimulated or the reference spine - which was usually chosen at approximately 10-30 µm from the soma. Every dendritic portion was sub-divided in 7 regions of interest (ROIs) of 2 µm length, with the central one being centered below the spine. The width of each region was adjusted to the thickness of the dendrite. In each region, changes in the Rhod-2 fluorescence intensities induced by the LFS or LFS + MNI-glutamate uncaging were calculated as $\Delta F/F_0$, where ΔF is the difference between the average fluorescence intensities at plateau and that before the delivery of the protocol. F_0 is the average fluorescence intensity measured before the stimulation. In order to quantify calcium variations induced by the pairing of MNI-glutamate uncaging with respect to LFS alone, the $\Delta F/F_0$ recorded upon LFS+MNI-glutamate uncaging was normalized to that observed upon LFS (i.e.,

Figure 5D and 5E). When considering the spatial spread of calcium variations induced by the stimulating protocols (Figure 5E), the aforementioned normalization was computed for each ROI.

Quantum dot labelling and imaging:

In the experiments aimed at monitoring the modulation of GABAA receptor lateral mobility during spatially-regulated synaptic plasticity, we combined SPT experiments with electrophysiology and plasticity induction (see sections above). Non-Hebbian or Hebbian stimulation protocols were delivered to neurons expressing the HA-tagged α1 subunit of GABAA receptor along with Homer1c-DsRed and gephyrin-GFP. The surface labelling of the HA tag with QDs allowed to selectively probe the mobility of GABAARs belonging to the neuron that received the plasticity protocol.

Before the experiment, QDs 655 (Invitrogen) were diluted in PBS and pre-exposed to casein 1X (Vectorlab, Italy) for 15 min to prevent QD non-specific binding. Then, living neurons were incubated with the anti-HA antibody (Roche) 1 μg/ml in the electrophysiology external recording solution for 4 minutes and subsequently with the diluted QDs solution for 3 minutes. The final concentration of QD was 0.1 nM. Control experiments omitting the anti-HA antibody were performed to validate the antibody-specific labelling of HA-tagged GABAARs.

SPT experiments were acquired by live-cell imaging on a wide field inverted fluorescence microscope (Olympus IX 70) equipped with a diode-based illumination device (Lumencor, SpectraX Light Engine, Optoprim, Italy), an EM-CCD camera (QuantEM:512SC, Photometrics, pixel size 16 μm) and an Apo-plan oil-immersion 100X objective 1.4 NA (Olympus). For each neuron, we chose a dendritic portion where we first localized glutamatergic and GABAergic synapses by Homer1c-DsRed and gephyrin-GFP fluorescence acquired with appropriate excitation and emission filter sets (ex: 543/22, 472/30, em: 593/40, 520/35, respectively) to achieve a 2D map of the relative localization of excitatory and inhibitory synapses. QD fluorescence acquired with specific filters (ex: 435/40 and em: 655/15 filters, Semrock, Italy) was monitored over time by recording movies of 600 consecutive frames at 20 Hz using the Metamorph 7.8 software (Molecular Devices, USA). The mobility of GABAAR-QD complexes was probed in the same field of view before and 30 minutes after the induction of synaptic plasticity, either with the LFS or with LFS paired with MNI-glutamate uncaging. During the experiments, neurons were kept at 28°C (TC-324B Warner

Instrument Corporation, CT, USA) in an open chamber and continuously superfused with the recording solution at 12 ml/h.

Single particle tracking:

Tracking of QD-labelled GABAAR was performed as previously described (de Luca et al., 2017; Petrini et al., 2009). The spatial coordinates of single QDs were identified in each frame as sets of > 4 connected pixels using two-dimensional object wavelet-based localization at sub-diffraction limited resolution (~ 40 nm) using the MIA software which is based on simulated annealing algorithm. Continuous tracking between blinks was performed with an implemented version of custom software originally written in MATLAB (The Mathworks Inc., Italy) in Dr Choquet's lab, based on a QD maximal allowable displacement (4 pixels) during a maximal allowable duration of the dark period. This stringent reconnection of trajectories across QD blinking combined with the highly diluted QD labelling have been set to avoid erroneous reconnection of neighbouring QDs in the same trajectory and to provide unambiguous observations of individual receptor-QD complex trajectories. When, occasionally, two QDs were too close to be unambiguously identified, they both were discarded from the analysis. Receptor trajectories were defined as synaptic (or extrasynaptic) when their spatial coordinates matched (or not) those of clustered gephyrin-GFP fluorescence. Although the definition of the synaptic compartments was diffraction limited, the sub-wavelength resolution of the single particle detection (~40 nm) allowed accurate description of receptor mobility within such small regions. For each receptor-QD complex, the instantaneous diffusion coefficient, *D*, was calculated from the linear fits of the *n*=1–4 values of the MSD versus time plot, using a custom-made software developed by Dr Choquet (Bordeaux, France). For two-dimensional free diffusion, MSD is represented by the equation: $MSD(t)=\langle r^2\rangle=4Dt$.

MSD(t) was calculated according to the formula:

$$\langle r^2\rangle = [\Sigma_{i=1}^{N-n}(X_{i+n} - X_i)^2 + (Y_{i+n} - Y_i)^2 /(N-n)]dt$$

Only reconstructed trajectories with >80 frames were retained for the analysis. The diffusion coefficients are presented as median and IQR (i.e. the interquartile range) defined as the interval between 25–75% percentiles. The immobile fraction is defined as the relative duration of the residency of a receptor-QD complex in a given compartment with coefficient <0.0075 $\mu m^2 s^{-1}$. This

threshold represents the local minimum of the bimodal distribution of synaptic $GABA_AR$ diffusion coefficients. To achieve a more complete characterization of GABAA receptor diffusion, we also measured the percentage of time spent by each receptor-QD in a given compartment (synaptic or extrasynaptic). In the case of local iLTD, when GABAAR disperse from inhibitory synapses, leaving few receptor-QD complexes for quantification, we also calculated the percentage of receptor number found at synapses after plasticity induction as compared to before the protocol.

Quantification and statistical analysis:

For each experiment quantifications and statistical details (statistical significance and test used) can be always found in the main text and figure legends. Unless otherwise stated, normally distributed data are presented as mean ± SEM (standard error of the mean), whereas non-normally distributed data are given as medians ± IQR (inter quartile range). For electrophysiological experiments in the paired-patch configuration as well as for gephyrin live-cell imaging and intracellular calcium imaging experiments n represents the number of neurons observed. In uncaging experiments, the number of synapses (n) is reported along with the number of neurons considered. For SPT experiments, n indicates the number of receptor trajectories, followed by the number of neurons observed. Each experiment was repeated on neurons obtained from at least three different cultures. The sample size used in each experiment was based on previous electrophysiological, live-cell imaging and SPT experiments (de Luca et al., 2017; Petrini et al., 2014). Data and statistical analysis was performed using Prism 5.0 and 6.0 Software (GraphPad Prism, USA). Normally distributed data sets were compared using the two-tailed unpaired Student's t-test or, in the case of paired data, with the paired t-test. Non–Gaussian data sets were tested by two-tailed non-parametric Mann-Whitney U-test, or in the case of paired data, Wilcoxon paired test. In paired-patch experiments, statistical differences in time course data within a group was quantified by one-way ANOVA variance test followed by Turkey's multiple comparison test. For time course of uncaging and imaging experiments exhibiting only one time point at the baseline, one-way ANOVAs were performed followed by Dunnett's multiple comparisons test. When possible, RM ANOVA was used, as indicated. Statistical significance between more than two normally distributed data-sets was tested by two-way ANOVA variance

test followed by Bonferroni's multiple comparisons test. Indications of significance correspond to p-values as follows: $p<0.05$ (*), $p<0.01$ (**), $p<0.001$ (***) and non-significant (ns), i.e. $p>0.05$.

RESULTS

In previous work of our laboratory, we demonstrated that the application of NMDA and CNQX induced moderate calcium influx, and promoted the recruitment of Gephyrin and GABAA receptors at inhibitory synapses thus leading to inhibitory LTP (iLTP) (Petrini et al., 2014). Such enhancement of inhibitory synapses is mediated by the CaMKII-mediated phosphorylation of GABAA receptor. CaMKII is known also to be required in excitatory plasticity, prompting us to consider a possible interaction between excitatory and inhibitory plasticity

Electrophysiological induction of inhibitory long term potentiation (iLTP):

As first step, we identified an electrical stimulation protocol able to induce an iLTP in hippocampal neurons. To this end, we performed paired-patch recordings between a presynaptic parvalbumin positive interneuron (PV+) and a postsynaptic putative pyramidal neuron in hippocampal (Fig 1.A). The application of an action potential train at 2 Hz for 40 seconds (low frequency stimulation, LFS) to the pyramidal neuron was able to induce an increase of inhibitory post-synaptic currents (IPSCs) recorded from pyramidal neurons up to 30 minutes after stimulation (Fig 1.B). Synaptic plasticity is usually promoted by modification that may occur at presynaptic or postsynaptic level. To point out the expression site for this form of plasticity we first decided to measure the “paired pulse ratio” (PPR). The lack of changes in PPR before and after the delivery of the LFS protocol suggested a postsynaptic mechanism (Fig S.1). Previous studies have shown that inhibitory synaptic potentiation could be induced by the retrograde action of nitric oxide (NO). In order to assess whether this mechanisms could underlie the IPSCs increase observed in our experiments, inhibitory plasticity was induced in the presence L-NAME, a blocker for nitric oxide. However L-NAME failed to change the LFS-induced potentiation of GABAergic synaptic currents thus arguing against a postsynaptic expression of this form of inhibitory plasticity (Fig S.2). In order to further investigate the source of our plasticity we used a GABA uncaging approach. In this technique, the GABA molecule is covalently bound to a chemical “cage” (DPNI-GABA) making the neurotransmitter unable to bind GABAA receptors. Following illumination with UV light, GABA can be readily separated from its cage, thus inducing an “uncaging” inhibitory current. Interestingly, by using diffraction-limited UV laser spot (about 500 nm) we can elicit uncaging postsynaptic currents (IPSCs) at individual inhibitory

synapses. In particular inhibitory synapses were identified by overexpressing vGAT-DsRED, a presynaptic marker specific for inhibitory vesicles (Fig 1.C). By coupling this technique with electrophysiology, we observed an increase in IPSCs following the application of LFS protocols, thus indicating the postsynaptic origin of this form of electrically-induced iLTP (Fig 1.D). Moreover, we focused on the possible molecular mechanisms which underlie this type of plasticity. Remindful of our previous work focusing on chem-iLTP, we studied the possible role of the CaMKII. To this aim, we first administered KN-93, an inhibitor for the CaMKII. Interestingly this CaMKII blocker prevented the increase of IPSCs amplitude, while the application KN-92, an inactive analogue of KN-93, left IPSCs unchanged, thus suggesting the involvement of CaMKII in this form of LFS-induced iLTP (Fig 1.E). Since CaMKII is activated by calcium we subsequently investigated the possible sources of calcium during iLTP induction. Calcium entry through NMDA receptors (and consequent activation of CaMKII) has been often implicated in excitatory plasticity. However the application of APV, a NMDA did not prevent iLTP indicating that NMDAR activity is not required in this iLTP (Fig S.3). Another important source of calcium influx is represented by the voltage gated calcium channels (VGCC). We blocked selectively L-type VGCC using Nifedipine, and P/Q and N type VGCC, using Ω-conotoxin MVIIC, but the IPSCS enhancement by LFS was not prevented (Fig 1.F). However, the simultaneous block of all this type of VGCC could abolish iLTP, suggesting that for the induction of this plasticity is sufficient the activation of a reduce number of VGCC and the influx of mild calcium. We also tested Ω-conotoxin GVIA, a specific blocker for N-type VGCC to further discriminate between P/Q or N-type involvement, since in literature is demonstrated that P/Q type are not postsynaptically expressed on hippocampal neuron (Higley and Sabatini, 2008), confirming a blockage of the iLTP. Altogether these results suggest that the application of a LFS is able to induce an CaMKII mediated increase in IPSCs amplitude promoted by a moderate influx of calcium through L and N type VGCC.

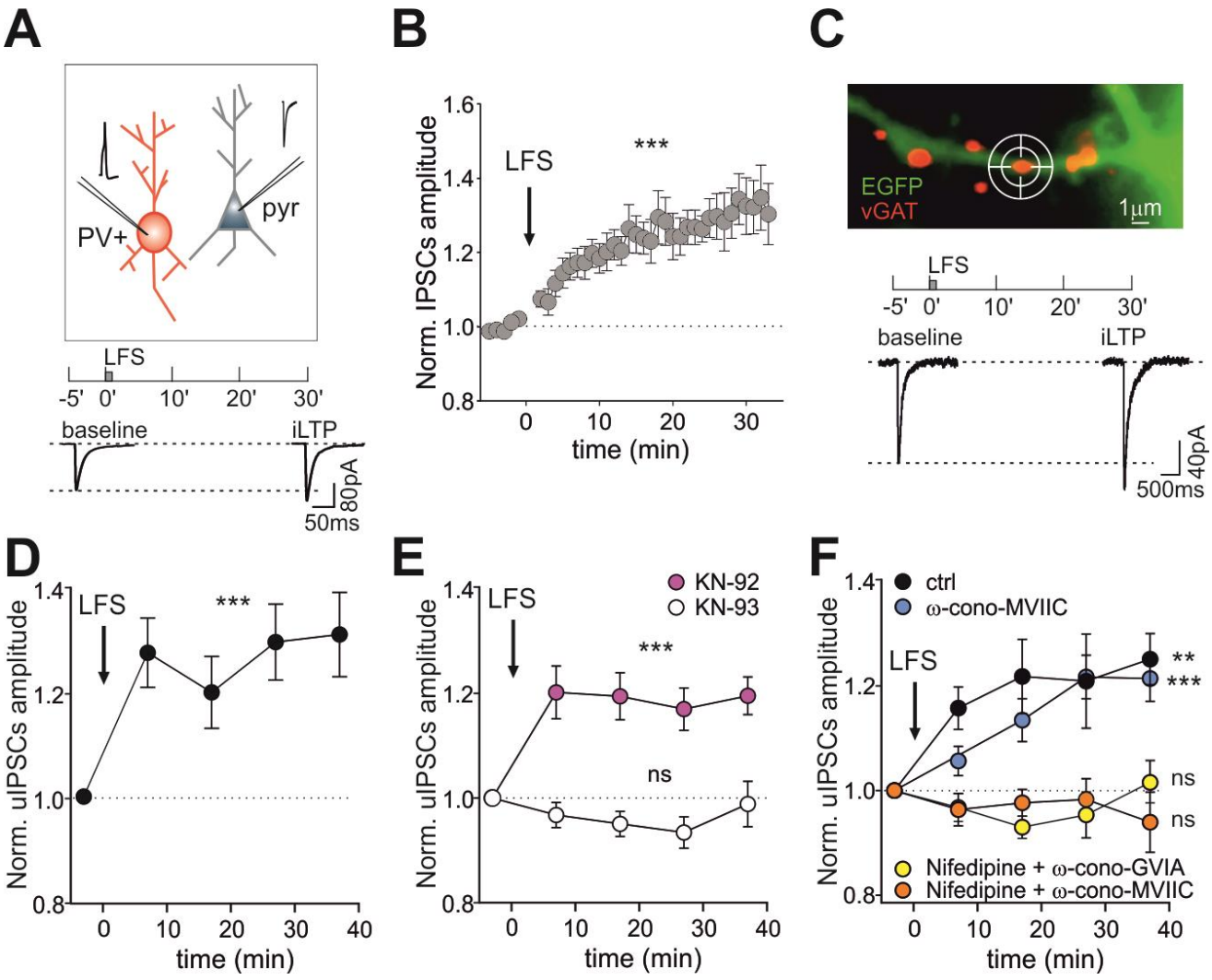

Figure 1: LFS induces iLTP

A. Top: Experimental configuration of paired patch recordings including a presynaptic parvalbumin-tdTomato positive (PV+) interneuron (red) and a postsynaptic pyramidal cell (grey). The schematic shows the low-frequency protocol (2 Hz APs train for 40 s, LFS) to induce synaptic plasticity. Bottom: Representative average traces of inhibitory postsynaptic response (IPSCs) before and 30 min after the protocol. **B.** Potentiation of IPSC amplitude after LFS (arrow; n = 24 neurons, $F_{37,708} = 5.3$, $p < 0.001$, one-way ANOVA followed by Turkey's multiple comparison test post-hoc test). **C.** Top: Identification of GABAergic synapses by live labeling of vGAT (red, see Star Methods) in an EGFP-expressing neuron (green). The "target" symbol indicates an individual GABAergic synapse where a diffraction-limited 378 nm UV laser spot was directed to uncage DPNI-GABA (see Star Methods). Scale bar, 1 µm. Timeline of the experiment (LFS, as in A). Bottom: Representative averaged traces of uncaging IPSCs (uIPSCs) before (baseline) and 30 min after LFS (iLTP). **D.** uIPSCs are potentiated after LFS (n = 23 synapses from 7 neurons; $F_{4,87} = 5.0$, $p = 0.001$; one-way ANOVA followed by Dunnett's post-test). **E.** CaMKII is required for LFS-induced iLTP. uIPSC amplitude normalized to baseline values in the presence of KN-93 (white; n = 19 synapses from 5 neurons; $F_{4,61} = 1.4$, $p = 0.24$, one-way ANOVA followed by Dunnett's post-test) and the inactive analogue KN-92 (pink; n = 26 synapses from 7 neurons; $F_{4,92} = 6.5$, $p < 0.001$; one-way ANOVA followed by Dunnett's post-test). **F.** Influence of voltage-gated calcium channels (VGCCs) on iLTP expression. Relative (after/before) uIPSC amplitude upon LFS in control conditions (black; n = 24 synapses from 9 neurons; $F_{4,78} = 5.1$, $p = 0.001$), or in the presence of the following VGCCs blockers: ω-conotoxin MVIIC for P/Q and N-type (blue; n =16 synapses from 4 neurons; $F_{4,64} = 9.1$, $p < 0.001$), or nifedipine, for L-type and

ω-conotoxin MVIIC (orange; n = 24 synapses from 6 neurons; $F_{4,80}$ = 0.3, p = 0.88) or nifedipine and ω-conotoxin GVIA for N-type (yellow; n = 17 synapses from 6 neurons; $F_{4,52}$ = 1.9, p = 0.13). All statistical comparisons were performed with one-way ANOVA followed by Dunnett's post-test. Values are expressed as mean ± SEM. **p < 0.01, ***p < 0.001, ns = not significant. See also Figure S1.

LFS induces excitatory long term depression (LTD):

In the attempt to investigate the coordinated plasticity at excitatory and inhibitory synapses we next sought to assess the effect of LFS on the excitatory transmission. To this end, we decided to use paired-patch recordings between two putative pyramidal neurons (Fig 2.A). In line with previous studies, the induction of LFS determined a decrease in the amplitude of EPSCs (LTD) that lasted up to thirty minutes (Fig 2.B). By following a similar experimental approach as in figure 1 we next used glutamate uncaging to demonstrate that this form of excitatory LTD is expressed at postsynaptic side. In this case we used MNI-glutamate uncaged at glutamatergic spines identified by overexpression of Homer1c-GFP, a proteins composing the excitatory postsynaptic density (PSD) (Fig 2.C). In line with the paired recordings data, we observed that after the delivery of the LFS protocol, uEPSC were depressed suggesting that this LTD is expressed postsynaptically (Fig 2.D). Overall, this set of experiments shows that the delivery of LFS protocols induces opposite effects at excitatory and inhibitory synaptic transmission by depressing glutamatergic synapses and enhancing the GABAergic ones. It is worth to mention that these activity-induced modifications were selectively observed at postsynaptic level.

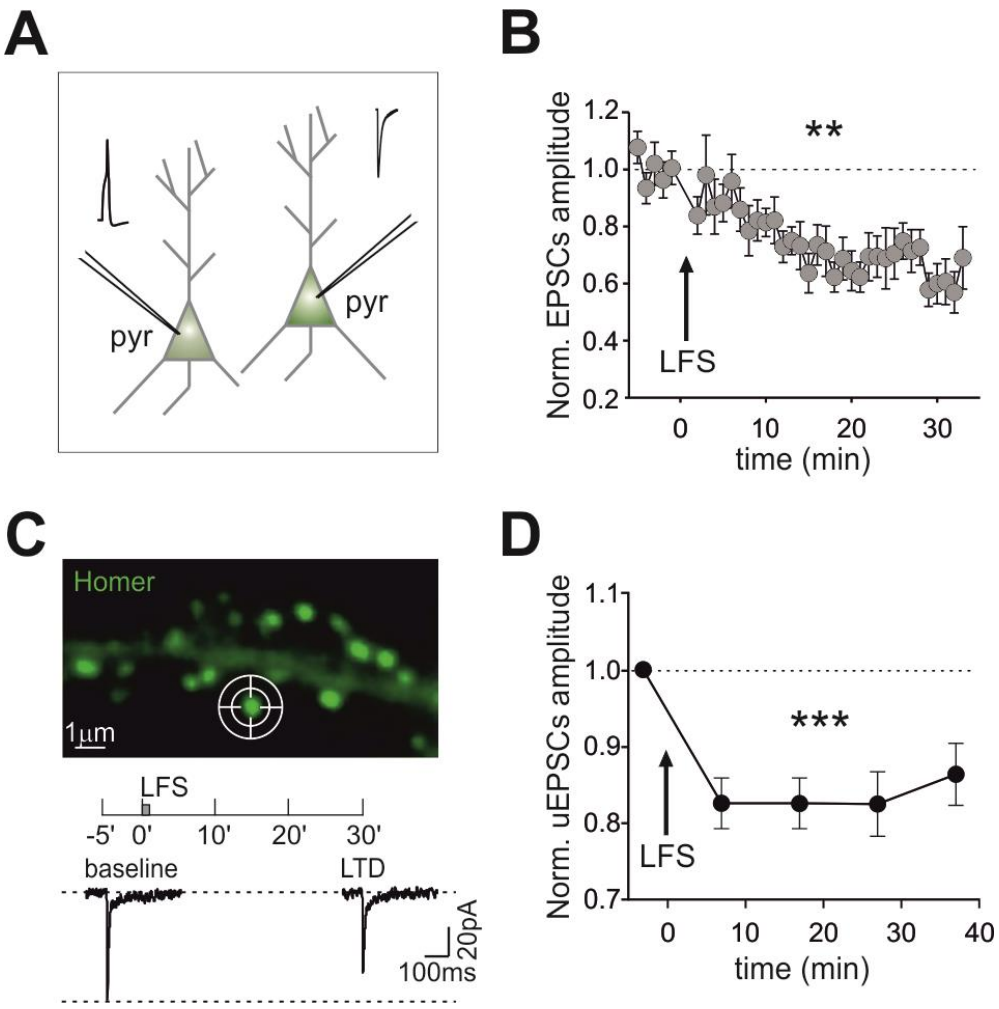

Figure 2: iLTP-inducing protocol promotes LTD at excitatory synapses

A. Experimental configuration of paired patch recordings used to probe excitatory postsynaptic currents (EPSCs) in a pyramidal neuron interconnected with another pyramidal cell. Synaptic plasticity was induced following the protocol outlined in Figure 1A. **B.** LFS induces long-term depression (LTD). Time course of normalized EPSC amplitude after LFS delivery (arrow) over 30 min (n = 15 synapses, $F_{39,438} = 2.8$, $p < 0.001$, one-way ANOVA followed by Turkey's test). **C.** Top: Identification of glutamatergic spines by Homer1c-GFP fluorescence. Scale bar, 1 μm. The target symbol indicates where a diffraction-limited 378 nm UV laser spot was directed to uncage MNI-glutamate at an individual spine. Bottom: Timeline of the experiment (as in Figure 1C) and representative average uncaging EPSC (uEPSC) traces recorded before (baseline) and at 30 minutes after LFS (LTD). **D.** Persistent reduction of uEPSC amplitude upon LFS as compared to baseline (n = 16 synapses from 11 neurons, $F_{4,68} = 6.0$, $p < 0.001$; one-way ANOVA followed by Dunnett's post-test). Values are expressed as mean ± SEM. $^{**}p < 0.01$, $^{***}p < 0.001$.

Gephyrin recruitment is involved in the iLTP :

Gephyirin is one of the main scaffold proteins at inhibitory synapses by stabilizing the inhibitory postsynaptic density (iPSD). Our previous work demonstrates that the accumulation of gephyrin at synapses played an important role in the expression of chem-iLTP. Next we studied whether changes in gephyrin synaptic expression were also involved in this form of electrically-induced iLTP. To this end, we transfected neurons with gephyrin-GFP and we studied on the variations of fluorescence intensity of gephyrin clusters before and after the application of the iLTP protocol (Fig 3.A). We decided to use overexpressed gephyrin-GFP to maintain the same experimental conditions as in previous electrophysiology experiments. We observed that, after LFS application gephyrin fluorescence clearly increased over time (Figure 3.B and 3.C) thus matching the electrophysiological data showing the increase of inhibitory synaptic current amplitude. These experiment shows that following LFS, gephyrin is recruited at inhibitory synapses concomitantly with the increase of the inhibitory synaptic currents.

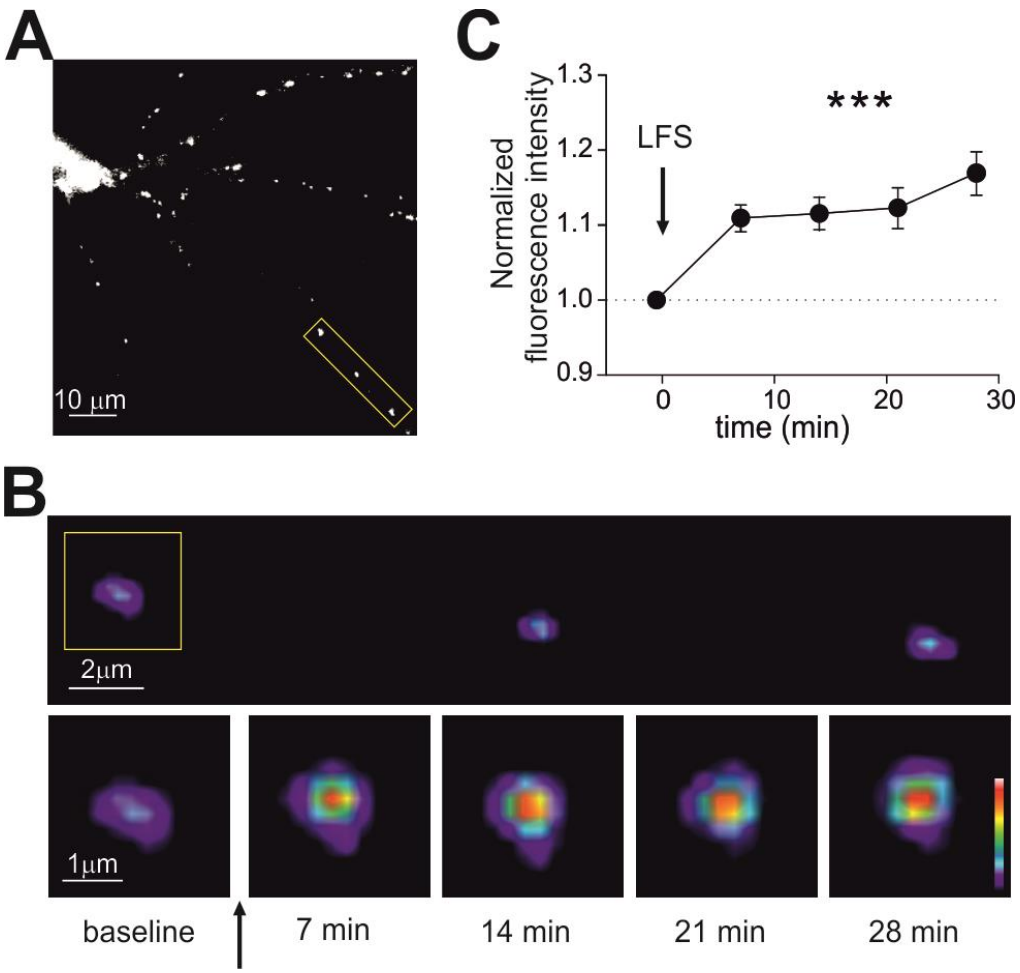

Figure 3: Enhanced gephyrin clustering during iLTP

A. Representative epifluorescence image of a neuron expressing GFP-tagged gephyrin. Scale bar, 10 μm. **B.** Top: Pseudocolor magnification of the dendritic portion framed in A. Scale bar, 2 μm. Please note that the fluorescence scale has been enhanced to visualize small clusters. Bottom: Pseudocolor images of the gephyrin cluster framed above at different time points before and after LFS (arrow). Scale bar, 1 μm. **C.** Summary of the normalized gephyrin fluorescence increase (after/before) observed upon iLTP induction with LFS (arrow; n = 13, $F_{4,48}$ = 21.5,, p < 0.001, RM one-way ANOVA followed by Dunnett's post-test). Values are expressed as mean ± SEM. ***p < 0.001.

Interaction between excitatory and inhibitory plasticity:

It has been shown that dendritic glutamatergic and GABAergic synapses are closely intercalated in the dendritic tree (Megías et al., 2001). Thus, in the attempt to investigate the interaction between synaptic excitation and inhibition, we assumed that dendritic synapses might interplay due to their spatial contiguity. To test this hypothesis, we induced LTP at an individual glutamatergic spine and we examined the changes of the synaptic strength at GABAergic synapses nearby the stimulated spine. Previous studies showed that by pairing the depolarization of a pyramidal neuron with repetitive glutamate uncaging at a single spine it is possible to induce an Hebbian-like LTP that remains confined to the stimulated spine (Harvey and Svoboda, 2007; Matsuzaki et al., 2004). In our experiments we performed a protocol of single spine LTP, by pairing MNI-glutamate uncaging with a frequency of 4 Hz for 40 seconds, together with the aforementioned protocol of LFS (Fig. 4A bottom panel). In a typical experiment layout, we identified two different spines and two different GABAergic synapses located on the dendritic portion of 10-20 μm identified by homer1C-DsRed and gephyrin-GFP overexpression, respectively (Fig. 4A upper panel). Baseline uncaging currents at glutamatergic spines and GABAergic synapses (uEPSCs and uIPSCs) were recorded by using the uncaging of MNI-glutamate and DPNI-GABA, respectively. Next, after the induction of single spine LTP as described above, we studied the changes of uEPSCs and uIPSCs amplitude at the same synaptic location (Fig. 4B). In the example reported in the figure 4A, the pairing of LFS and repetitive uncaging at spine 1, induced a clear LTP, thus confirming the efficacy of the single spine LTP protocol. We also observed that spine 3 and GABAergic synapse 4, that were relatively far from the potentiated spine, showed depression (LTD) and potentiation (iLTP), respectively. The behavior of spine 3 and GABAergic synapse 4 matched the results obtained in the previous experiments after the LFS i.e. depression of glutamatergic synapses and potentiation of the GABAergic ones. Interestingly, we observed that GABAergic synapse 2 located in the close proximity of the potentiated spine showed iLTD (Fig. 4.B). Thus these experiments suggest that the “vicinity” of a GABAergic synapses to a potentiated glutamatergic spine is able to “revert” the sign of GABAergic plasticity from iLTP to iLTD. We next decided to study the spatial rules of such plasticity interplay between excitatory and inhibitory plasticity. To this end we systematically studied the sign and the extent of GABAergic plasticity in relation to their distance from the potentiated spine and we found that GABAergic synapses located within ±3 μm from the stimulated spine were depressed while at locations >3 μm they showed iLTP (Fig 4.C). Next, we studied the role of calcium in this distance-

dependent plasticity interplay, and we observed that the application of nifedipine prevented the expression of iLTD at inhibitory synapses located near the potentiated spine, suggesting that the activation of L-type VGCC is required for this “inversion” of inhibitory plasticity (Fig 4.C blue line). In addition the “local” inhibitory iLTD was also blocked by the calpain inhibitor MDL28170 (Fig 4.C red line). Calpain is a protease that has been already implicated in GABAergic synaptic depression (Mele et al., 2016; Tyagarajan and Fritschy, 2014; Tyagarajan et al., 2011). Interestingly, gephyrin is a calpain substrate thus providing a potential mechanistic insight for the form of GABAergic iLTD we described. Overall, we demonstrate that the induction of single spine LTP determines the expression of a GABAergic iLTD that is spatially restricted to GABAergic synapses located in a range of 3 microns from the potentiated spine.

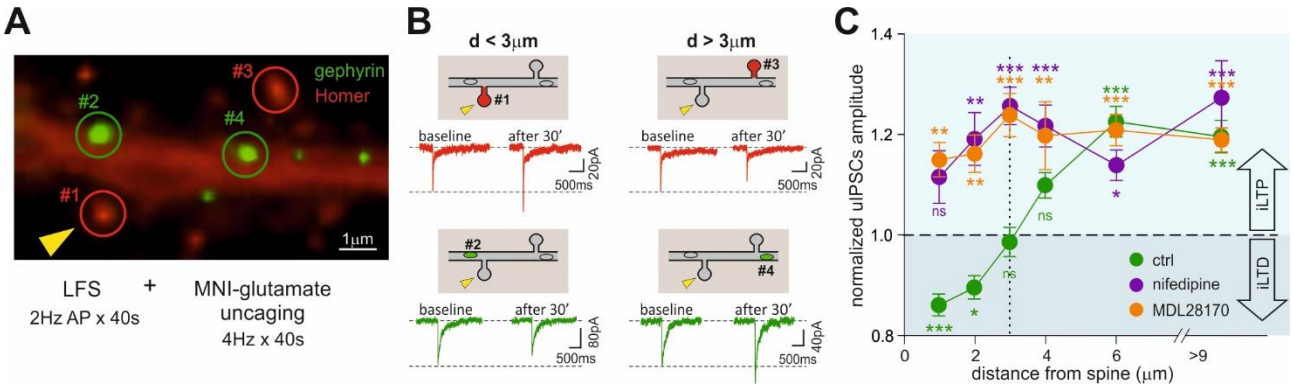

Figure 4: Plasticity interplay between potentiated spine and neighboring GABAergic synapses

A. Epifluorescence image showing a typical experimental layout. Top: Dendritic portion of a neuron expressing Homer1c-DsRed (red) to identify excitatory spines and Gephyrin-GFP (green) to identify inhibitory synapses. Scale bar, 1 µm. Excitatory and inhibitory synaptic responses were probed by uncaging MNI-glutamate at two glutamatergic spines (#1 and #3) and DPNI-GABA at two GABAergic synapses (#2 and #4), respectively. The yellow arrowhead indicates the stimulated spine (see below). Bottom: Induction of synaptic plasticity. LFS (2Hz AP train) delivered to the whole neuron through the patch pipette was paired with diffraction-limited 4 Hz MNI-glutamate uncaging (yellow arrowhead) selectively at spine #1 (LFS + MNI-glutamate uncaging). **B.** Representative average traces of uEPSCs (top, red) and uIPSCs (bottom, green) recorded from glutamatergic synapses (#1 and #3) and GABAergic synapses (#2 and #4) before (baseline) and 30 min after the induction of synaptic plasticity. The relative localization of each spine with respect to #1 (receiving the single spine LTP protocol, yellow arrowhead) is schematized above the traces. Please note that the stimulated synapse #1 displays LTP, while glutamatergic synapse #3 and GABAergic synapse #4, both located relatively far from the potentiated spine, show LTD and iLTP, respectively. Interestingly, GABAergic synapse #2, close to the potentiated spine, shows iLTD. **C.** Spatial distribution of GABAergic plasticity at inhibitory synapses located at different distances from the potentiated spine. Please note that uIPSCs at GABAergic synapses located in close proximity of the stimulated spine (d < 3 µm) were depressed, whereas those located at d > 3 µm displayed potentiation (green, for each data point n = 18-39 synapses from 20 neurons, $F_{6,603}$ = 30.6, p< 0.001, one-way ANOVA followed by Dunnett's post-test). In the presence of nifedipine, the same protocol (LFS + MNI-glutamate uncaging) does not elicit iLTD at synapses at d < 3 µm. In these conditions, all GABAergic synapses exhibit iLTP regardless of their distance from the stimulated spine (purple, for each data point n = 7-16 synapses from 7 neurons, $F_{6,68}$ = 6.6, p < 0.001, one-way ANOVA followed by Dunnett's post-test). The blockade of calpain activity with MDL28170 prevents the local iLTD (orange, for each data point n = 9-67 synapses from 24 neurons, $F_{6,223}$ = 13.0, p < 0.001, one-way ANOVA followed by Dunnett's post-test). Values are expressed as mean ± SEM.*p < 0.05, **p < 0.01, ***p < 0.001, ns = not significant. See also Figure S2.

Spatial dendritic calcium dynamics during iLTP and LTP:

As shown in previous studies, iLTP might be induced by moderate calcium entry through a CaMKII-mediated mechanisms (Chiu et al., 2018; Marsden et al., 2007, 2010; Petrini et al., 2014) while sustained calcium entry could lead to iLTD due to the activation of calcineurin or calpain (Mele et al., 2016; Niwa et al., 2012). This evidence allowed us to hypothesize that the "local" iLTD observed in the range of 3 microns from the potentiated spine could be induced by "local" high calcium influx through L-type VGCC activated during the induction of single spine LTP. To verify this hypothesis we used a calcium imaging approach to study the dendritic calcium dynamics during both LFS alone (non-Hebbian) and LFS+uncaging (Hebbian) protocols. In particular, neurons expressing homer-GFP to identify glutamatergic spines, were filled with the calcium indicator Rhod-2 through the patch pipette and the variations of fluorescence in whole dendrite and in the dendritic portion below the spine were evaluated after the delivery of the LFS or the LFS+uncaging. These experiments showed that calcium influx was significantly higher after the application of the LFS+uncaging with respect to the LFS alone (Fig. 5C). Calcium concentration was measured 5 seconds after the protocol onsets since both LFS and LFS+uncaging protocols already reached a plateau. Moreover, we studied the variation of fluorescence intensity at increasing distances from the stimulated spine (Fig 5.D). Interestingly, the calcium increase in the dendritic region of ≈ ±3 μm from the stimulated was higher in LFS+uncaging with respect to LFS (Fig. 5.E). These findings are in line with our hypothesis that higher calcium concentration in the dendritic region right below the spine, may activate a signaling vascade that leading to depression instead of a potentiation of inhibitory synapses. In our previous experiments we observed that in the presence of L-type VGCC blocker nifedipine, "local" iLTD was reverted in iLTP. Thus, in a subsequent set of calcium imaging experiments we focused on the local calcium dynamics in presence of the drug. The administration of nifedipine significantly reduces the calcium influx in the postsynaptic neuron after the single spine LTP protocol compared with the simple LFS (Fig S3). Hence, the block of L-type VGCC significantly reduces the local calcium entry in the dendritic area below the stimulated spine. These calcium dynamics support the hypothesis that in the proximity of the spine, local high calcium concentrations can locally induce iLTD instead of iLTP.

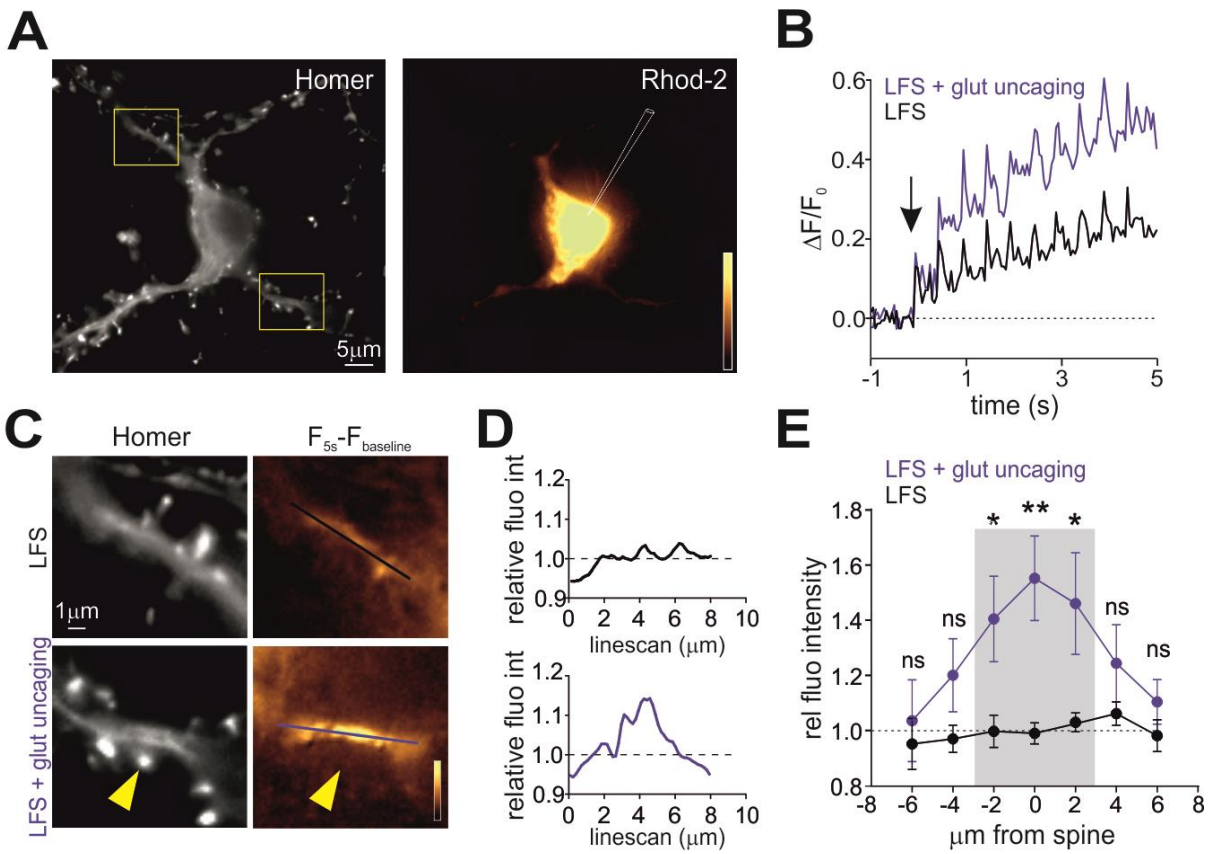

Figure 5: Spatial dynamics of dendritic calcium during iLTP and LTD

A. Representative epifluorescence image of a Homer1c-GFP expressing neuron (left) loaded with Rhod-2 through the patch pipette (gold, right). Scale bar, 5 µm. **B.** Relative Rhod-2 fluorescence intensity quantified during the LFS protocol (black) and the LFS paired with glutamate uncaging protocol (blue) in two 4 µm-long dendritic portions of the same neuron centered below a reference and stimulated spine, respectively. The arrow indicates the beginning of the protocol. **C.** Left: Magnifications of the dendritic portions framed in A, stimulated with LFS (top) or LFS paired with MNI-glutamate uncaging (bottom). The yellow arrowhead indicates the stimulated spine. Scale bar, 1 µm. Right: Gold pseudocolor representation of Rhod-2 fluorescence intensity changes at plateau (5 s) of the stimulating protocols (i.e., LFS, top and LFS paired with glutamate uncaging, bottom) with respect to baseline values (F_{5s}-$F_{baseline}$). The lines indicate the position of the linescans quantified in D. **D**. Relative fluorescence variation induced by "LFS + glut uncaging" protocol with respect to LFS alone. The fluorescence intensities quantified along the two linescans in C are normalized to the average fluorescence detected along the linescan in LFS. **E.** Changes in the relative dendritic Rhod-2 fluorescence intensity (as measured in Figure 5D) as a function of the distance from a reference or stimulated spine during the LFS (black) or the LFS+ glut uncaging (blue), respectively. The grey area indicates the range of ± 3µm from the potentiated spine where significant changes in Rhod-2 fluorescence are quantified as compared to the LFS protocol (LFS: n = 23 neurons, LFS+ glut uncaging: n = 22 neurons, $F_{1,265}$ = 22.1, $p < 0.001$, two-way ANOVA followed by Bonferroni's multiple comparison test). Statistical significance for each data point is shown. Values are expressed as mean ± SEM. *$p < 0.05$, **$p < 0.01$, ns = not significant.

Gephyrin dynamics during single spine LTP protocol:

Previous work from our laboratory showed that iLTP involves the increase of gephyrin expression at synapses. In contrast inhibitory synaptic depression is associated with the loss of synaptic gephyrin Thus, to corroborate our electrophysiology data we focused on the dynamics of gephyrin clusters intensity after the induction of single spine LTP. In these experiments we decided to label gephyrin by using finger-GFP, an intrabody-based strategy yielding the best signal to noise ratio, a fundamental requisite to visualize subtle fluorescence variation as those occurring during inhibitory synaptic plasticity. By combining quantitative imaging experiments with electrophysiology we observed that following the induction of single spine LTP, gephyrin clusters located ≈ ±3 μm from the potentiated spine were undergoing a decrease of fluorescence intensity, indicating a loss of gephyrin (Fig. 6A). In contrast, after the single inhibitory clusters located at distance > 3 μm from the potentiated spine showed higher fluorescence, in line with inhibitory iLTP (Fig 6.B and C). Importantly, the detection of the fluorescence increase after the induction of single spine LTP was also observed by overexpressing gephyrin-GFP. This indicate that the gephyrin increase associated with iLTP is not affected by the gephyrin labeling strategy. Overall, these experiments show that the dependence of the gephyrin synaptic clustering on the relative distance from the potentiated spine matches the observations made by electrophysiological experiments, thus reinforcing our paradigm that LFS alone potentiates GABAergic synapses while the potentiation of a single spine creates a region of low inhibition in the dendritic portion of ±3 μm from the potentiated spine

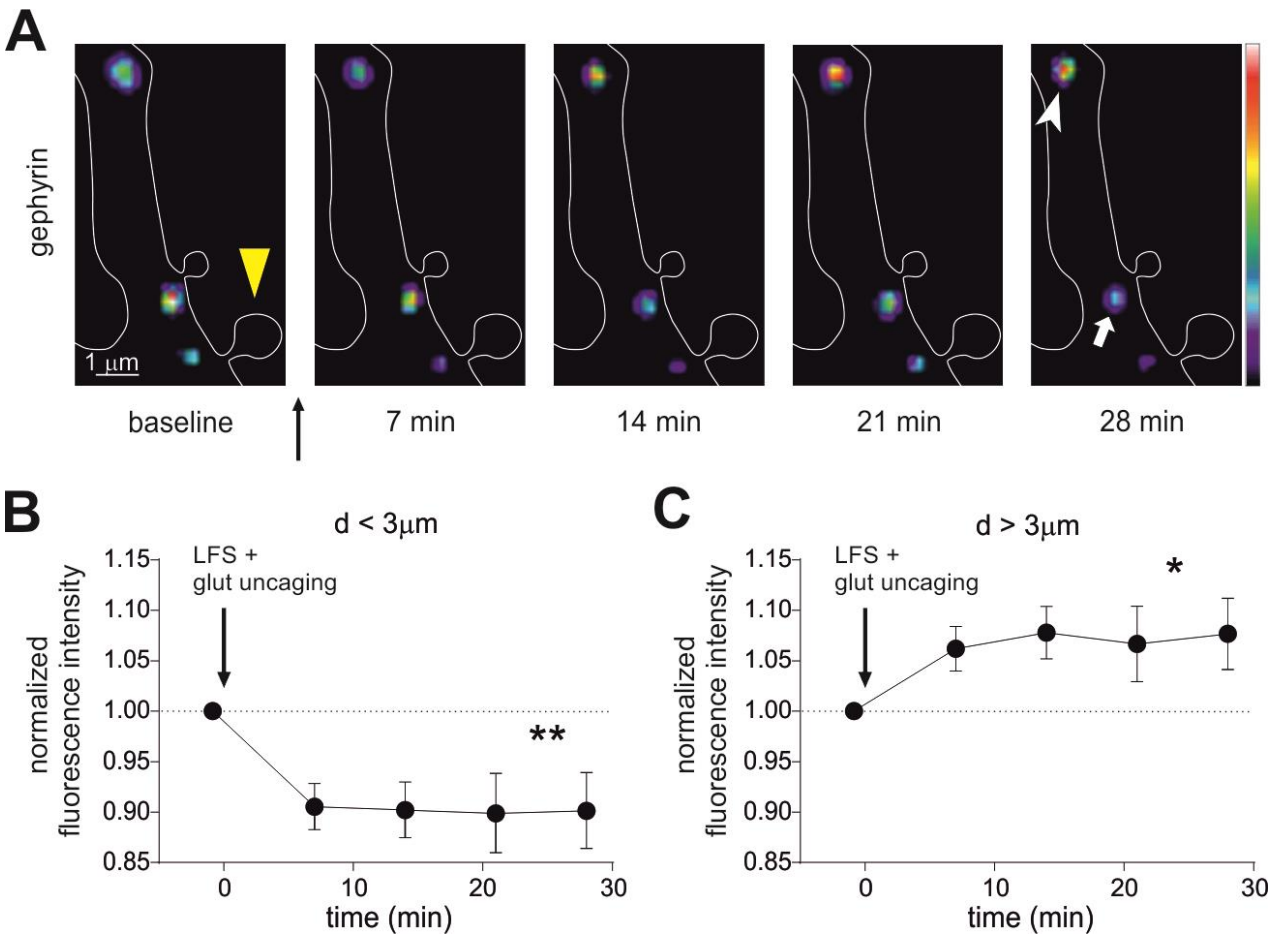

Figure 6: Gephyrin dynamics after single-spine LTP protocol

A. Representative dendritic portion of a Homer1c-DsRed expressing neuron (white outline) showing pseudocolored FingR-gephyrin fluorescent clusters at different time points before (baseline) and after the delivery of the LFS+glutamate uncaging protocol (yellow arrowhead). Clusters at distance > 3 µm (white arrowhead) from the stimulated spine (yellow arrowhead) were potentiated, whereas clusters at distance < 3 µm (white arrow) from the stimulated spine were depressed. Scale bar, 1 µm. **B.** Summary of the relative changes (after/before) in gephyrin fluorescence intensity quantified in clusters located at d < 3µm from the stimulated spine (n = 13, $F_{4,48}$ = 4.8, p=0.02, RM one-way ANOVA followed by Dunnett's post-test). **C.** Summary of the relative changes in gephyrin fluorescence intensity quantified in clusters located at d > 3µm from the stimulated spine (n = 13; $F_{4,48}$ = 2.7, p = 0.04, RM one-way ANOVA followed by Dunnett's post-test). Data are presented as mean ± SEM. *p < 0.05, **p < 0.01.

Surface dynamics of GABA receptors after induction of single spine LTP :

Postsynaptic long-term potentiation and long-term depression are associated with decreased or increased lateral mobility of postsynaptic receptors, respectively (Choquet and Triller, 2013; Petrini and Barberis, 2014). We next aimed to understand whether the opposing gephyrin modifications at increasing distances from a single spine expressing LTP is accompanied by differential surface dynamics of GABAA receptors (GABAARs). For this purpose, the lateral mobility of α1 subunit-containing GABAARs was analyzed by quantum dots-based single particle tracking (SPT). In particular, with observations before and after the expression of single-spine LTP, we monitored the mobility of synaptic receptors at GABAergic synapses located either in the dendrite at a distance of ± 3 μm from an individual potentiated glutamatergic spine or further away (> 3 μm) (Figure 7A). Interestingly, at inhibitory synapses located > 3 μm from the potentiated spine – that is, those exhibiting iLTP (Figure 4B and S2B) – GABAARs were less mobile after the single spine LTP induction protocol, as indicated by reduced paired diffusion coefficient (before = 0.013 $\mu m^2 s^{-1}$ and interquartile range (IQR) 0.008 - 0.029; after = 0.006 $\mu m^2 s^{-1}$ and IQR: 0.002 - 0.011; n = 31 trajectories from 9 neurons, $p<0.001$; Figure 7B), increased immobile fraction (before = 0.29 ± 0.07; after = 0.58 ± 0.07; n = 31, $p<0.001$; Figure 7C) and prolonged time spent at synapses (before = 36% ± 5%; after = 61% ± 6%; n=31, p=0.002; Figure 7D). We next considered GABAARs diffusing at synapses within a 3 μm range from the potentiated spine (d < 3 μm). Before the protocol, they exhibited diffusive properties comparable to GABAARs at synapses located > 3 μm from potentiated spine ($n_{d>3}$ = 31; $n_{d<3}$ = 9, p>0.05; Figure 7B-7D). After the stimulation, GABAARs at synapses close to the potentiated spine (d < 3 μm), (i.e., exhibiting iLTD in response to the single-spine LTP protocol, see Figure 4B and S2B), displayed markedly increased mobility (Figure 7A) as quantified in the diffusion coefficient (before = 0.012 $\mu m^2 s^{-1}$ and IQR: 0.007 - 0.017; after = 0.022 $\mu m^2 s^{-1}$ and IQR: 0.017 - 0.030; n = 9 trajectories from 5 neurons, p=0.04; Figure 7B) and immobile fraction (before = 0.29 ± 0.12; after = 0.04 ± 0.03; n=9, p=0.04; Figure 7C) after the stimulation. As expected, in these conditions of increased mobility, GABAARs escaped more frequently from the synaptic area, thus depleting inhibitory synapses of GABAARs during local iLTD (-61 % ± 11, n = 19; $p<0.001$; Figure 7E). As a control, we quantified the fraction of residual GABAARs at synapses within 3 μm of non-photo-stimulated spines at the end of each experiment (-6 % ± 3, n = 12; p = 0.25; Figure 7E). The negligible variation in synaptic GABAAR number in this control suggests that GABAARs selectively disperse from inhibitory synapses during local iLTD. However, the few GABAARs that remained at synapses

during iLTD spent the same time in that compartment before and after single spine LTP induction (before = 39% ± 6%; after = 34% ± 8%; n = 9, p=0.49; Figure 7D). In line with these data, following the single spine LTP protocol, the steady state of the mean square displacement vs time curve (MSD) for GABAARs at synapses far from the potentiated spine (d > 3 μm) was reduced, thus indicating higher receptor confinement (n = 19 from 8 neurons, p=0.01; Figure 7F, left). In contrast, after the delivery of the same plasticity induction protocol, GABAARs in the dendritic range of ± 3 μm from the potentiated spine were less confined, as indicated by an increased MSD steady state (n = 9 from 5 neurons, p=0.01; Figure 7F, right).

It is worth noting that the single spine LTP protocol did not change the lateral diffusion properties of extrasynaptic receptors at distances > 3 μm (Figure S4A and S4B). Likewise, matched observations of individual extra-synaptic GABAARs in the range of 3 μm (d < 3 μm) from the potentiated spine showed unchanged diffusion coefficients and immobile fractions before and after the single spine LTP protocol (Figure S4C and S4D), while the percentage of time spent at the extrasynaptic domain increased (Figure S4C right). In order to rule out that the effect of the single spine LTP protocol on GABAAR diffusion was due to UV laser illumination, but instead required MNI-glutamate uncaging, we performed a control experiment in which the same protocol was performed without puffing MNI-glutamate (i.e., LFS paired with UV illumination). Synaptic GABAARs close to the illuminated spine (d < 3 μm) showed reduced mobility (before = 0.017 $\mu m^2 s^{-1}$; IQR: 0.006 – 0.025; after = 0.005 $\mu m^2 s^{-1}$; IQR: 0.004 - 0.09; n = 7 from 4 neurons; p=0.01; Figure S4E), increased immobile fraction (before = 0.22 ± 0.13; after = 0.62 ± 0.16; n=7; p=0.03; Figure S4E) and enhanced confinement (n = 4, p<0.001; Figure S4F), similarly to GABAARs at d > 3 μm from the potentiated spine, i.e. during iLTP (compare with Figure 7B-7D). Therefore, UV illumination (without MNI-glutamate) is not sufficient to reproduce the modifications of GABAAR dynamics observed during local iLTD. Overall, these results show that following the induction of single spine LTP, the spatial dependence of dendritic lateral diffusion of GABAAR faithfully corresponds with modulation of IPSC amplitude and gephyrin synaptic clustering.

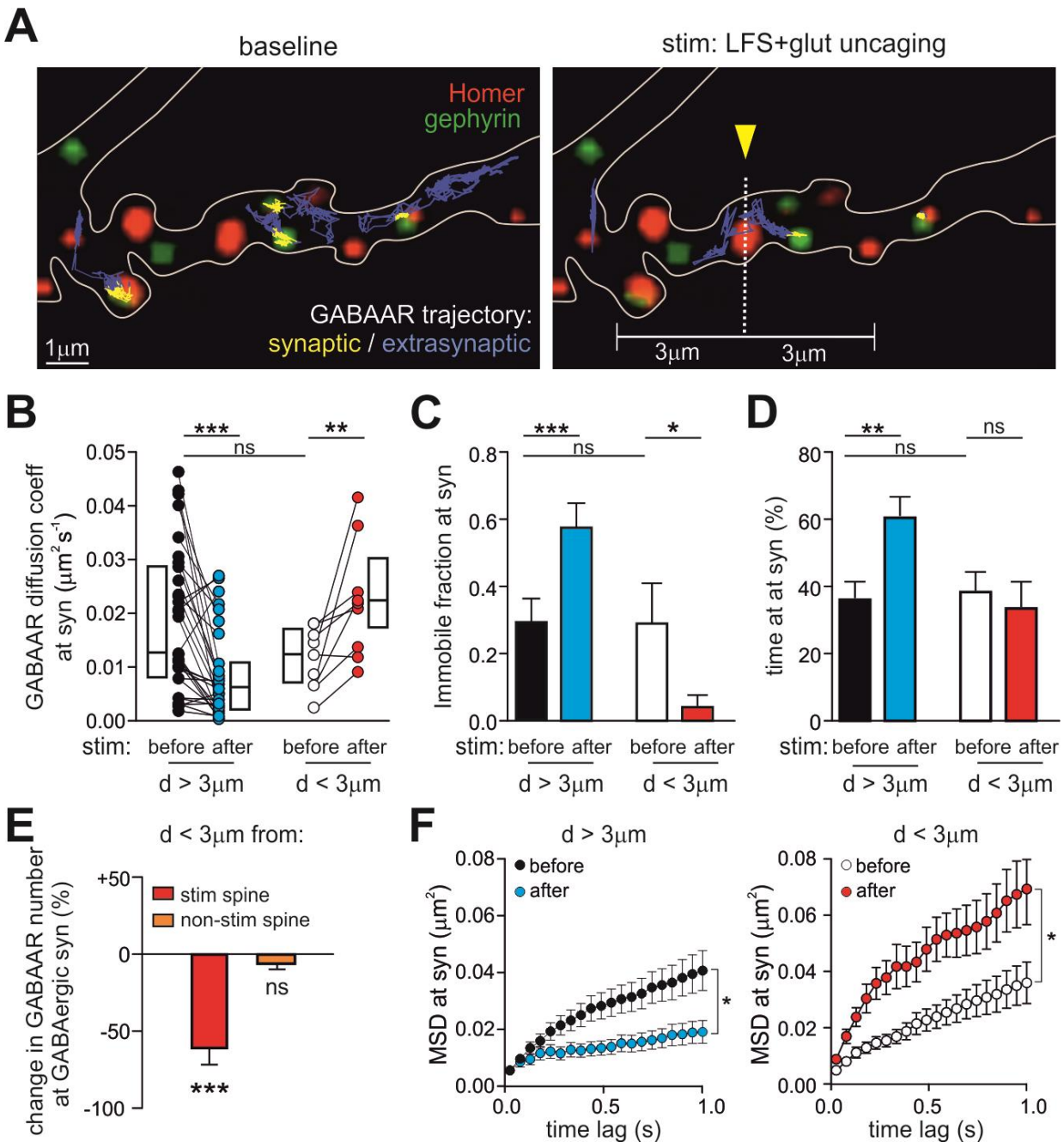

Figure 7: GABAA receptor lateral diffusion after the single-spine LTP protocol

A. Representative synaptic (yellow) and extrasynaptic (blue) trajectories of individual GABAARs diffusing on a gephyrin-GFP and Homer1c-DsRed expressing neuron, before (left) and after (right) the delivery of the LFS + MNI-glutamate uncaging protocol at the indicated spine (yellow arrowhead). Scale bar, 1 µm. **B-D.** Effect of LFS+glut uncaging on the surface mobility of GABAA receptors at synapses located at d > 3 or d < 3 µm from the potentiated spine. **B.** Paired diffusion coefficient values of synaptic GABAARs before and after the stimulating protocol (d > 3 µm: n = 31 trajectories from 9 neurons, p < 0.001, paired Wilcoxon test; d < 3 µm: n = 9 trajectories from 5 neurons, p = 0.04, paired Wilcoxon test). Comparison 'before stim" d > 3 µm vs d < 3 µm: p = 0.19, Mann-Whitney test. **C.** Immobile fraction of synaptic GABAARs before and after the stimulating protocol (d > 3 µm: n = 31 from 9 neurons, p < 0.001, paired Wilcoxon test; d < 3 µm: n = 9 from 5 neurons, p = 0.03, paired Wilcoxon test). Comparison before d > 3 µm vs d < 3 µm: p = 0.62, Mann-Whitney test. **D.** Percentage of time spent at synapses of synaptic GABAARs before and after the stimulating protocol (d > 3 µm: n = 31, p = 0.003, paired Wilcoxon test; d < 3 µm: n = 9, p = 0.50, paired Wilcoxon test. Comparison

'before stim" d > 3 µm vs d < 3 µm: p = 0.54, Mann-Whitney test. **E.** Variation in the number of synaptic GABAARs at GABAergic synapses close (d < 3 µm) to the potentiated spine (red; n = 19, p < 0.001, paired Wilcoxon test) or to a spine receiving the same protocol in the absence of MNI-glutamate (orange; n = 12, p = 0.25, paired Wilcoxon test). **F.** MSD versus time values of matched observations of individual GABAARs localized at d > 3µm (left) and d < 3µm (right) from the potentiated spine, before and after LFS+glut uncaging (d > 3 µm: n = 19 from 8 neurons, $F_{1,36}$ = 7.0, p = 0.01; d < 3 µm: n = 9 from 5 neurons, $F_{1,16}$ = 8.5, p = 0.01; RM two-way ANOVA followed by Bonferroni's multiple comparison test). Unless otherwise stated, values are expressed as mean ± SEM.*p < 0.05, **p < 0.01, ***p < 0.001, ns = not significant. See also Figure S4.

Most studies investigate synaptic modifications occurring either few milliseconds (short-term plasticity) or several minutes or hours (long term plasticity) following the plasticity induction. However, the different processes that precede the expression of long term potentiation have been less investigated. In the second part of my thesis I've been studying on the molecular mechanisms occurring in the early stages of expression of the aforementioned plasticity paradigms. In particular I focused on how early events after the induction of plasticity impact on the formation and maintenance of long-term plasticity.

iLTP is preceded by a transient depression:

In the previous section of the present thesis, we highlighted that gephyrin is recruited at inhibitory synapses after the delivery of the iLTP-inducing protocols. Interestingly, during the delivery of the same protocols, we observed opposite gephyrin dynamics. Indeed, in gephyrin-GFP transfected neurons, during a 40 second depolarization step at 0 mV, we observed a marked decrease of gephyrin fluorescence that progressively increased in the following minutes to reach the gephyrin increase (iLTP) shown in the first part of this thesis (Fig. 8A). Thus the gephyrin accumulation following iLTP is preceded by a transient gephyrin dispersal. Subsequently, we investigated the role of depolarization duration in this transient gephyrin depression and we observed that, with respect 40 second pulses, longer depolarization induced more pronounced depression while shorter depolarization resulted in lower depression (Fig. 8B). Having established that the amount of depression depends on the depolarization length we next explored the possibility that such transient gephyrin depression could impact on the subsequent gephyrin accumulation. To this end, we studied the long term effect of the same depolarization protocols and we found that the increase of the depolarization length to 80 seconds abolished the gephyrin increase (Fig. 8B). In contrast by shortening the depolarization duration to 20, 10 and 5 seconds induced a pronounced increase of the long-term accumulation of gephyrin that was maximum at 10 seconds (Fig. 8B). The further shortening of the depolarization pulse to 1 second abolished the gephyrin accumulation (Fig. 8B). These results reveal that the transient gephyrin depression is not required for the following long-term increase of gephyrin iLTP, and, at least in a specific range of pulse durations, gephyrin transient depression and the following gephyrin potentiation seem to be oppositely regulated. This also

allowed to hypothesize that this two phenomenon might be modulated by different and molecular mechanisms.

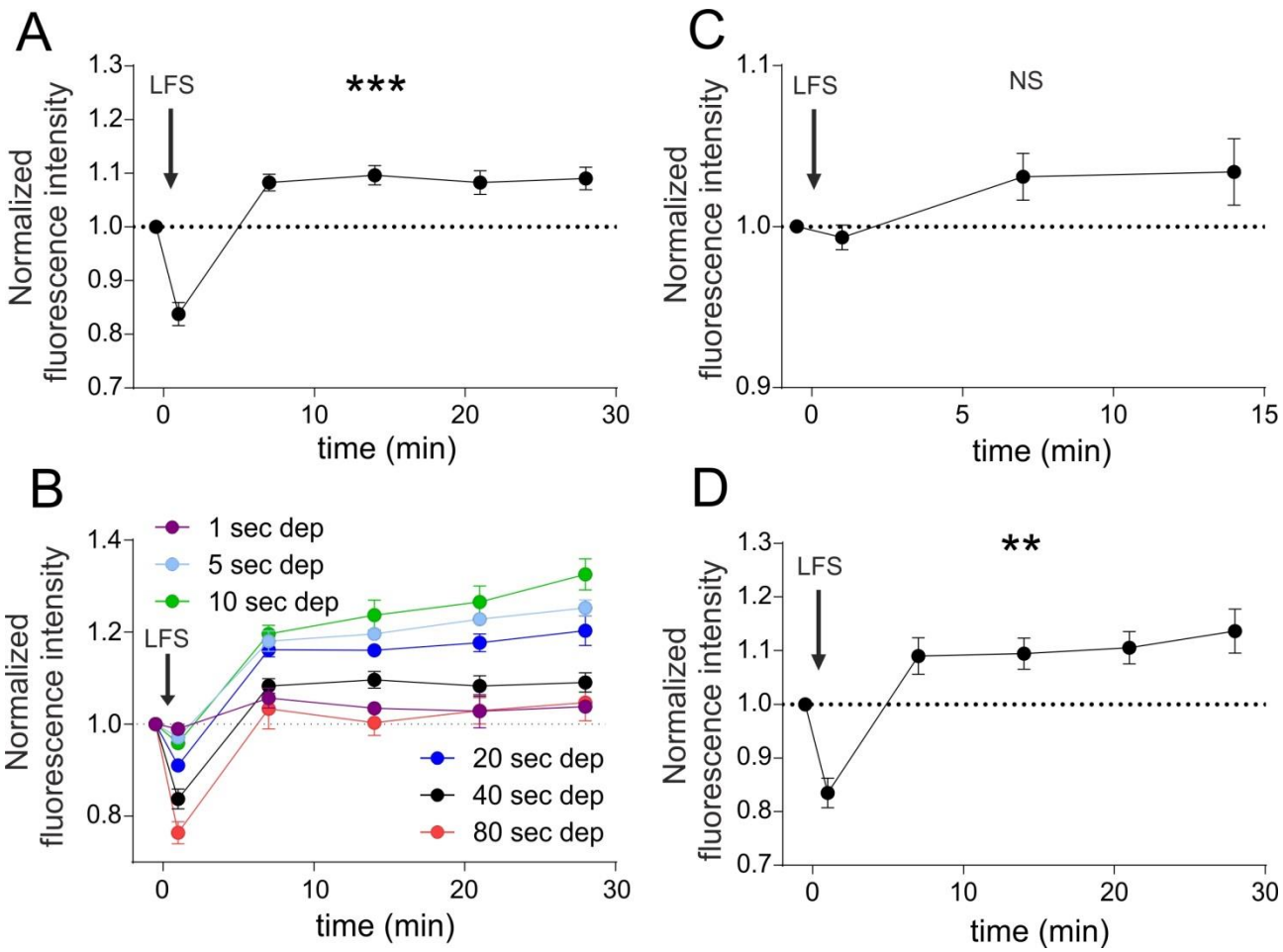

Figure 8: siSTD precedes gephyrin recruitment after LFS induction

A. Summary of the normalized gephyrin fluorescence variation (after/before) observed upon iLTP induction with 40 seconds depolarization (n = 17, $F_{4,48}$ = 21.5,, p < 0.001, RM one-way ANOVA followed by Dunnett's post-test). **B.** Summary of the normalized gephyrin fluorescence variation (after/before) observed after the delivery depolarization of 1 second (purple, n=3), 5 seconds (light blue, n=3), 10 seconds (green, n=5), 20 seconds (blue, n=6), 40 seconds (black, n=17) and 80 seconds (red, n=6). **C.** Summary of the normalized gephyrin fluorescence variation (after/before) observed upon iLTP induction with 40 seconds depolarization in extracellular solution with 0 calcium (n=9, p < 0.001, RM one-way ANOVA followed by Dunnett's post-test). **D.** Summary of the normalized gephyrin fluorescence variation (after/before) observed upon iLTP induction with 40 seconds depolarization in presence of calcineurin inhibitor cyclosporin (n = 8, p < 0.001, RM one-way ANOVA followed by Dunnett's post-test). Values are expressed as mean ± SEM. ***p < 0.001.

Calpain is crucial for the induction of the transient loss of gephyrin:

As mentioned above, synaptic plasticity is mostly dependent on variations of intracellular calcium concentration. In this framework, we studied the role of calcium during the induction of the transient gephyrin depression induced by depolarization. In a first set of experiments the depolarization delivered in the presence of extracellular solution nominal zero calcium failed to induce the transient gephyrin depression (Figure 8C) indicating that this phenomenon is calcium dependent. In line with previous data, also the gephyrin potentiation was prevented by the absence of calcium (Petrini et al., 2014). Sustained calcium influx has been shown to be required for GABAergic depression due to the activation of both calcineurin and calpain (Bannai et al., 2015; Mele et al., 2016; Niwa et al., 2012; Tyagarajan et al., 2011). In a second set of experiments the application of cyclosporine, calcineurin inhibitor, left unchanged the transient gephyrin depression induced by depolarization and the following gephyrin accumulation (Figure 8D). Next, the depolarization was delivered in presence of the calpain inhibitor MDL28170. In these conditions the transient gephyrin depression was abolished (Fig. 9A). In addition, we observed that the gephyrin increase (iLTP) was significantly higher with respect to that in 40 second depolarization without MDL28170 (figure 8A). Thus calpain is involved not only in the early transient depression but also in the late potentiation.

In analogy with the experiments shown in Fig. 8B, we studied both the transient depression and the potentiation induced by different stimulation intensities in MDL28170. Interestingly, the inhibition of calpain completely abolished the dependence of both gephyrin depression and potentiation on the depolarization duration (Figure 9A). Interestingly, we noticed that the strength of the potentiation attained in presence of MDL28170 was comparable with the “maximal potentiation” obtained in control conditions following the delivery of 10 seconds depolarization (Compare Fig. 9A and Fig. 8B). Moreover, further test the role of calpain in these types of inhibitory plasticity, we performed the same experiments on neurons transfected with a mutant form of gephyrin (gephyrin-D269) that shows a 269 aminoacid deletion that make gephyrin insensitive to the calpain proteolytic action (Figure 9B). In this conditions, the transient gephyrin depression was strongly reduced with respect to wild type conditions, although not completely abolished. In line with these data the gephyrin late potentiation persisted and at depolarization durtions of 20 and 40 seconds it reached a value comparable to that obtained in the presence of MDL28170 (Figure 9A). At 80 seconds pulses, however the gephyrin time course of gephyrin potentiation was significantly slower than that

observed in MDL28170. In summary, we observed that calcium and calpain are crucial for the induction of the transient gephyrin depression and the subsequent potentiation observed following the delivery of a depolarization step. Previously we demonstrated that CaMKII is involved in iLTP, with an opposite action respect to the calpain. Thus, the effects of neuronal depolarization seem to be ruled by the opposite action of calpain and CaMKII, that may be activated by different calcium concentrations and at specific time points after plasticity induction.

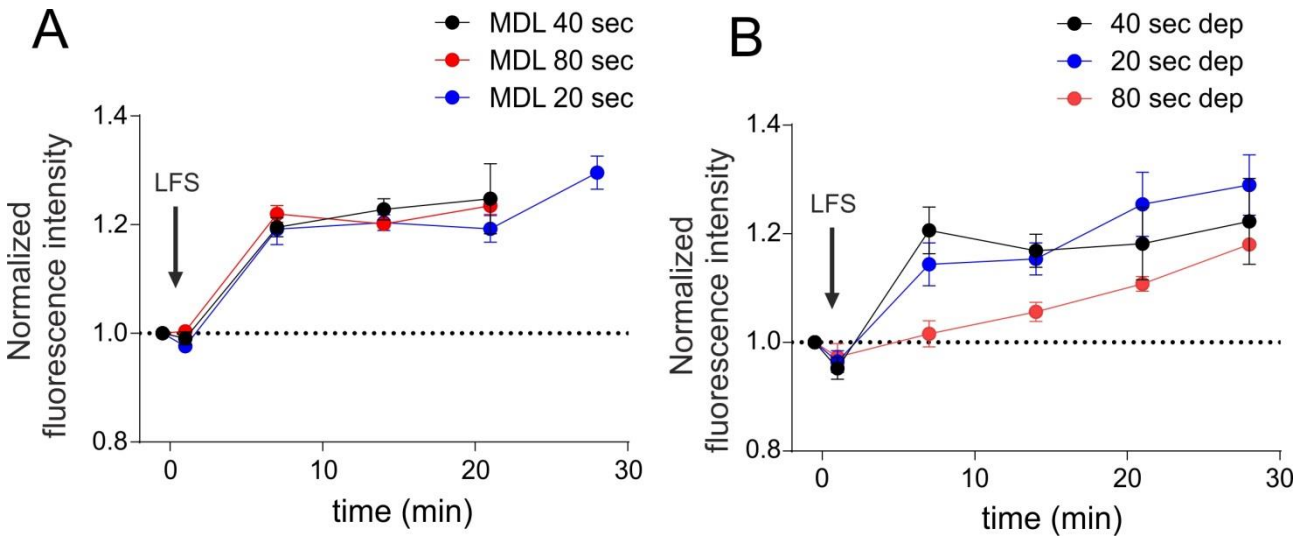

Figure 9: Calpain is crucial for the transient dispersion of gephyrin

A. Summary of the normalized gephyrin fluorescence variation (after/before) observed in presence of calpain ibhibitor MDL28170 after the depolarization of 40 seconds (black, n=9), 80 seconds (red, n=4) and 20 seconds (blue, n=12). **B.** Summary of the normalized mutated gephyrin fluorescence variation (after/before) observed after the depolarization of 40 second (black, n=10), 20 seconds (blue, n=5) and 80 seconds (red, n=5).

SUPPLEMENTARY FIGURES

Figure S 1

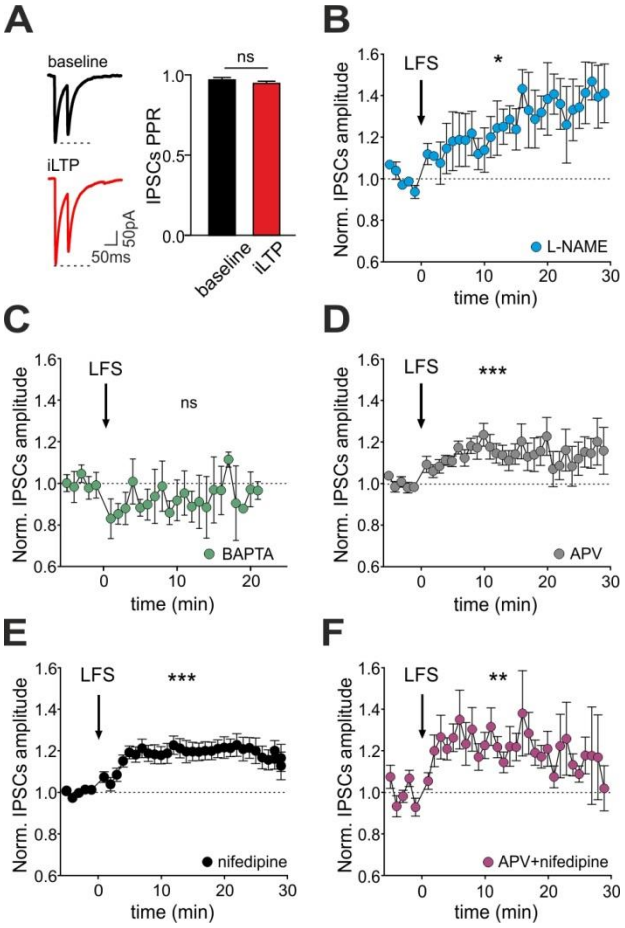

Figure S1 (related to Figure 1): Postsynaptic mechanism and Ca^{2+} dependence of LFS-induced iLTP

A-B. Unlikely presynaptic mechanisms of iLTP. **A.** Left: Representative IPSC paired pulses traces recorded before (baseline) and after (iLTP) the delivery of the LFS. Right: Quantification of the paired pulse ratio (PPR) (n = 25; p = 0.14, paired Student's t-test). **B.** The nitric oxide synthase blocker L-NAME does not prevent LFS-induced iLTP (n = 5, $F_{33,136}$= 1.6, p = 0.03; one-way ANOVA followed by Turkey's multiple comparison test). **C-E.** Time course of relative IPSC amplitude increase before and after the delivery of the LFS protocol (arrow), in the presence of the fast Ca^{2+} chelator BAPTA (**C**; n = 4, $F_{25,69}$ = 0.4, p = 0.99), APV (**D**; n = 11, $F_{33,241}$ = 2.2, p < 0.001), nifedipine (**E**; n = 21, $F_{33,640}$ = 3.6, p < 0.001), and APV + nifedipine (**F**; n = 6, $F_{33,162}$ = 2.1, p = 0.002). One-way ANOVA followed by Turkey's multiple comparison test. Values are expressed as mean ± SEM. *p < 0.05, **p < 0.01, ****p < 0.001, ns = not significant.

Figure S 2

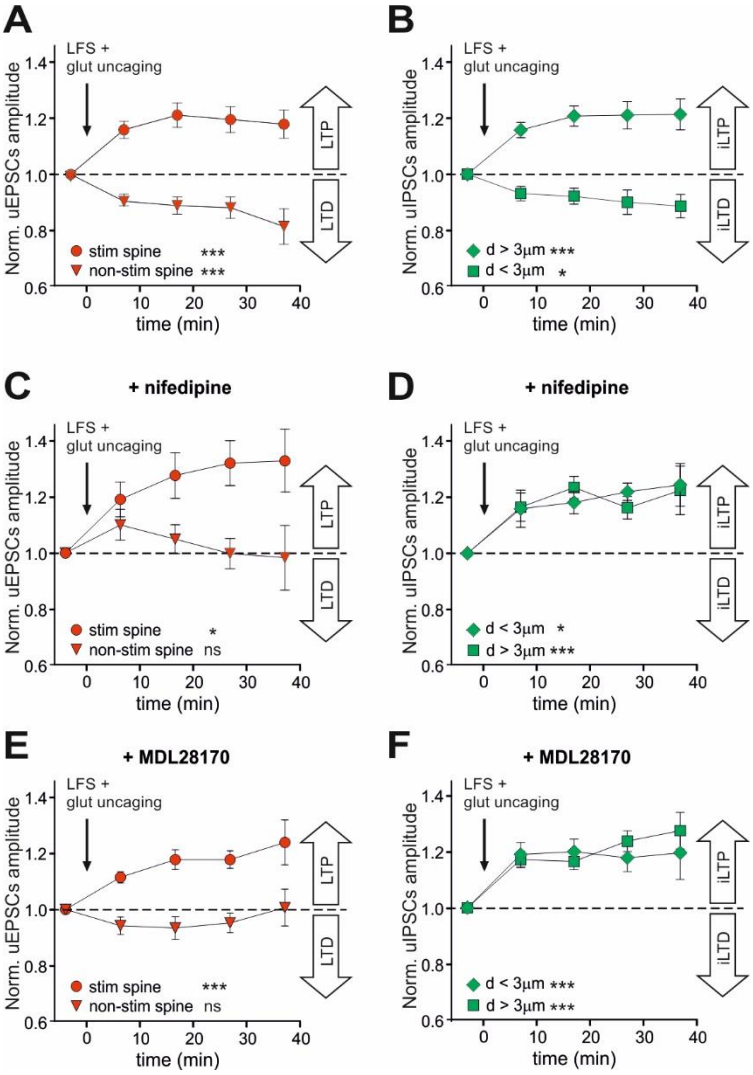

Figure S2 (related to Figure 4): Spatial coordination of the plasticity of excitatory and inhibitory synapses upon single spine LTP

A. After the "LFS+glut uncaging" protocol, the stimulated spine is selectively potentiated (circle, n = 7-20 synapses from 20 neurons, $F_{4,61}$ = 9.3, p< 0.001) and the non-photostimulated ("non-stim") spines (putatively exposed only to LFS) are depressed (triangle, n = 6-16 from 20 neurons, $F_{4,51}$ = 6.3, p< 0.001). All the statistical comparison shown here are performed with one-way ANOVA followed by Dunnett's post-test. **B.** After the "LFS+glut uncaging protocol", GABAergic synapses located at d > 3 µm from the stimulated spine are potentiated (diamond, n = 7-41 synapses from 20 neurons, $F_{4,127}$ = 11.4, p< 0.001) and those located at d < 3 µm are depressed (square, n = 11-30 20 neurons, $F_{4,103}$ = 3.0, p = 0.02). **C.** Same as in A in presence of nifedipine. Stimulated spine, n = 4-7 synapses from 7 neurons, $F_{4,26}$ = 3.9, p = 0.01; non-photostimulated spine, n = 3-6 synapses from 7 neurons, $F_{4,20}$ = 0.8, p = 0.51. **D.** Same as in B, in presence of nifedipine. d < 3 µm, n = 3-9 synapses from 7 neurons, $F_{4,27}$ = 4.0, p = 0.01; d > 3 µm, n = 4-14 synapses from 7 neurons, $F_{4,45}$ = 6.1,

p <0.001. **E.** Same as in A in presence of MDL28170. Stimulated spine, n = 3-24 synapses from 24 neurons, $F_{4,78}$ = 11.9, p <0.001; non-photostimulated spine, n = 3-25 synapses from 24 neurons, $F_{4,70}$ = 1.2, p = 0.31. **F.** Same as in B, in presence of MDL28170. d < 3 µm, n = 5-24 synapses from 24 neurons, $F_{4,71}$ = 7.1, p <0.001; d > 3, n = 6-68 synapses from 24 neurons, $F_{4,174}$ = 20.0, p <0.001. Values are expressed as mean ± SEM. *p < 0.05, ***p < 0.001, ns = not significant.

Figure S 3

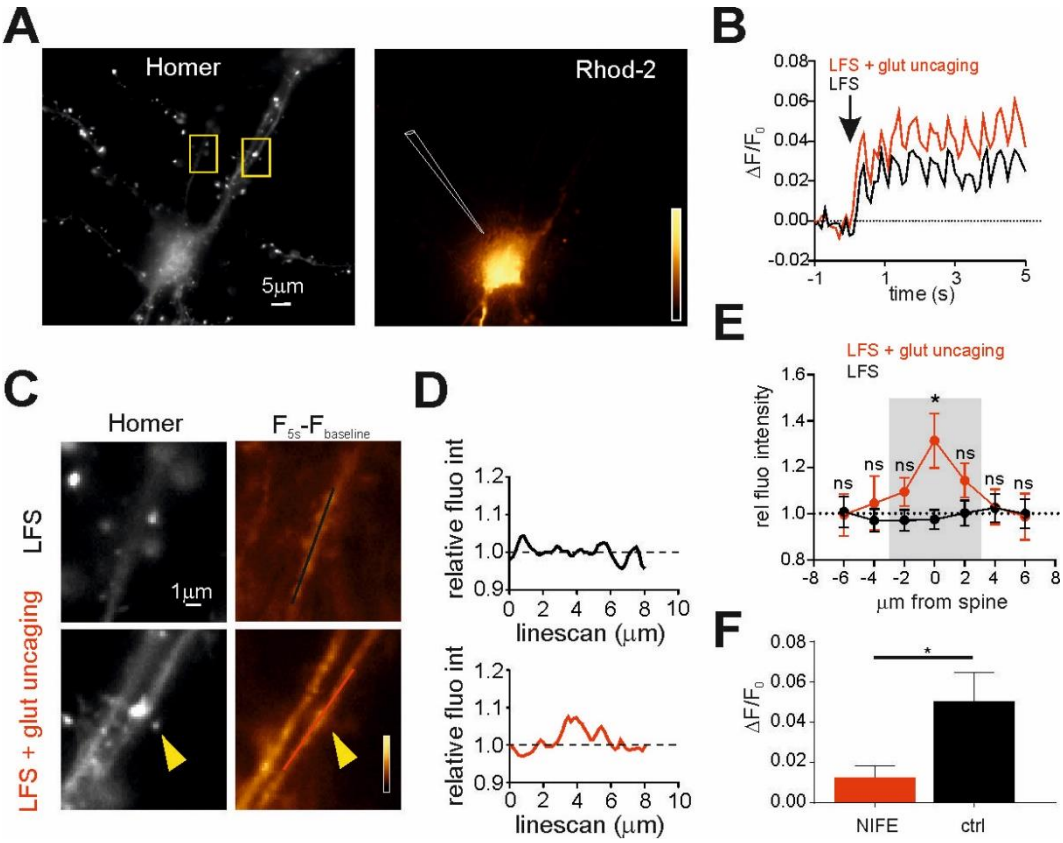

Figure S3 (related to Figure 5): Spatial dynamics of dendritic calcium during iLTP and LTD in presence of nifedipine

A. Representative epifluorescence image of a Homer1c-GFP expressing neuron (left) loaded with Rhod-2 through the patch pipette (gold, right). Scale bar, 5 µm. **B.** Relative Rhod-2 fluorescence intensity variation in presence of nifedipine during the LFS protocol (black) and the LFS paired with glutamate uncaging protocol (red) in two 4 µm-long dendritic portions of the same neuron centered below a reference and stimulated spine, respectively. The arrow indicates the beginning of the protocol. **C.** Left: Magnifications of the dendritic portions framed in A, stimulated with LFS (top) or LFS paired with MNI-glutamate uncaging (bottom). The yellow arrowhead indicates the stimulated spine. Scale bar, 1 µm. Right: Gold pseudocolor representation of Rhod-2 fluorescence intensity changes at plateau (5 s) of the stimulating protocols (i.e., LFS, top and LFS paired with glutamate uncaging, bottom) with respect to baseline values (F_{5s}-$F_{baseline}$). The lines indicate the position of the linescans quantified in D. **D**. Relative fluorescence variation induced by "LFS + glut uncaging" protocol with respect to LFS alone. The fluorescence intensities quantified along the two linescans in C are normalized to the average fluorescence detected along the linescan in LFS. **E.** Changes in the relative dendritic Rhod-2 fluorescence intensity (as measured in Figure 5D) as a function of the distance from a reference or stimulated spine during the LFS (black) or the LFS+ glut uncaging (red), respectively. The grey area indicates the range of ± 3µm from the potentiated spine where significant changes in Rhod-2 fluorescence are quantified

as compared to the LFS protocol. **F.** The larger intracellular calcium increase induced by single spine LTP as compared to LFS is attenuated in the presence of Nifedipine. Bars represent the difference between the DF/F0 induced upon single spine LTP and upon LFS, quantified in the dendritic portion centered below the stimulated and reference spine respectively. Values in the presence of Nifedipine (red) are compared to control conditions (black) (LFS: n = 13 neurons, LFS+ glut uncaging: n = 13 neurons, $p < 0.001$, two-way ANOVA followed by Bonferroni's multiple comparison test). Statistical significance for each data point is shown. Values are expressed as mean ± SEM. *$p < 0.05$, **$p < 0.01$, ns = not significant.

Figure S 4

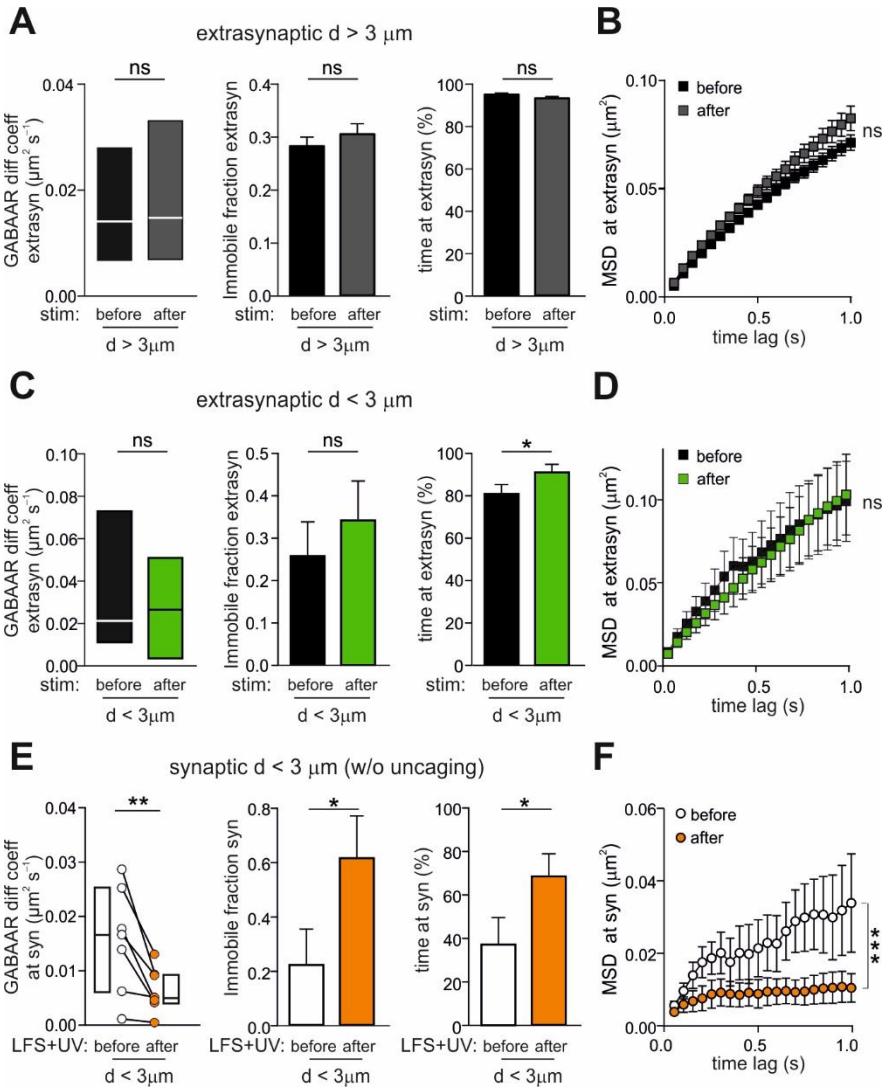

Figure S4 (related to Figure 7): Supplementary data on the modulation of GABAAR lateral mobility upon single spine LTP

A-B. Characterization of the lateral mobility of extrasynaptic GABAARs located at d > 3 µm from the potentiated spine, before (black) and after (grey) the single spine LTP protocol. **A**. Left: Median diffusion coefficient and interquartile range (IQR; n = 526-620 trajectories from 22 neurons; p = 0.63, Mann-Whitney test). Middle: Immobile fraction (n = 526-620 trajectories from 22 neurons; p = 0.40, Mann-Whitney test). Right: Percentage of time spent by GABAA receptors in the extrasynaptic compartment (n = 526-638 trajectories; p = 0.16, Mann-Whitney test). **B.** MSD versus time plot (n= 526-617 from 22 neurons; ns, ordinary two-way ANOVA followed by Bonferroni's post hoc test). **C-D.** Characterization of the lateral mobility of extrasynaptic GABAARs located at d < 3 µm from the stimulated spine, before (black) and after (green) the single spine LTP protocol. **C**. Left: Paired median diffusion coefficient (n = 25 trajectories from 14 neurons; p = 0.34, paired Wilcoxon test). Middle: Paired IF (n = 25 trajectories from 14 neurons; p = 0.24, paired

Wilcoxon test). Right: Paired values of percentage time spent by GABAA receptors in the extrasynaptic compartments at d < 3 μm from the stimulated spine (n = 25 trajectories from 14 neurons; p = 0.01, paired Wilcoxon test). **D.** MSD versus time plot of paired extrasynaptic GABAA receptors close to the potentiated spine (d < 3 μm), n = 18 from 14 neurons, ns, RM two-way ANOVA followed by Bonferroni's post hoc test. **E**-**F**. Same as in C-D, except for the uncaging. Please note that in this set of experiments the stimulating protocol was LFS + 4Hz UV-light pulses train on a spine (ctrl spine) in absence of MNI-glutamate. Only synaptic GABAAR trajectories localized in the range of 3μm from the ctrl spine were considered. **E**. Left: Paired median diffusion coefficient (n = 7 from 4 neurons; p = 0.01, paired Wilcoxon test). Middle: Paired IF (n = 7 from 4 neurons; p = 0.03, paired Wilcoxon test). Right: Paired values of percentage of time spent by GABAA receptors at synapses close to the control spine (n = 7 from 4 neurons; p = 0.01, paired Wilcoxon test). **F.** Paired MSD values of synaptic GABAA receptors close to the control spine (d < 3 μm; n = 4 from 4 neurons, p < 0.001, RM two-way ANOVA). Unless stated otherwise, values are expressed as mean ± SEM. *p < 0.05, **p < 0.01, ns = not significant.

DISCUSSION AND CONCLUSIONS

In the present thesis, by using different experimental approaches, we analysed the interplay between dendritic excitatory and inhibitory synaptic plasticity. In addition, we have characterized the mechanisms of the early stage of long-term inhibitory plasticity. In particular, we observed that the delivery an action potential train of 40 seconds at the frequency of 2 Hz (low frequency stimulation, LFS) induces the potentiation in inhibitory transmission (iLTP) and, concomitantly, depresses excitatory transmission (LTD). Moreover, we demonstrate that the induction of a Hebbian protocol of glutamatergic LTP on a single spine (obtained by pairing LFS with repetitive glutamate uncaging at an individual spine) influences the plasticity of neighbouring GABAergic synapses. In particular, we show that, after the induction of single spine LTP, GABAergic synapses located within ±3 μm from the potentiated spine were depressed (local iLTD). Our findings strongly support the existence of dendritic "plasticity micro-domains" that involve both excitatory and inhibitory synapses. In this view, the synaptic signal can be modulated in specific dendritic portions thus potentially operating a higher-order regulation of dendritic integration that is expected to ultimately impact on the neuronal output. In addition, we have also observed that, during the delivery of LFS, before iLTP expression, gephyrin clusters undergo a transient depression. Such early modulation of inhibitory postsynaptic density (iPSD) might regulate the expression of long-term inhibitory plasticity.

In the first part, we demonstrate that LFS is able to induce plasticity of opposite sign at excitatory and inhibitory synapses, respectively. Previous work at glutamatergic synapses has shown that mild calcium entry induces LTD, while sustained calcium influx leads to LTP (Coultrap et al., 2014; Lisman, 2001) an experimental paradigm that is in line with the original Bienenstock, Cooper, and Munro (BCM) theory (Bienenstock et al., 1982). Interesting, our data converges with the hypothesis (validated also by previous studies, Marsden et al., 2010; Petrini et al., 2014) that, at inhibitory synapses, this paradigm could be opposite – i.e. moderate and sustained calcium entry induce iLTP and iLTD, respectively. However, the potentiation of inhibition (iLTP), similarly to classical excitatory LTP, is mediated by the activation of CaMKII. A possible mechanism for this apparent discrepancy is that high and low calcium concentrations may induce the selective translocation of CaMKII at excitatory or inhibitory synapses, respectively (Marsden et al., 2010).

The “opposite calcium rule” at inhibitory synapses seems also to be confirmed in our Hebbian paradigm in which LFS is paired with repetitive glutamate uncaging at an individual spine. In these conditions, a local massive influx of calcium that require both L and P/Q type of VGCC is responsible for the induction of the (local) iLTD. We propose that VGCCs may be likely activated by backpropagating action potential during LFS thus leading to iLTP. In contrast, the local depolarization due to repetitive glutamate uncaging might induce a stronger VGCC activation leading to further calcium increase nearby the spine. Although it has been shown that the voltage in the spine is markedly attenuated in the parent dendrite due to heavy neck filtering (Yuste, 2013), it is possible that the very strong uncaging stimulation we deliver (160 pulses in 40 seconds) might still induce a significant dendritic depolarization, thus contributing to the further elevation of calcium in the proximity of the stimulated spine. In contrast, it is unlikely that calcium in the spine might permeate to the parent dendrite due to i) the strong calcium buffering and extrusion mechanisms in the spine and ii) the low calcium permeation rate through the spine neck (Sabatini et al., 2001, 2002).

This mechanisms of local iLTD induced by high calcium concentration is in line with previous works showing that massive influx of calcium is responsible for the depression of inhibitory transmission (Bannai et al., 2009, 2015; Muir et al., 2010). In our experiments, iLTD is induced by calpain activation that, in high calcium concentration, may overcome CaMKII signalling. In previous studies, calpain was demonstrated to be involved in the proteolysis of gephyrin clusters and the consequent reduction of GABAergic synapses (Costa et al., 2016; Tyagarajan et al., 2013). Calpain could be either activated in dendrites, or, diffuse from activated spines to parent dendrites. The latter mechanism has been extensively shown for several signaling molecule in the heyerosynaptic interaction between glutamatergic spines (Chen and Sabatini, 2012; El-Boustani et al., 2018; Harvey et al., 2008; Murakoshi et al., 2011; Oh et al., 2015; Yasuda, 2017).

While from our electrophysiology and uncaging experiments it is clear that the plasticity forms reported here are expressed at postsynaptic level, it is still possible that reduction of inhibitory strength could result from increased intracellular chloride concentration following coordinated neuronal stimulations thus leading to the reduction of the chloride electrochemical gradient (Woodin et al., 2003). Although our experiments have been performed in whole cell conditions where the intracellular chloride concentration is “imposed” by intracellular solution, as recently shown in Khirug et al., 2008 and Otsu et al., 2020, it still possible that, due to the local reduction of

chloride transporters, a different chloride gradient could be still maintained, especially in dendritic regions far from the soma. In this case, our local iLTP could be hypothetically due to local alterations of chloride concentration. However several observations rule against this possibility: i) the synapses we considered are located rather proximally (around 30 μm from the soma) where the "chloride concentration clamp error" should be limited, ii) the local iLTP has been efficiently blocked by nifedipine, a pharmacological manipulation that is unlikely to alter chloride gradient, iii) postsynaptic modifications not related to chloride gradient such as gephyrin depression and increased of GABAA receptor dynamics at synapses have been associated to local iLTD.

We propose here that the mechanisms underlying the "local iLTP" occurring in the vicinity of a potentiated glutamatergic synapse would involve diffusive intracellular processes (e.g. calcium and activated calpain) that are expected to depend on the dendritic microscale topology. In the present study, experiments were carried on putative pyramidal neurons where most glutamatergic synapses are located on spines. In these conditions, it is likely that the biochemical compartmentalization imposed by spines significantly shapes the rate and the range of dendritic diffusion. In this concern, it would be interesting to study the aforementioned paradigm of "local iLTP" in interneurons that, typically, do not show spines. In particular, future experiments will clarify how the potential lower dendritic compartmentalization in these two neuronal types will affect the short-range interaction between plasticity at excitatory and inhibitory synapses. In addition to the dendritic compartmentalization, the different expression of receptor/channels between pyramidal neurons and interneurons may further contribute to specific pyramidal and interneuronal "dendritic local plasticity patterns". For instance, while NMDA receptors are abundantly expressed in pyramidal neurons, they are less expressed on interneurons where the glutamate-activated calcium entry is mainly supported by calcium permeable AMPA receptors (CP-AMPAR). Whereas calcium entry of an individual glutamatergic synapse on spine requires dendritic depolarization to remove the NMDA magnesium block, the activation of glutamatergic synapses on interneurons would be achieved through CP-AMPARs activation that in contrast, due the polyamines block, requires hyperpolarization. Thus, such differential expression of glutamate receptors is expected to be very relevant in shaping dendritic plasticity topology in particular in relation to the coincidence between synaptic stimulation and back-propagating action potentials bpAP. In this concern, since bpAP are heavily attenuated in distal dendrites due to cable filtering, the different expression of NMDA and CP-AMPA receptors in pyramidal neurons and interneurons is also expected to vary the "plasticity rules" in relation to the synapse electro-tonic distance from the cell soma.

In this work, we highlight the importance of the coordination of synaptic excitation and inhibition with special emphasis on the short-range interaction of glutamatergic and GABAergic synapse in specific spatial compartments. Previous work shows that, following monocular deprivation (MD), glutamatergic and GABAergic synapses were modulated locally in dendritic subregions of 10μm (Chen et al., 2012). Moreover, it has been recently demonstrated that after the Hebbian potentiation of a specific spine in visual cortex pyramidal neuron, obtained by the pairing of visual stimulation with an optogenetic activation, spines neighboring the potentiated spine were depressed (El-Boustani et al., 2018). Similarly, the potentiation of an individual spine following a protocol of motor skill training determined the shrinkage of spines adjacent to the potentiated spine. All the aforementioned studies are in line with our conclusions that synapses can locally interplay in dendritic microdomains and underline the importance to study the role of GABAergic synapses within such functional dendritic units. Recently it has been shown that GABAergic inhibitory synapses are very dynamic structures being frequently formed and eliminated in relation to neuronal activity and in concert with excitatory synapses (Chen et al., 2012; Villa et al., 2016). Our findings reinforce the concept that modifications of GABAergic synapses are highly influenced by plasticity occurring at glutamatergic synapses, suggesting that the activity-dependent remodeling of the network is shaped by concerted synaptic excitation and inhibition plasticity.

In the present experiment, we focused on the interplay of spines and GABAergic synapses located in proximity of the soma (≈ 20 to 50 um). Since these synapses are electrotonically relatively close to the soma, the LFS combined with a photorelease of glutamate at 4Hz is probably sufficient to ensure summation between synaptic stimulation and bpAP and to trigger the biochemical event to induce spine LTP and local iLTD. In more distal dendritic regions, the back-propagating action potentials generated by the LFS stimulation may not attain the membrane depolarization needed to allow the influx of calcium required for iLPT (see discussion above on NMDA and CP-AMPA receptors). On the other hand, in the distal regions, the phenomenon of “synaptic scaling” together with the higher dendritic impedance in thin dendrites, would maximize the impact of local of synaptic glutamate release on the variation of the membrane potential. In this scenario, at this stage, it is difficult to predict how the interplay between excitatory and inhibitory synaptic plasticity and the local spatiotemporal dynamics of calcium can be modulated at distal synapses, since the strength of the depolarization by bpAP and local activation of glutamatergic synapses are heavily and oppositely modulated by the distance from the soma. In future studies it will be crucial to assess how these factors interact to shape distal dendritic microdomains.

As mentioned above, we find that LFS alone induces glutamatergic LTD and GABAergic iLTP while opposite trend (glutamatergic LTP and GABAergic iLTD) has been observed with LFS+uncaging. In this concern, it is interesting to note that, in both conditions, synaptic excitation and inhibition follow an “anti-homeostatic” rule. This might be considered an unexpected result, since previous studies found that during network activity, the strengthening/weakening of excitation and inhibition are regulated to preserve the neuronal output (homestatic plasticity). Even if our model show a possible altered excitation to inhibition (E/I) unbalance, we should consider that this disequilibrium is local. In fact, the different microdomains undergoing either non-Hebbian or Hebbian plasticity could still balance each other at the larger spatial domains such as the whole neuron level or in longer dendritic portions. In these conditions the overall E/I balance could still be preserved even in the presence of local unbalance.

A disruption of the E/I balance has been proposed to be at the base of several neurological diseases including autism and schizophrenia (Antoine et al., 2019; Lewis et al., 2012; Rubenstein and Merzenich, 2003). However, it is worth noting that drugs that effectively act on the E/I balance have only limited efficacy in treating these diseases. This might be due to the fact that these drugs act at the whole brain level. We propose that specific E/I alterations in specific dendritic micro-domains might account for the physiopathology of such neurological diseases. In this scenario, new specific pharmacological tools may be required to target specific dendritic portions and possibly correct the E/I unbalance in specific “dendritic nodes”.

In the second part of this thesis, I focused on the transient loss of gephyrin from inhibitory synapses during the delivery of the depolarization protocol we used for the induction iLTP. We show that the structural inhibitory short term depression is proportional to the length of the depolarization pulse, suggesting a close relationship between the amount of calcium influx and the strength of the transient gephyrin depression. In particular, we demonstrated that longer depolarization are able to activate the protease calpain that promotes the dispersion of gephyrin, competing with CaMKII, that on contrary promotes the recruitment of the scaffold protein. Thus, in our model, calpain and CamKII pathways (activated at different calcium concentrations) induce opposite effect on gephyrin assembly. Further experiments will be needed to assess the physiological role for this gephyrin transient depression. Our working hypothesis is that the transient loss of inhibition could favour excitation, a process that might be necessary to trigger specific intracellular signalling shaping long-

term plasticity. In order to further explore this topic, we plan to study the dynamics of excitatory synapses during the aforementioned depolarization pulses.

Our results reinforce the idea that synaptic plasticity is a highly dynamic process where synapses undergo profound remodelling even during plasticity induction. Our future work will be devoted to understand the coordination between excitatory and inhibitory plasticity with the ultimate goal to study how the early dynamics of GABAergic and glutamatergic synapses influence the remodelling of the neuronal circuits by regulating synaptic plasticity in the long-term and consolidation phases.

BIBLIOGRAPHY

Abidin, I., Eysel, U.T., Lessmann, V., and Mittmann, T. (2008). Impaired GABAergic inhibition in the visual cortex of brain-derived neurotrophic factor heterozygous knockout mice. J. Physiol. *586*, 1885–1901.

Aguado, F. (2003). BDNF regulates spontaneous correlated activity at early developmental stages by increasing synaptogenesis and expression of the K+/Cl- co-transporter KCC2. Development *130*, 1267–1280.

Antoine, M.W., Langberg, T., Schnepel, P., and Feldman, D.E. (2019). Increased Excitation-Inhibition Ratio Stabilizes Synapse and Circuit Excitability in Four Autism Mouse Models. Neuron.

Araya, R., Vogels, T.P., and Yuste, R. (2014). Activity-dependent dendritic spine neck changes are correlated with synaptic strength. Proc. Natl. Acad. Sci. *111*, E2895–E2904.

Arellano, J.I. (2007). Ultrastructure of dendritic spines: correlation between synaptic and spine morphologies. Front. Neurosci. *1*, 131–143.

Atwal, J.K., Massie, B., Miller, F.D., and Kaplan, D.R. (2000). The TrkB-Shc site signals neuronal survival and local axon growth via MEK and PI3-Kinase. Neuron *27*, 265–277.

Bacci, A., Rudolph, U., Huguenard, J.R., and Prince, D.A. (2003). Major differences in inhibitory synaptic transmission onto two neocortical interneuron subclasses. J. Neurosci. *23*, 9664–9674.

Bailey, C.H., Giustetto, M., Huang, Y.Y., Hawkins, R.D., and Kandel, E.R. (2000). Is Heterosynaptic modulation essential for stabilizing hebbian plasiticity and memory. Nat. Rev. Neurosci. *1*, 11–20.

Balena, T., and Woodin, M.A. (2008). Coincident pre- and postsynaptic activity downregulates NKCC1 to hyperpolarize E(Cl) during development. Eur. J. Neurosci. *27*, 2402–2412.

Bannai, H., Lévi, S., Schweizer, C., Inoue, T., Launey, T., Racine, V., Sibarita, J.B., Mikoshiba, K., and Triller, A. (2009). Activity-Dependent Tuning of Inhibitory Neurotransmission Based on GABAAR Diffusion Dynamics. Neuron *62*, 670–682.

Bannai, H., Niwa, F., Sherwood, M.W., Shrivastava, A.N., Arizono, M., Miyamoto, A., Sugiura, K., Lévi, S., Triller, A., and Mikoshiba, K. (2015). Bidirectional Control of Synaptic GABAAR Clustering by Glutamate and Calcium. Cell Rep. *13*, 2768–2780.

Barnard, E.A., Skolnick, P., Olsen, R.W., Mohler, H., Sieghart, W., Biggio, G., Braestrup, C., Bateson, A.N., and Langer, S.Z. (1998). International Union of Pharmacology. XV. Subtypes of gamma-aminobutyric acidA receptors: classification on the basis of subunit structure and receptor function. Pharmacol. Rev. *50*, 291–313.

Bartos, M., Vida, I., and Jonas, P. (2007). Synaptic mechanisms of synchronized gamma oscillations in inhibitory interneuron networks. Nat. Rev. Neurosci. *8*, 45–56.

Bartos, M., Alle, H., and Vida, I. (2011). Role of microcircuit structure and input integration in hippocampal interneuron recruitment and plasticity. Neuropharmacology *60*, 730–739.

Baudouin, S.J., Gaudias, J., Gerharz, S., Hatstatt, L., Zhou, K., Punnakkal, P., Tanaka, K.F., Spooren, W., Hen, R., De Zeeuw, C.I., et al. (2012). Shared synaptic pathophysiology in syndromic and nonsyndromic rodent models of autism. Science (80-.).

Beffert, U., Weeber, E.J., Durudas, A., Qiu, S., Masiulis, I., Sweatt, J.D., Li, W.P., Adelmann, G., Frotscher, M., Hammer, R.E., et al. (2005). Modulation of synaptic plasticity and memory by Reelin involves differential splicing of the lipoprotein receptor Apoer2. Neuron *47*, 567–579.

Ben-Ari, Y. (2001). Developing networks play a similar melody. Trends Neurosci. *24*, 353–360.

Ben-Ari, Y. (2002). Excitatory actions of gaba during development: the nature of the nurture. Nat. Rev. Neurosci. *3*, 728–739.

Ben-Ari, Y., and Spitzer, N.C. (2004). Nature and nurture in brain development. Trends Neurosci. *27*, 361.

Benes, F. (2001). GABAergic Interneurons Implications for Understanding Schizophrenia and Bipolar Disorder. Neuropsychopharmacology *25*, 1–27.

Benes, F.M. (1991). Deficits in Small Interneurons in Prefrontal and Cingulate Cortices of Schizophrenic and Schizoaffective Patients. Arch. Gen. Psychiatry *48*, 996.

Berger, T., Larkum, M.E., and Lüscher, H.-R. (2001). High I h Channel Density in the Distal Apical Dendrite of Layer V Pyramidal Cells Increases Bidirectional Attenuation of EPSPs. J. Neurophysiol. *85*, 855–868.

Bernard, C. (2012). Alterations in synaptic function in epilepsy.

Bienenstock, E., Cooper, L., and Munro, P. (1982). Theory for the development of neuron selectivity: orientation specificity and binocular interaction in visual cortex. J. Neurosci. *2*, 32–48.

Bloodgood, B.L., and Sabatini, B.L. (2005). Neuronal Activity Regulates Diffusion Across the Neck of Dendritic Spines. Science (80-.). *310*, 866–869.

Bloodgood, B.L., and Sabatini, B.L. (2007). Nonlinear Regulation of Unitary Synaptic Signals by CaV2.3 Voltage-Sensitive Calcium Channels Located in Dendritic Spines. Neuron *53*, 249–260.

Bowery, N.G., Hill, D.R., and Hudson, A.L. (1983). Characteristics of GABAB receptor binding sites on rat whole brain synaptic membranes. Br. J. Pharmacol. *78*, 191–206.

Bozzi, Y., Provenzano, G., and Casarosa, S. (2018). Neurobiological bases of autism-epilepsy comorbidity: a focus on excitation/inhibition imbalance. Eur. J. Neurosci. *47*, 534–548.

Bragin, a, Jandó, G., Nádasdy, Z., Hetke, J., Wise, K., and Buzsáki, G. (1995). Gamma (40-100 Hz) oscillation in the hippocampus of the behaving rat. J. Neurosci. *15*, 47–60.

Brenman, J.E., Chao, D.S., Gee, S.H., McGee, A.W., Craven, S.E., Santillano, D.R., Wu, Z., Huang, F., Xia, H., Peters, M.F., et al. (1996). Interaction of nitric oxide synthase with the postsynaptic density protein PSD-95 and α1-syntrophin mediated by PDZ domains. Cell *84*, 757–767.

Breustedt, J., Vogt, K.E., Miller, R.J., Nicoll, R.A., and Schmitz, D. (2003). α1E-Containing Ca2+ channels are involved in synaptic plasticity. Proc. Natl. Acad. Sci. U. S. A. *100*, 12450–12455.

Briz, V., and Baudry, M. (2017). Calpains: Master Regulators of Synaptic Plasticity. Neuroscientist *23*, 221–231.

Brünig, I., Penschuck, S., Berninger, B., Benson, J., and Fritschy, J.M. (2001). BDNF reduces miniature inhibitory postsynaptic currents by rapid downregulation of GABAA receptor surface expression. Eur. J. Neurosci. *13*, 1320–1328.

Bywalez, W.G., Patirniche, D., Rupprecht, V., Stemmler, M., Herz, A.V.M., Pálfi, D., Rózsa, B., and Egger, V. (2015). Local Postsynaptic Voltage-Gated Sodium Channel Activation in Dendritic Spines of Olfactory Bulb Granule Cells. Neuron *85*, 590–601.

Cane, M., Maco, B., Knott, G., and Holtmaat, A. (2014). The relationship between PSD-95 clustering and spine stability In Vivo. J. Neurosci. *34*, 2075–2086.

Capani, F., Martone, M.E., Deerinck, T.J., and Ellisman, M.H. (2001). Selective localization of high concentrations of F-actin in subpopulations of dendritic spines in rat central nervous system: A three-dimensional electron microscopic study. J. Comp. Neurol. *435*, 156–170.

Capogna, M. (2011). Neurogliaform cells and other interneurons of stratum lacunosum-moleculare gate entorhinal-hippocampal dialogue. J. Physiol. *589*, 1875–1883.

Castillo, P.E. (2012). Presynaptic LTP and LTD of excitatory and inhibitory synapses. Cold Spring Harb. Perspect. Biol. *4*.

Castillo, P.E., Chiu, C.Q., and Carroll, R.C. (2011). Long-term plasticity at inhibitory synapses. Curr. Opin. Neurobiol. *21*, 328–338.

Chang, J.-Y., Nakahata, Y., Hayano, Y., and Yasuda, R. (2019). Mechanisms of Ca2+/calmodulin-dependent kinase II activation in single dendritic spines. Nat. Commun. *10*, 2784.

Chen, Y., and Sabatini, B.L. (2012). Signaling in dendritic spines and spine microdomains. Curr. Opin. Neurobiol.

Chen, Z.-W., and Olsen, R.W. (2007). GABA A receptor associated proteins: a key factor regulating GABA A receptor function. J. Neurochem. *100*, 279–294.

Chen, J.L., Villa, K.L., Cha, J.W., So, P.T.C., Kubota, Y., and Nedivi, E. (2012). Clustered Dynamics of Inhibitory Synapses and Dendritic Spines in the Adult Neocortex. Neuron *74*, 361–373.

Chen, L., Wang, H., Vicini, S., and Olsen, R.W. (2000). The γ-aminobutyric acid type A (GABA(A)) receptor-associated protein (GABARAP) promotes GABA(A) receptor clustering and modulates the channel kinetics. Proc. Natl. Acad. Sci. U. S. A. *97*, 11557–11562.

Chevaleyre, V., Takahashi, K.A., and Castillo, P.E. (2006). ENDOCANNABINOID-MEDIATED SYNAPTIC PLASTICITY IN THE CNS. Annu. Rev. Neurosci. *29*, 37–76.

Chidambaram, S.B., Rathipriya, A.G., Bolla, S.R., Bhat, A., Ray, B., Mahalakshmi, A.M., Manivasagam, T., Thenmozhi, A.J., Essa, M.M., Guillemin, G.J., et al. (2019). Dendritic spines: Revisiting the physiological role. Prog. Neuro-Psychopharmacology Biol. Psychiatry *92*, 161–193.

Chiu, C.Q., Lur, G., Morse, T.M., Carnevale, N.T., Ellis-Davies, G.C.R., and Higley, M.J. (2013). Compartmentalization of GABAergic inhibition by dendritic spines. Science (80-.). *340*, 759–762.

Chiu, C.Q., Martenson, J.S., Yamazaki, M., Natsume, R., Sakimura, K., Tomita, S., Tavalin, S.J., and Higley, M.J. (2018). Input-Specific NMDAR-Dependent Potentiation of Dendritic GABAergic Inhibition. Neuron *97*, 368-377.e3.

Chiu, C.Q., Barberis, A., and Higley, M.J. (2019). Preserving the balance: diverse forms of long-term GABAergic synaptic plasticity. Nat. Rev. Neurosci. *20*, 272–281.

Chklovskii, D.B., Mel, B.W., and Svoboda, K. (2004). <Nature03012.Pdf>. *431*.

Choquet, D., and Triller, A. (2013). The dynamic synapse. Neuron *80*, 691–703.

Collins, T.J., Lipp, P., Berridge, M.J., and Bootman, M.D. (2001). Mitochondrial Ca2+ Uptake Depends on the Spatial and Temporal Profile of Cytosolic Ca2+ Signals. J. Biol. Chem.

Contestabile, A. (2000). Roles of NMDA receptor activity and nitric oxide production in brain development. Brain Res. Rev. *32*, 476–509.

Costa, J.T., Mele, M., Baptista, M.S., Gomes, J.R., Ruscher, K., Nobre, R.J., de Almeida, L.P., Wieloch, T., and Duarte, C.B. (2016). Gephyrin Cleavage in In Vitro Brain Ischemia Decreases GABAA Receptor Clustering and Contributes to Neuronal Death. Mol. Neurobiol.

Coultrap, S.J., Freund, R.K., O'Leary, H., Sanderson, J.L., Roche, K.W., Dell'Acqua, M.L., and Bayer, K.U. (2014). Autonomous CaMKII mediates both LTP and LTD using a mechanism for differential substrate site selection. Cell Rep.

Croarkin, P.E., Levinson, A.J., and Daskalakis, Z.J. (2011). Evidence for GABAergic inhibitory deficits in major depressive disorder. Neurosci. Biobehav. Rev. *35*, 818–825.

Dan, Y., and Poo, M.-M. (2006). Spike timing-dependent plasticity: from synapse to perception. Physiol. Rev. *86*, 1033–1048.

Davenport, C.M., Rajappa, R., Katchan, L., Taylor, C.R., Tsai, M.C., Smith, C.M., de Jong, J.W., Arnold, D.B., Lammel, S., and Kramer, R.H. (2021). Relocation of an Extrasynaptic GABAA Receptor to Inhibitory Synapses Freezes Excitatory Synaptic Strength and Preserves Memory. Neuron *109*, 123-134.e4.

Daw, M.I., Tricoire, L., Erdelyi, F., Szabo, G., and McBain, C.J. (2009). Asynchronous Transmitter Release from Cholecystokinin-Containing Inhibitory Interneurons Is Widespread and Target-Cell Independent. J. Neurosci. *29*, 11112–11122.

Diering, G.H., and Huganir, R.L. (2018). The AMPA Receptor Code of Synaptic Plasticity. Neuron *100*, 314–329.

Doyon, N., Prescott, S.A., Castonguay, A., Godin, A.G., Kröger, H., and De Koninck, Y. (2011). Efficacy of Synaptic Inhibition Depends on Multiple, Dynamically Interacting Mechanisms Implicated in Chloride Homeostasis. PLoS Comput. Biol. *7*, e1002149.

Drake, C.T., Milner, T.A., and Patterson, S.L. (1999). Ultastructural localization of full-length trkB immunoreactivity in rat hippocampus suggests multiple roles in modulating activity-dependent synaptic plasticity. J. Neurosci. *19*, 8009–8026.

El-Boustani, S., Ip, J.P.K., Breton-Provencher, V., Knott, G.W., Okuno, H., Bito, H., and Sur, M. (2018). Locally coordinated synaptic plasticity of visual cortex neurons in vivo. Science (80-.). *360*, 1349–1354.

Eliasson, M.J.L., Blackshaw, S., Schell, M.J., and Snyder, S.H. (1997). Neuronal nitric oxide synthase alternatively spliced forms: Prominent functional localizations in the brain. Proc. Natl. Acad. Sci. U. S. A. *94*, 3396–3401.

Falcón-Moya, R., Pérez-Rodríguez, M., Prius-Mengual, J., Andrade-Talavera, Y., Arroyo-García, L.E., Pérez-Artés, R., Mateos-Aparicio, P., Guerra-Gomes, S., Oliveira, J.F., Flores, G., et al. (2020). Astrocyte-mediated switch in spike timing-dependent plasticity during hippocampal development. Nat. Commun. *11*.

Fifková, E., and Anderson, C.L. (1981). Stimulation-induced changes in dimensions of stalks of

dendritic spines in the dentate molecular layer. Exp. Neurol. *74*, 621–627.

Fifková, E., and Delay, R.J. (1982). Cytoplasmic actin in neuronal processes as a possible mediator of synaptic plasticity. J. Cell Biol. *95*, 345–350.

Fiumelli, H., and Woodin, M.A. (2007). Role of activity-dependent regulation of neuronal chloride homeostasis in development. Curr. Opin. Neurobiol. *17*, 81–86.

Flores, C.E., Nikonenko, I., Mendez, P., Fritschy, J.-M., Tyagarajan, S.K., and Muller, D. (2015). Activity-dependent inhibitory synapse remodeling through gephyrin phosphorylation. Proc. Natl. Acad. Sci. *112*, E65–E72.

Freund, T.F., and Buzsáki, G. (1998). Interneurons of the hippocampus. Hippocampus *6*, 347–470.

Freund, T.F., and Katona, I. (2007). Perisomatic Inhibition. Neuron *56*, 33–42.

Froemke, R.C., Merzenich, M.M., and Schreiner, C.E. (2007). A synaptic memory trace for cortical receptive field plasticity. Nature *450*, 425–429.

Fuentealba, P., Tomioka, R., Dalezios, Y., Márton, L.F., Studer, M., Rockland, K., Klausberger, T., and Somogyi, P. (2008). Rhythmically active enkephalin-expressing GABAergic cells in the CA1 area of the hippocampus project to the subiculum and preferentially innervate interneurons. J. Neurosci. *28*, 10017–10022.

Gabernet, L., Jadhav, S.P., Feldman, D.E., Carandini, M., and Scanziani, M. (2005). Somatosensory Integration Controlled by Dynamic Thalamocortical Feed-Forward Inhibition. Neuron *48*, 315–327.

Garthwaite, J. (2008). Concepts of neural nitric oxide-mediated transmission. Eur. J. Neurosci. *27*, 2783–2802.

Geiger, J.R.P., Lübke, J., Roth, A., Frotscher, M., and Jonas, P. (1997). Submillisecond AMPA receptor-mediated signaling at a principal neuron- interneuron synapse. Neuron *18*, 1009–1023.

Gordon, G.R.J., Mulligan, S.J., and MacVicar, B.A. (2007). Astrocyte control of the cerebrovasculature. Glia *55*, 1214–1221.

Gorkiewicz, T., Szczuraszek, K., Wyrembek, P., Michaluk, P., Kaczmarek, L., and Mozrzymas, J.W. (2010). Matrix Metalloproteinase-9 reversibly affects the time course of NMDA-induced currents in cultured rat hippocampal neurons. Hippocampus *20*, 1105–1108.

Gross, G.G., Junge, J.A., Mora, R.J., Kwon, H.-B., Olson, C.A., Takahashi, T.T., Liman, E.R., Ellis-Davies, G.C.R., McGee, A.W., Sabatini, B.L., et al. (2013). Recombinant Probes for Visualizing Endogenous Synaptic Proteins in Living Neurons. Neuron *78*, 971–985.

Haas, J.S., Nowotny, T., and Abarbanel, H.D.I. (2006). Spike-Timing-Dependent Plasticity of Inhibitory Synapses in the Entorhinal Cortex. J. Neurophysiol. *96*, 3305–3313.

Hardingham, N., and Fox, K. (2006). The role of nitric oxide and GluR1 in presynaptic and postsynaptic components of neocortical potentiation. J. Neurosci. *26*, 7395–7404.

Harnett, M.T., Xu, N.-L., Magee, J.C., and Williams, S.R. (2013). Potassium Channels Control the Interaction between Active Dendritic Integration Compartments in Layer 5 Cortical Pyramidal Neurons. Neuron *79*, 516–529.

Harnett, M.T., Magee, J.C., and Williams, S.R. (2015). Distribution and Function of HCN Channels in the Apical Dendritic Tuft of Neocortical Pyramidal Neurons. J. Neurosci. *35*, 1024–1037.

Harris, K., and Stevens, J. (1989). Dendritic spines of CA 1 pyramidal cells in the rat hippocampus: serial electron microscopy with reference to their biophysical characteristics. J. Neurosci. *9*, 2982–2997.

Harris, K., Jensen, F., and Tsao, B. (1992). Three-dimensional structure of dendritic spines and synapses in rat hippocampus (CA1) at postnatal day 15 and adult ages: implications for the maturation of synaptic physiology and long-term potentiation [published erratum appears in J Neurosci 1992 Aug;1. J. Neurosci. *12*, 2685–2705.

Harvey, C.D., and Svoboda, K. (2007). Locally dynamic synaptic learning rules in pyramidal neuron dendrites. Nature *450*, 1195–1200.

Harvey, C.D., Yasuda, R., Zhong, H., and Svoboda, K. (2008). The spread of Ras activity triggered by activation of a single dendritic spine. Science (80-.).

He, Q., Duguid, I., Clark, B., Panzanelli, P., Patel, B., Thomas, P., Fritschy, J.M., and Smart, T.G. (2015a). Interneuron- and GABA<inf>A</inf> receptor-specific inhibitory synaptic plasticity in cerebellar Purkinje cells. Nat. Commun. *6*, 1–13.

He, Q., Duguid, I., Clark, B., Panzanelli, P., Patel, B., Thomas, P., Fritschy, J.M., and Smart, T.G. (2015b). Interneuron- and GABAA receptor-specific inhibitory synaptic plasticity in cerebellar Purkinje cells. Nat. Commun. *6*.

Hefft, S., and Jonas, P. (2005). Asynchronous GABA release generates long-lasting inhibition at a hippocampal interneuron–principal neuron synapse. Nat. Neurosci. *8*, 1319–1328.

Heifets, B.D., and Castillo, P.E. (2009). Endocannabinoid Signaling and Long-Term Synaptic Plasticity. Annu. Rev. Physiol. *71*, 283–306.

Higley, M. J. and Contreras, D. (2006). Balanced Excitation and Inhibition Determine Spike Timing during Frequency Adaptation. J. Neurosci. *26*, 448–457.

Higley, M.J., and Sabatini, B.L. (2008). Calcium Signaling in Dendrites and Spines: Practical and Functional Considerations. Neuron *59*, 902–913.

Hill, T.C., and Zito, K. (2013). LTP-Induced Long-Term Stabilization of Individual Nascent Dendritic Spines. J. Neurosci. *33*, 678–686.

Hlushchenko, I., Koskinen, M., and Hotulainen, P. (2016). Dendritic spine actin dynamics in neuronal maturation and synaptic plasticity. Cytoskeleton *73*, 435–441.

Hoffman, D.A., Magee, J.C., Colbert, C.M., and Johnston, D. (1997). K+ channel regulation of signal propagation in dendrites of hippocampal pyramidal neurons. Nature *387*, 869–875.

Hölscher, C. (1997). Nitric oxide, the enigmatic neuronal messenger: Its role in synaptic plasticity. Trends Neurosci. *20*, 298–303.

Hromádka, T., and Zador, A.M. (2007). Toward the mechanisms of auditory attention. Hear. Res. *229*, 180–185.

Huang, Y.Y., and Kandel, E.R. (2005). θ frequency stimulation up-regulates the synaptic strength of the pathway from CA1 to subiculum region of hippocampus. Proc. Natl. Acad. Sci. U. S. A. *102*, 232–237.

Humeau, Y., Herry, C., Kemp, N., Shaban, H., Fourcaudot, E., Bissière, S., and Lüthi, A. (2005).

Dendritic spine heterogeneity determines afferent-specific Hebbian plasticity in the amygdala. Neuron *45*, 119–131.

Hussman, J.P. (2001). Suppressed GABAergic inhibition as a common factor in suspected etiologies of autism. J. Autism Dev. Disord. *31*, 247–248.

Inagaki, T., Begum, T., Reza, F., Horibe, S., Inaba, M., Yoshimura, Y., and Komatsu, Y. (2008). Brain-derived neurotrophic factor-mediated retrograde signaling required for the induction of long-term potentiation at inhibitory synapses of visual cortical pyramidal neurons. Neurosci. Res. *61*, 192–200.

Isaacson, J.S., and Scanziani, M. (2011). How Inhibition Shapes Cortical Activity. Neuron *72*, 231–243.

Isaacson, J.S., Solis, J.M., and Nicoll, R.A. (1993). Local and diffuse synaptic actions of GABA in the hippocampus. Neuron *10*, 165–175.

Ito, M. (2001). Cerebellar long-term depression: Characterization, signal transduction, and functional roles. Physiol. Rev. *81*, 1143–1195.

Jovanovic, J.N., Thomas, P., Kittler, J.T., Smart, T.G., and Moss, S.J. (2004). Brain-Derived Neurotrophic Factor Modulates Fast Synaptic Inhibition by Regulating GABAA Receptor Phosphorylation, Activity, and Cell-Surface Stability. J. Neurosci. *24*, 522–530.

Kaiser, K.M.M., Lübke, J., Zilberter, Y., and Sakmann, B. (2004). Postsynaptic Calcium Influx at Single Synaptic Contacts between Pyramidal Neurons and Bitufted Interneurons in Layer 2/3 of Rat Neocortex Is Enhanced by Backpropagating Action Potentials. J. Neurosci. *24*, 1319–1329.

Kang, H., and Schuman, E.M. (1996). Kang&Schuman1996. *273*, 1–5.

Kang, H.J., and Schuman, E.M. (1995). Neurotrophin-induced modulation of synaptic transmission in the adult hippocampus. J. Physiol. - Paris *89*, 11–22.

Kang, J., Jiang, L., Goldman, S.A., and Nedergaard, M. (1998). Astrocyte-mediated potentiation of inhibitory synaptic transmission. Nat. Neurosci. *1*, 683–692.

Kano, M., Rexhausen, U., Dreessen, J., and Konnerth, A. (1992). Synaptic excitation produces a long-lasting rebound potentiation of inhibitory synaptic signals in cerebellar Purkinje cells. Nature *356*, 601–604.

Kano, M., Kano, M., Fukunaga, K., and Konnerth, A. (1996). Ca2+-induced rebound potentiation of γ-aminobutyric acid-mediated currents requires activation of Ca2+/calmodulin-dependent kinase II. Proc. Natl. Acad. Sci. U. S. A. *93*, 13351–13356.

Karayannis, T., Elfant, D., Huerta-Ocampo, I., Teki, S., Scott, R.S., Rusakov, D.A., Jones, M. V, and Capogna, M. (2010). Slow GABA transient and receptor desensitization shape synaptic responses evoked by hippocampal neurogliaform cells. J. Neurosci. *30*, 9898–9909.

Katz, Y., Menon, V., Nicholson, D.A., Geinisman, Y., Kath, W.L., and Spruston, N. (2009). Synapse Distribution Suggests a Two-Stage Model of Dendritic Integration in CA1 Pyramidal Neurons. Neuron *63*, 171–177.

Kawaguchi, S., and Hirano, T. (2007). Sustained structural change of GABA(A) receptor-associated protein underlies long-term potentiation at inhibitory synapses on a cerebellar Purkinje neuron. J. Neurosci. *27*, 6788–6799.

Kawaguchi, Y., and Kubota, Y. (1997). GABAergic cell subtypes and their synaptic connections in rat frontal cortex. Cereb. Cortex *7*, 476–486.

Khirug, S., Yamada, J., Afzalov, R., Voipio, J., Khiroug, L., and Kaila, K. (2008). GABAergic depolarization of the axon initial segment in cortical principal neurons is caused by the Na-K-2Cl cotransporter NKCC1. J. Neurosci. *28*, 4635–4639.

Kittler, J.T., and Moss, S.J. (2001). Neurotransmitter Receptor Trafficking and the Regulation of Synaptic Strength. Traffic *2*, 437–448.

Klausberger, T., and Somogyi, P. (2008). Neuronal Diversity and Temporal Dynamics: The Unity of Hippocampal Circuit Operations. Science (80-.). *321*, 53–57.

Kneussel, M. (2002). Dynamic regulation of GABAA receptors at synaptic sites. Brain Res. Rev. *39*, 74–83.

Kneussel, M., Haverkamp, S., Fuhrmann, J.C., Wang, H., Wassle, H., Olsen, R.W., and Betz, H. (2000). The gamma -aminobutyric acid type A receptor (GABAAR)-associated protein GABARAP interacts with gephyrin but is not involved in receptor anchoring at the synapse. Proc. Natl. Acad. Sci. *97*, 8594–8599.

Kobayashi, K., Manabe, T., and Takahashi, T. (1996). Presynaptic Long-Term Depression at the Hippocampal Mossy Fiber--CA3 Synapse. Science (80-.). *273*, 648–650.

Kobayashi, K., Toshiya, M., and Tomoyuki, T. (1999). Calcium-dependent mechanisms involved in presynaptic long-term depression at the hippocampal mossy fibreCA3 synapse. Eur. J. Neurosci. *11*, 1633–1638.

Koch, C., and Zador, A. (1993). The function of dendritic spines: devices subserving biochemical rather than electrical compartmentalization. J. Neurosci. *13*, 413–422.

Kohara, K., Yasuda, H., Huang, Y., Adachi, N., Sohya, K., and Tsumoto, T. (2007). A Local Reduction in Cortical GABAergic Synapses after a Loss of Endogenous Brain-Derived Neurotrophic Factor, as Revealed by Single-Cell Gene Knock-Out Method. J. Neurosci. *27*, 7234–7244.

Korkotian, E., and Segal, M. (1999). Release of calcium from stores alters the morphology of dendritic spines in cultured hippocampal neurons. Proc. Natl. Acad. Sci. *96*, 12068–12072.

Korte, M., Kang, H., Bonhoeffer, T., and Schuman, E. (1998). A role for BDNF in the late-phase of hippocampal long-term potentiation. Neuropharmacology *37*, 553–559.

Kovalchuk, Y., Hanse, E., Kafitz, K.W., and Konnerth, A. (2002). Postsynaptic induction of BDNF-mediated long-term potentiation. Science (80-.). *295*, 1729–1734.

Kreitzer, A.C., and Regehr, W.G. (2001). Retrograde inhibition of presynaptic calcium influx by endogenous cannabinoids at excitatory synapses onto Purkinje cells. Neuron *29*, 717–727.

Kuczewski, N., Langlois, A., Fiorentino, H., Bonnet, S., Marissal, T., Diabira, D., Ferrand, N., Porcher, C., and Gaiarsa, J.-L. (2008). Spontaneous glutamatergic activity induces a BDNF-dependent potentiation of GABAergic synapses in the newborn rat hippocampus. J. Physiol. *586*, 5119–5128.

Kullmann, D.M., and Lamsa, K.P. (2007). Long-term synaptic plasticity in hippocampal interneurons. Nat. Rev. Neurosci. *8*, 687–699.

Kurotani, T., Yamada, K., Yoshimura, Y., Crair, M.C., and Komatsu, Y. (2008). State-Dependent

Bidirectional Modification of Somatic Inhibition in Neocortical Pyramidal Cells. Neuron *57*, 905–916.

Lachamp, P.M., Liu, Y., and Liu, S.J. (2009). Glutamatergic modulation of cerebellar interneuron activity is mediated by an enhancement of GABA release and requires protein kinase A/RIM1alpha signaling. J. Neurosci. *29*, 381–392.

Lamsa, K., Heeroma, J.H., and Kullmann, D.M. (2005). Hebbian LTP in feed-forward inhibitory interneurons and the temporal fidelity of input discrimination. Nat. Neurosci. *8*, 916–924.

Lange, M.D., Doengi, M., Lesting, J., Pape, H.C., and Jüngling, K. (2012). Heterosynaptic long-term potentiation at interneuron-principal neuron synapses in the amygdala requires nitric oxide signalling. J. Physiol. *590*, 131–143.

Larkum, M.E., Zhu, J.J., and Sakmann, B. (1999). A new cellular mechanism for coupling inputs arriving at different cortical layers. Nature *398*, 338–341.

Larkum, M.E., Nevian, T., Sandler, M., Polsky, A., and Schiller, J. (2009). Synaptic Integration in Tuft Dendrites of Layer 5 Pyramidal Neurons: A New Unifying Principle. Science (80-.). *325*, 756–760.

Lee, H.-K., and Kirkwood, A. (2011). AMPA receptor regulation during synaptic plasticity in hippocampus and neocortex. Semin. Cell Dev. Biol. *22*, 514–520.

Lee, E., Lee, J., and Kim, E. (2017). Excitation/Inhibition Imbalance in Animal Models of Autism Spectrum Disorders. Biol. Psychiatry *81*, 838–847.

Lee, S.-J.R., Escobedo-Lozoya, Y., Szatmari, E.M., and Yasuda, R. (2009). Activation of CaMKII in single dendritic spines during long-term potentiation. Nature *458*, 299–304.

Lei, W., Omotade, O.F., Myers, K.R., and Zheng, J.Q. (2016). Actin cytoskeleton in dendritic spine development and plasticity. Curr. Opin. Neurobiol. *39*, 86–92.

Leil, T.A., Chen, Z.-W., Chang, C.-S.S., and Olsen, R.W. (2004). GABAA receptor-associated protein traffics GABAA receptors to the plasma membrane in neurons. J. Neurosci. *24*, 11429–11438.

Levitt, P., Eagleson, K.L., and Powell, E.M. (2004). Regulation of neocortical interneuron development and the implications for neurodevelopmental disorders. Trends Neurosci. *27*, 400–406.

Lewis, D.A., Curley, A.A., Glausier, J.R., and Volk, D.W. (2012). Cortical parvalbumin interneurons and cognitive dysfunction in schizophrenia. Trends Neurosci.

Lien, C.-C., Mu, Y., Vargas-Caballero, M., and Poo, M. (2006). Visual stimuli–induced LTD of GABAergic synapses mediated by presynaptic NMDA receptors. Nat. Neurosci. *9*, 372–380.

Lisman, J.E. (2001). Three Ca2+ levels affect plasticity differently: The LTP zone, the LTD zone and no man's land. J. Physiol.

Liu, S.J., and Lachamp, P. (2006). The activation of excitatory glutamate receptors evokes a long-lasting increase in the release of GABA from cerebellar stellate cells. J. Neurosci. *26*, 9332–9339.

Liu, Y., Zhang, L.I., and Tao, H.W. (2007). Heterosynaptic scaling of developing GABAergic synapses: dependence on glutamatergic input and developmental stage. J. Neurosci. *27*, 5301–5312.

Llinas, R., Nicholson, C., Freeman, J.A., and Hillman, D.E. (1968). Dendritic Spikes and Their Inhibition in Alligator Purkinje Cells. Science (80-.). *160*, 1132–1135.

Losonczy, A., and Magee, J.C. (2006). Integrative Properties of Radial Oblique Dendrites in Hippocampal CA1 Pyramidal Neurons. Neuron *50*, 291–307.

Lourenço, J., Pacioni, S., Rebola, N., van Woerden, G.M., Marinelli, S., DiGregorio, D., and Bacci, A. (2014). Non-associative Potentiation of Perisomatic Inhibition Alters the Temporal Coding of Neocortical Layer 5 Pyramidal Neurons. PLoS Biol. *12*, e1001903.

Lourenço, J., De Stasi, A.M., Deleuze, C., Bigot, M., Pazienti, A., Aguirre, A., Giugliano, M., Ostojic, S., and Bacci, A. (2020a). Modulation of Coordinated Activity across Cortical Layers by Plasticity of Inhibitory Synapses. Cell Rep. *30*, 630-641.e5.

Lourenço, J., Koukouli, F., and Bacci, A. (2020b). Synaptic inhibition in the neocortex: Orchestration and computation through canonical circuits and variations on the theme. Cortex *132*, 258–280.

de Luca, E., Ravasenga, T., Petrini, E.M., Polenghi, A., Nieus, T., Guazzi, S., and Barberis, A. (2017). Inter-Synaptic Lateral Diffusion of GABAA Receptors Shapes Inhibitory Synaptic Currents. Neuron *95*, 63-69.e5.

Lüscher, B., and Keller, C.A. (2004). Regulation of GABAA receptor trafficking, channel activity, and functional plasticity of inhibitory synapses. Pharmacol. Ther. *102*, 195–221.

Maffei, A., and Turrigiano, G.G. (2008). Multiple Modes of Network Homeostasis in Visual Cortical Layer 2/3. J. Neurosci. *28*, 4377–4384.

Maffei, A., Nataraj, K., Nelson, S.B., and Turrigiano, G.G. (2006). Potentiation of cortical inhibition by visual deprivation. Nature *443*, 81–84.

Magee, J.C. (1998). Dendritic Hyperpolarization-Activated Currents Modify the Integrative Properties of Hippocampal CA1 Pyramidal Neurons. J. Neurosci. *18*, 7613–7624.

Magee, J.C., and Johnston, D. (1995). Characterization of single voltage-gated Na+ and Ca2+ channels in apical dendrites of rat CA1 pyramidal neurons. J. Physiol. *487*, 67–90.

Magee, J.C., and Johnston, D. (1997). A synaptically controlled, associative signal for Hebbian plasticity in hippocampal neurons. Science *275*, 209–213.

Magee, J., Hoffman, D., Colbert, C., and Johnston, D. (1998). ELECTRICAL AND CALCIUM SIGNALING IN DENDRITES OF HIPPOCAMPAL PYRAMIDAL NEURONS. Annu. Rev. Physiol. *60*, 327–346.

Majewska, A., Brown, E., Ross, J., and Yuste, R. (2000). Mechanisms of Calcium Decay Kinetics in Hippocampal Spines: Role of Spine Calcium Pumps and Calcium Diffusion through the Spine Neck in Biochemical Compartmentalization. J. Neurosci. *20*, 1722–1734.

Marín, O. (2012). Interneuron dysfunction in psychiatric disorders. Nat. Rev. Neurosci. *13*, 107–120.

Markram, H., Lübke, J., Frotscher, M., and Sakmann, B. (1997). Regulation of synaptic efficacy by coincidence of postsynaptic APs and EPSPs. Science *275*, 213–215.

Marsden, K.C., Beattie, J.B., Friedenthal, J., and Carroll, R.C. (2007). NMDA Receptor Activation Potentiates Inhibitory Transmission through GABA Receptor-Associated Protein-Dependent Exocytosis of GABAA Receptors. J. Neurosci. *27*, 14326–14337.

Marsden, K.C., Shemesh, A., Bayer, K.U., and Carroll, R.C. (2010). Selective translocation of Ca2+/calmodulin protein kinase II (CaMKII) to inhibitory synapses. Proc. Natl. Acad. Sci. *107*,

20559–20564.

Marty, S., Wehrlé, R., and Sotelo, C. (2000). Neuronal activity and brain-derived neurotrophic factor regulate the density of inhibitory synapses in organotypic slice cultures of postnatal hippocampus. J. Neurosci. *20*, 8087–8095.

Matsuzaki, M., Ellis-Davies, G.C., Nemoto, T., Miyashita, Y., Iino, M., and Kasai, H. (2001). Dendritic spine geometry is critical for AMPA receptor expression in hippocampal CA1 pyramidal neurons. Nat. Neurosci. *4*, 1086–1092.

Matsuzaki, M., Honkura, N., Ellis-Davies, G.C.R., and Kasai, H. (2004). Structural basis of long-term potentiation in single dendritic spines. Nature *429*, 761–766.

McBain, C.J., and Fisahn, A. (2001). Interneurons unbound. Nat. Rev. Neurosci. *2*, 11–23.

McKinney, R.A. (2010). Excitatory amino acid involvement in dendritic spine formation, maintenance and remodelling. J. Physiol. *588*, 107–116.

Megías, M., Emri, Z., Freund, T.., and Gulyás, A.. (2001). Total number and distribution of inhibitory and excitatory synapses on hippocampal CA1 pyramidal cells. Neuroscience *102*, 527–540.

Mele, M., Leal, G., and Duarte, C.B. (2016). Role of GABAAR trafficking in the plasticity of inhibitory synapses. J. Neurochem. *139*, 997–1018.

Mellor, J., and Nicoll, R.A. (2001). Hippocampal mossy fiber LTP is independent of postsynaptic calcium. Nat. Neurosci. *4*, 125–126.

Migliore, M., and Shepherd, G.M. (2002). Emerging rules for the distributions of active dendritic conductances. Nat. Rev. Neurosci. *3*, 362–370.

Minta, A., Kao, J.P.Y., and Tsien, R.Y. (1989). Fluorescent indicators for cytosolic calcium based on rhodamine and fluorescein chromophores. J. Biol. Chem.

Mizoguchi, Y., Kanematsu, T., Hirata, M., and Nabekura, J. (2003). A Rapid Increase in the Total Number of Cell Surface Functional GABA A Receptors Induced by Brain-derived Neurotrophic Factor in Rat Visual Cortex. J. Biol. Chem. *278*, 44097–44102.

Moss, S.J., and Smart, T.G. (2001). Constructing inhibitory synapses. Nat. Rev. Neurosci. *2*, 240–250.

Muir, J., Arancibia-Carcamo, I.L., MacAskill, A.F., Smith, K.R., Griffin, L.D., and Kittler, J.T. (2010). NMDA receptors regulate GABAA receptor lateral mobility and clustering at inhibitory synapses through serine 327 on the 2 subunit. Proc. Natl. Acad. Sci. *107*, 16679–16684.

Mulkey, R.M., Endo, S., Shenolikar, S., and Malenka, R.C. (1994a). Involvement of a calcineurin/inhibitor-1 phosphatase cascade in hippocampal long-term depression. Nature *369*, 486–488.

Mulkey, R.M., Endo, S., Shenolikar, S., and Malenka, R.C. (1994b). Involvement of a calcineurin/inhibitor-1 phosphatase cascade in hippocampal long-term depression. Nature *369*, 486–488.

Murakoshi, H., Wang, H., and Yasuda, R. (2011). Local, persistent activation of Rho GTPases during plasticity of single dendritic spines. Nature.

Nevian, T., Larkum, M.E., Polsky, A., and Schiller, J. (2007). Properties of basal dendrites of layer 5

pyramidal neurons: a direct patch-clamp recording study. Nat. Neurosci. *10*, 206–214.

Nicoll, R.A. (2017). A Brief History of Long-Term Potentiation. Neuron *93*, 281–290.

Nimchinsky, E.A., Sabatini, B.L., and Svoboda, K. (2002). Structure and Function of Dendritic Spines. Annu. Rev. Physiol. *64*, 313–353.

Niwa, F., Bannai, H., Arizono, M., Fukatsu, K., Triller, A., and Mikoshiba, K. (2012). Gephyrin-independent GABAAR mobility and clustering during plasticity. PLoS One *7*.

Noguchi, J., Matsuzaki, M., Ellis-Davies, G.C.R., and Kasai, H. (2005). Spine-neck geometry determines NMDA receptor-dependent Ca2+ signaling in dendrites. Neuron *46*, 609–622.

Noguchi, J., Nagaoka, A., Watanabe, S., Ellis-Davies, G.C.R., Kitamura, K., Kano, M., Matsuzaki, M., and Kasai, H. (2011). In vivo two-photon uncaging of glutamate revealing the structure-function relationships of dendritic spines in the neocortex of adult mice. J. Physiol. *589*, 2447–2457.

Nusser, Z., Hájos, N., Somogyi, P., and Mody, I. (1998). Increased number of synaptic GABAA receptors underlies potentiation at hippocampal inhibitory synapses. Nature *395*, 172–177.

Nymann-Andersen, J., Wang, H., Chen, L., Kittler, J.T., Moss, S.J., and Olsen, R.W. (2002). Subunit specificity and interaction domain between GABAA receptor-associated protein (GABARAP) and GABAA receptors. J. Neurochem. *80*, 815–823.

O'Dell, T.J., Hawkins, R.D., Kandel, E.R., and Arancio, O. (1991). Tests of the roles of two diffusible substances in long-term potentiation: Evidence for nitric oxide as a possible early retrograde messenger. Proc. Natl. Acad. Sci. U. S. A. *88*, 11285–11289.

Oh, W.C., Parajuli, L.K., and Zito, K. (2015). Heterosynaptic structural plasticity on local dendritic segments of hippocampal CA1 neurons. Cell Rep. *10*, 162–169.

Ohno-Shosaku, T., Maejima, T., and Kano, M. (2001). Endogenous cannabinoids mediate retrograde signals from depolarized postsynaptic neurons to presynaptic terminals. Neuron *29*, 729–738.

Orekhova, E. V., Stroganova, T.A., Nygren, G., Tsetlin, M.M., Posikera, I.N., Gillberg, C., and Elam, M. (2007). Excess of High Frequency Electroencephalogram Oscillations in Boys with Autism. Biol. Psychiatry *62*, 1022–1029.

Otsu, Y., Donneger, F., Schwartz, E.J., and Poncer, J.C. (2020). Cation–chloride cotransporters and the polarity of GABA signalling in mouse hippocampal parvalbumin interneurons. J. Physiol. *598*, 1865–1880.

Payne, J.A., Rivera, C., Voipio, J., and Kaila, K. (2003). Cation-chloride co-transporters in neuronal communication, development and trauma. Trends Neurosci. *26*, 199–206.

Pelkey, K.A., Chittajallu, R., Craig, M.T., Tricoire, L., Wester, J.C., and McBain, C.J. (2017). Hippocampal GABAergic Inhibitory Interneurons. Physiol. Rev. *97*, 1619–1747.

Peters, A., and Kaiserman-Abramof, I.R. (1970). The small pyramidal neuron of the rat cerebral cortex. The perikaryon, dendrites and spines. Am. J. Anat. *127*, 321–355.

Petrini, E.M., and Barberis, A. (2014). Diffusion dynamics of synaptic molecules during inhibitory postsynaptic plasticity. Front. Cell. Neurosci. *8*, 1–16.

Petrini, E.M., Lu, J., Cognet, L., Lounis, B., Ehlers, M.D., and Choquet, D. (2009). Endocytic

Trafficking and Recycling Maintain a Pool of Mobile Surface AMPA Receptors Required for Synaptic Potentiation. Neuron *63*, 92–105.

Petrini, E.M., Ravasenga, T., Hausrat, T.J., Iurilli, G., Olcese, U., Racine, V., Sibarita, J.-B., Jacob, T.C., Moss, S.J., Benfenati, F., et al. (2014). Synaptic recruitment of gephyrin regulates surface GABAA receptor dynamics for the expression of inhibitory LTP. Nat. Commun. *5*.

Phillips, K.G., Hardingham, N.R., and Fox, K. (2008). Postsynaptic action potentials are required for nitric-oxide-dependent long-term potentiation in CA1 neurons of adult GluR1 knock-out and wild-type mice. J. Neurosci. *28*, 14031–14041.

Pizzorusso, T; Medini, P; Berardi, N; Chierzi, S; Fawcett , J.W; Maffei, L. (2002). Reactivation of Ocular Dominance Plasticity in the Adult Visual Cortex. Science (80-.). *298*, 1248–1251.

Poirazi, P., and Mel, B.W. (2001). Impact of active dendrites and structural plasticity on the memory capacity of neural tissue. Neuron *29*, 779–796.

Polsky, A., Mel, B.W., and Schiller, J. (2004). Computational subunits in thin dendrites of pyramidal cells. Nat. Neurosci. *7*, 621–627.

Qiu, S., Zhao, L.F., Korwek, K.M., and Weeber, E.J. (2006). Differential reelin-induced enhancement of NMDA and AMPA receptor activity in the adult hippocampus. J. Neurosci. *26*, 12943–12955.

Rall, W., and Shepherd, G.M. (1968). Theoretical reconstruction of field potentials and dendrodendritic synaptic interactions in olfactory bulb. J. Neurophysiol. *31*, 884–915.

Rinke, I., Artmann, J., and Stein, V. (2010). ClC-2 voltage-gated channels constitute part of the background conductance and assist chloride extrusion. J. Neurosci. *30*, 4776–4786.

Rivera, C., Voipio, J., Payne, J.A., Ruusuvuori, E., Lahtinen, H., Lamsa, K., Pirvola, U., Saarma, M., and Kaila, K. (1999). The K+/Cl- co-transporter KCC2 renders GABA hyperpolarizing during neuronal maturation. Nature *397*, 251–255.

Rivera, C., Voipio, J., and Kaila, K. (2005). Two developmental switches in GABAergic signalling: the K + -Cl − cotransporter KCC2 and carbonic anhydrase CAVII. J. Physiol. *562*, 27–36.

De Roo, M., Klauser, P., Garcia, P.M., Poglia, L., and Muller, D. (2008). Chapter 11 Spine dynamics and synapse remodeling during LTP and memory processes. pp. 199–207.

Rubenstein, J.L.R., and Merzenich, M.M. (2003a). Model of autism: increased ratio of excitation/inhibition in key neural systems. Genes, Brain Behav. *2*, 255–267.

Rubenstein, J.L.R., and Merzenich, M.M. (2003b). Model of autism: Increased ratio of excitation/inhibition in key neural systems. Genes, Brain Behav. *2*, 255–267.

Sabatini, B.L., Maravall, M., and Svoboda, K. (2001). Ca2+ signaling in dendritic spines. Curr. Opin. Neurobiol. *11*, 349–356.

Sabatini, B.L., Oertner, T.G., and Svoboda, K. (2002). The Life Cycle of Ca2+ Ions in Dendritic Spines. Neuron *33*, 439–452.

Sanacora, G., Mason, G.F., Rothman, D.L., Behar, K.L., Hyder, F., Petroff, O.A.C., Berman, R.M., Charney, D.S., and Krystal, J.H. (1999). Reduced Cortical γ-Aminobutyric Acid Levels in Depressed Patients Determined by Proton Magnetic Resonance Spectroscopy. Arch. Gen. Psychiatry *56*, 1043.

Sanhueza, M., Fernandez-Villalobos, G., Stein, I.S., Kasumova, G., Zhang, P., Bayer, K.U., Otmakhov,

N., Hell, J.W., and Lisman, J. (2011). Role of the CaMKII/NMDA Receptor Complex in the Maintenance of Synaptic Strength. J. Neurosci. *31*, 9170–9178.

Sanz-Clemente, A., Gray, J.A., Ogilvie, K.A., Nicoll, R.A., and Roche, K.W. (2013). Activated CaMKII Couples GluN2B and Casein Kinase 2 to Control Synaptic NMDA Receptors. Cell Rep. *3*, 607–614.

Scelfo, B., Sacchetti, B., and Strata, P. (2008). Learning-related long-term potentiation of inhibitory synapses in the cerebellar cortex. Proc. Natl. Acad. Sci. *105*, 769–774.

Segal, M. (1995). Imaging of calcium variations in living dendritic spines of cultured rat hippocampal neurons. J. Physiol. *486*, 283–295.

Segal, M., Clarke, D.J., Maddox, P., Salmon, E.D., Bloom, K., and Reed, S.I. (2000). Coordinated Spindle Assembly and Orientation Requires Clb5p-Dependent Kinase in Budding Yeast. J. Cell Biol. *148*, 441–452.

Sieghart, W. (2006). Structure, Pharmacology, and Function of GABAA Receptor Subtypes. pp. 231–263.

Sivakumaran, S., Mohajerani, M.H., and Cherubini, E. (2009). At Immature Mossy-Fiber-CA3 Synapses, Correlated Presynaptic and Postsynaptic Activity Persistently Enhances GABA Release and Network Excitability via BDNF and cAMP-Dependent PKA. J. Neurosci. *29*, 2637–2647.

Soderling, T.R. (2000). CaM-kinases: Modulators of synaptic plasticity. Curr. Opin. Neurobiol. *10*, 375–380.

Sohal, V.S., Zhang, F., Yizhar, O., and Deisseroth, K. (2009). Parvalbumin neurons and gamma rhythms enhance cortical circuit performance. Nature *459*, 698–702.

Somogyi, P., Tamás, G., Lujan, R., and Buhl, E.H. (1998). Salient features of synaptic organisation in the cerebral cortex1Published on the World Wide Web on 3 March 1998.1. Brain Res. Rev. *26*, 113–135.

Spencer, W.A., and Kandel, E.R. (1961). ELECTROPHYSIOLOGY OF HIPPOCAMPAL NEURONS: IV. FAST PREPOTENTIALS. J. Neurophysiol. *24*, 272–285.

Stuart, G., and Spruston, N. (1998). Determinants of Voltage Attenuation in Neocortical Pyramidal Neuron Dendrites. J. Neurosci. *18*, 3501–3510.

Stuart, G.J., and Sakmann, B. (1994). Active propagation of somatic action potentials into neocortical pyramidal cell dendrites. Nature *367*, 69–72.

Stuart, G.J., and Spruston, N. (2015). Dendritic integration: 60 years of progress. Nat. Neurosci. *18*, 1713–1721.

Szabadics, J., Tamás, G., and Soltesz, I. (2007). Different transmitter transients underlie presynaptic cell type specificity of GABAA,slow and GABAA,fast. Proc. Natl. Acad. Sci. U. S. A. *104*, 14831–14836.

Tanaka, J. -i., Horiike, Y., Matsuzaki, M., Miyazaki, T., Ellis-Davies, G.C.R., and Kasai, H. (2008). Protein Synthesis and Neurotrophin-Dependent Structural Plasticity of Single Dendritic Spines. Science (80-.). *319*, 1683–1687.

Tanaka, T., Saito, H., and Matsuki, N. (1997). Inhibition of GABA(A) synaptic responses by brain-derived neurotrophic factor (BDNF) in rat hippocampus. J. Neurosci. *17*, 2959–2966.

Tazerart, S., Mitchell, D.E., Miranda-Rottmann, S., and Araya, R. (2020). A spike-timing-dependent plasticity rule for dendritic spines. Nat. Commun. *11*.

Thompson, R.F. (2005). In Search of Memory Traces. Annu. Rev. Psychol. *56*, 1–23.

Tønnesen, J., and Nägerl, U.V. (2016). Dendritic Spines as Tunable Regulators of Synaptic Signals. Front. Psychiatry *7*.

Tønnesen, J., Katona, G., Rózsa, B., and Nägerl, U.V. (2014). Spine neck plasticity regulates compartmentalization of synapses. Nat. Neurosci. *17*, 678–685.

Treiman, D.M. (2001). GABAergic Mechanisms in Epilepsy. Epilepsia *42*, 8–12.

Tyagarajan, S.K., and Fritschy, J.M. (2014). Gephyrin: A master regulator of neuronal function? Nat. Rev. Neurosci. *15*, 141–156.

Tyagarajan, S.K., Ghosh, H., Yevenes, G.E., Nikonenko, I., Ebeling, C., Schwerdel, C., Sidler, C., Zeilhofer, H.U., Gerrits, B., Muller, D., et al. (2011). Regulation of GABAergic synapse formation and plasticity by GSK3 -dependent phosphorylation of gephyrin. Proc. Natl. Acad. Sci. *108*, 379–384.

Tyagarajan, S.K., Ghosh, H., Yévenes, G.E., Imanishi, S.Y., Zeilhofer, H.U., Gerrits, B., and Fritschy, J.M. (2013). Extracellular signal-regulated kinase and glycogen synthase kinase 3β regulate gephyrin postsynaptic aggregation and GABAergic synaptic function in a calpain-dependent mechanism. J. Biol. Chem. *288*, 9634–9647.

Tzounopoulos, T., Janz, R., Südhof, T.C., Nicoll, R.A., and Malenka, R.C. (1998). A role for cAMP in long-term depression at hippocampal mossy fiber synapses. Neuron *21*, 837–845.

Udakis, M., Pedrosa, V., Chamberlain, S.E.L., Clopath, C., and Mellor, J.R. (2020). Interneuron-specific plasticity at parvalbumin and somatostatin inhibitory synapses onto CA1 pyramidal neurons shapes hippocampal output. Nat. Commun. *11*.

Villa, K.L., Berry, K.P., Subramanian, J., Cha, J.W., Oh, W.C., Kwon, H.B., Kubota, Y., So, P.T.C., and Nedivi, E. (2016). Inhibitory Synapses Are Repeatedly Assembled and Removed at Persistent Sites In Vivo. Neuron *89*, 756–769.

Villacres, E.C., Wong, S.T., Chavkin, C., and Storm, D.R. (1998). Type I Adenylyl Cyclase Mutant Mice Have Impaired Mossy Fiber Long-Term Potentiation. J. Neurosci. *18*, 3186–3194.

Wang, J., Liu, S., Haditsch, U., Tu, W., Cochrane, K., Ahmadian, G., Tran, L., Paw, J., Wang, Y., Mansuy, I., et al. (2003). Interaction of calcineurin and type-A GABA receptor gamma 2 subunits produces long-term depression at CA1 inhibitory synapses. J. Neurosci. *23*, 826–836.

Wang, X. Bin, Bozdagi, O., Nikitczuk, J.S., Zu, W.Z., Zhou, Q., and Huntley, G.W. (2008). Extracellular proteolysis by matrix metalloproteinase-9 drives dendritic spine enlargement and long-term potentiation coordinately. Proc. Natl. Acad. Sci. U. S. A. *105*, 19520–19525.

Wardle, R.A., and Poo, M. (2003). Brain-derived neurotrophic factor modulation of GABAergic synapses by postsynaptic regulation of chloride transport. J. Neurosci. *23*, 8722–8732.

Weeber, E.J., Beffert, U., Jones, C., Christian, J.M., Förster, E., David Sweatt, J., and Herz, J. (2002). Reelin and apoE receptors cooperate to enhance hippocampal synaptic plasticity and learning. J. Biol. Chem. *277*, 39944–39952.

Weinberger, N.M. (2004). Specific long-term memory traces in primary auditory cortex. Nat. Rev. Neurosci. *5*, 279–290.

Weisskopf, M., Castillo, P., Zalutsky, R., and Nicoll, R. (1994). Mediation of hippocampal mossy fiber long-term potentiation by cyclic AMP. Science (80-.). *265*, 1878–1882.

Weitlauf, C., and Winder, D. (2001). Calcineurin, synaptic plasticity, and memory. ScientificWorldJournal. *1*, 530–533.

Wiera, G., Lebida, K., Lech, A.M., Brzdąk, P., Van Hove, I., De Groef, L., Moons, L., Petrini, E.M., Barberis, A., and Mozrzymas, J.W. (2020). Long-term plasticity of inhibitory synapses in the hippocampus and spatial learning depends on matrix metalloproteinase 3. Cell. Mol. Life Sci.

Williams, S.R., and Stuart, G.J. (2002). Dependence of EPSP efficacy on synapse location in neocortical pyramidal neurons. Science (80-.). *295*, 1907–1910.

Wilson, R.I., and Nicoll, R.A. (2001). Endogenous cannabinoids mediate retrograde signalling at hippocampal synapses. Nature *410*, 588–592.

Woodin, M.A., Ganguly, K., and Poo, M. (2003). Coincident Pre- and Postsynaptic Activity Modifies GABAergic Synapses by Postsynaptic Changes in Cl− Transporter Activity. Neuron *39*, 807–820.

Wosiski-Kuhn, M., and Stranahan, A.M. (2012). Transient increases in dendritic spine density contribute to dentate gyrus long-term potentiation. Synapse *66*, 661–664.

Xia, Z., and Storm, D.R. (2005). The role of calmodulin as a signal integrator for synaptic plasticity. Nat. Rev. Neurosci. *6*, 267–276.

Xue, J.G., Masuoka, T., Gong, X. Di, Chen, K.S., Yanagawa, Y., Alex Law, S.K., and Konishi, S. (2011). NMDA receptor activation enhances inhibitory GABAergic transmission onto hippocampal pyramidal neurons via presynaptic and postsynaptic mechanisms. J. Neurophysiol. *105*, 2897–2906.

Yang, G., Lai, C.S.W., Cichon, J., Ma, L., Li, W., and Gan, W.-B. (2014). Sleep promotes branch-specific formation of dendritic spines after learning. Science (80-.). *344*, 1173–1178.

Yasuda, R. (2017). Biophysics of Biochemical Signaling in Dendritic Spines: Implications in Synaptic Plasticity. Biophys. J.

Yasuda, H., Kinoshita, S., and Tsumoto, T. (1998). Localized contribution of N-methyl-D-aspartate receptors to synaptic input-induced rise of calcium in apical dendrites of layer II/III neurons in rat visual cortex. Neuroscience.

Yasuda, H., Higashi, H., Kudo, Y., Inoue, T., Hata, Y., Mikoshiba, K., and Tsumoto, T. (2003). Imaging of calcineurin activated by long-term depression-inducing synaptic inputs in living neurons of rat visual cortex. Eur. J. Neurosci. *17*, 287–297.

Yuste, R. (2013). Electrical Compartmentalization in Dendritic Spines. Annu. Rev. Neurosci. *36*, 429–449.

Zalutsky, R.A., and Nicoll, R.A. (1990). Comparison of two forms of long-term potentiation in single hippocampal neurons. Science (80-.). *248*, 1619–1624.

Zeng, H., Chattarji, S., Barbarosie, M., Rondi-Reig, L., Philpot, B.D., Miyakawa, T., Bear, M.F., and Tonegawa, S. (2001). Forebrain-specific calcineurin knockout selectively impairs bidirectional

synaptic plasticity and working/episodic-like memory. Cell *107*, 617–629.

Zorrilla de San Martin, J., Delabar, J.-M., Bacci, A., and Potier, M.-C. (2018). GABAergic over-inhibition, a promising hypothesis for cognitive deficits in Down syndrome. Free Radic. Biol. Med. *114*, 33–39.

ACKNOWLEDGMENTS

Firstly, I would like to thank my supervisor Dr. *Andrea Barberis* for give me the possibility to work in his laboratory and for the strong support during this journey. I would like to express my very great appreciation for encouraging my research and motivating me, for his patience, in particular during the writing of this thesis, and for trying to transfer to me his huge knowledge. I hope I caught at least half of his teachings.

A big thank also to my current colleagues, Dr. *Enrica Petrini* and Martina Bruno, and former ones, Dr. *Alice Polenghi* e Dr. *Tiziana Ravasenga*, for the crucial help in the times of needs, the stimulating discussions, the teamwork, and for all the funny moments that we had in the last three years.
In particular, a special mention goes to Dr. *Tiziana Ravasenga* for sharing with me happy and sad moments during the long journey of this project and for teaching me how to work in a laboratory.

I would also like to thank my referees, Dr. *Alberto Bacci* and Dr. *Jerzy Mozrzymas* for accepting this charge.

A special thanks to my *family*. Words cannot express how grateful I am to my mother and father for all of the sacrifices that they've made on my behalf. Thank also to my sister that was always supporting me. Although we do not always agree, I'm glad you're my sister.

I would also like to thank all of my friends who supported me. In particular, thanks to my amazing friends of *Jolly and Coi* for the good time we shared together, even if in this last year for reason of force majeure we have seen less but we continue to keep in contact.

Last but not the least, I would like to express my special appreciation to my girlfriend *Francesca* who was always my support in the difficult moments of this life journey. Even if we live in different cities and we can meet only during the weekend, you always make me feel near you and your kind support.